Investigation of Halogen Bond Interactions of Chiral Molecules Using Infrared, Vibrational Circular Dichroism, NMR, UV-vis Spectroscopy and Density Functional Theory Calculations

by

Amin Moazeni

A thesis submitted in partial fulfillment of the requirements for the degree of

Doctor of Philosophy

Department of Chemistry
University of Alberta

Abstract

This PhD thesis shows the application of different spectroscopic and theoretical tools to probe the extent and possible interaction between various Lewis acids (halogen bond donor) and Lewis bases (halogen bond acceptors). Vibrational circular dichroism (VCD) that is the chiral version of infrared (IR) spectroscopy is able to provide valuable information about the absolute configuration of a chiral molecule in the solution when coupled with theoretical calculations. This technique is also sensitive to intermolecular interactions. Since the strength and level of interaction between the halogen bond donors and halogen bond acceptors is unknown to us we have also decided to utilize other spectroscopy techniques such as ^{19}F-NMR, ^{1}H-NMR, and UV-vis spectroscopy.

In chapter 3, I studied the formation of the halogen bond between 4-benzyl-1,3-thiazolidine-2-one (NOS) and iodine. In order to probe the interaction between the two molecules I used FT-IR, VCD, ^{1}H-NMR, and UV-vis spectroscopy techniques. Density Functional Theory (DFT) calculations allowed me to find out what would be the conformers of the interacting species and which ones would contribute to the formation of final complexes. This study concluded with no interaction between the two species.

In chapter 4, I studied the formation of the halogen bond between 4-benzyl-1,3-thiazolidine-2-thione (NSS) and iodine in the solution using FT-IR, VCD, ^{1}H-NMR, and UV-vis spectroscopy techniques. DFT simulations were carried out to find out the most stable conformers of the interacting species and the formation of final

complexes. This study concluded with discovery of a new halogen bond interaction motif between the two species.

In chapter 5, I studied the formation of halogen bond between 4-benzyl-1,3-thiazolidine-2-one (NOS) and iodopentafluorobenzene (F_5BnI) in the solution using FT-IR, VCD, ^{1}H-NMR, and ^{19}F-NMR spectroscopy. Sensitivity of the VCD and ^{19}F-NMR spectroscopy allowed me to monitor small changes in the spectra of interacting species. Consequently with the aid of DFT simulations I was able to suggest the most probable conformer for the interaction between the donor and acceptor species.

In chapter 6, I studied the formation of halogen bond between 4-benzyl-1,3-thiazolidine-2-thione (NSS) and iodopentafluorobenzene (F_5BnI) in the solution using FT-IR, VCD, ^{1}H-NMR, and ^{19}F-NMR spectroscopy. ^{19}F-NMR signals does not suggest a strong interaction between the two species due to the low change in the chemical shift. Despite the fact that the interaction between these species is weak, we were able to collect signals from the VCD machine which together with the DFT data enabled us to suggest a possible structure in the formation of the complex.

Preface

The contents of this thesis are based on the research work that I have undertaken during my graduate study in the Department of Chemistry at the University of Alberta. The contribution made by each author in each research project is summarized below.

Chapters 3,4,5 and 6 are to be submitted for a journal publication. I carried out all the aqueous phase IR, VCD, NMR, and UV-vis measurements, and the simulations of spectra. Professor Y. Xu was the supervisory author and was involved in the concept formation. Professor Carlos A. Cruz-Noguez was the defense supervisor.

Acknowledgement

I’m grateful to my former supervisor Prof. Yunjie Xu for admitting me into her research group as a graduate student and also for all the assistance and guidance provided during my PhD research studies. I am extremely grateful to my current supervisor Prof. Carlos A. Cruz-Noguez who assisted me through the final stages of my PhD program.

I am indeed grateful to my wife and my little daughter who were the hope, and the force for me to get over the challenges during the final stages of my PhD degree and finish the line and get back to them physically and mentally.

Table of contents

List of Tables (Chapters)

Table Page

List of Figures (Chapters)

CHAPTER 1

Introduction

1.1 History of Halogen Bond

A halogen bond (X-bond) can be defined broadly as a non-covalent interaction between an electron deficient X-bond donor and an electron rich X-bond acceptor, in a similar fashion as a hydrogen bond (H-bond). One of the early studies of X-bond was by Guthrie[1] in 1863, when he added iodine powder to a solution of ammonia to form the complex, which he then suggested to be $I_2 \cdots NH_3$ and named it "iodide of iodammonium". Guthrie found that this complex decomposed upon treating with water, turned water into a reddish-brown color, and produced a residue, which exploded spontaneously under water.

Since then, there have been some notable discoveries in the field of X-bonds. In the 1950s Mulliken[2,3] observed a larger blue shift of the iodine visible absorption peak in aromatic solvents (Table 1.1). Mulliken recognized that the absorption intensity at the λ_{max} of iodine-benzene at about 500 nm is ~1000 times stronger than the λ_{max} of benzene in heptane, which is at 2600Å [2], and proposed the formation of an electron donor-acceptor complex, in which there is a ***transfer of charge*** from the *electron donor* D to the *electron acceptor* A:

$$D + A \leftrightarrow D^+A^- \leftrightarrow D^+ + A^-$$

Table 1.1 Maximum Absorbance of Iodine in Visible Region in six Different Solvents

Solvent	λ_{max} nm	Solvent	λ_{max}
n-Heptane	520	Benzene	500
CCl_4	520	Toluene	497
CH_3CHCl_2	503	o-Xylene	497

Significant progress over the last few decades has been made in studies of X-bonds in the solid state. Using X-ray diffraction, geometries of X-bond complexes were reported by a few research groups, including the 1969 Nobel Prize winner O. Hassel. A few interesting structures are shown in Fig. 1.1. In the bromine···1,4 dioxanate compound, the Br–Br distance is 2.31 Å, longer than that of the free bromine molecule at 2.28 Å[4], and the Br···O distance is 2.71 Å, a value between the van der Waals (3.37 Å) and covalent (1.87 Å) radii of bromine···oxygen. These bond distance values indicate a very strong interaction between the bromine and oxygen atom, as suggested by Hassel. The Br–Br distance in bromine hexamethylenetetraamine complex is 2.4 Å, while the Br···N distance is 2.3 Å, showing a strong interaction between the nitrogen and the bromine atom and a large weakening of the Br–Br covalent bond. Similarly, the Br–O distance of 2.82 Å is shorter than the sum of the van der Waals radii of bromine and oxygen, 3.37 Å, in the third example in Fig 1.1.

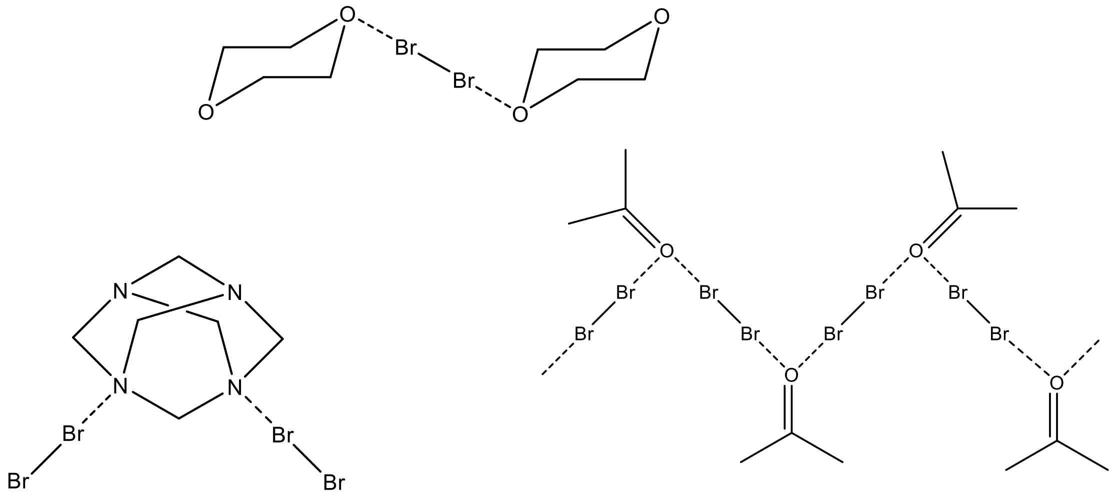

Figure 1.1. Examples of three X-bond complexes: bromine···1,4-dioxane[4], bromine···hexamethylenetetraamine,[5] and bromine···acetone.[6]

In general, an X-bond is characterized by a fairly short acceptor···X bond (which is referred to as a charge transfer bond in some instances) distance and a lengthening of the X–X bond length compared to that in free halogens. Table 2 shows some selected bond lengths of the addition complexes of halogens with ethers, ketones, and sulphides.[4, 6-7] In the benzyl sulphide···I_2 and the 1,4 dithian···I_2 compounds, the S···I distances are very short, 2.78 Å and 2.83 Å, respectively. For both of them, the I–I distance is approximately 0.2 Å larger than the I–I distance in the free iodine, which is 2.67 Å. By comparing the X···O distances and the sums of the van der Waals radii in the additional complexes of 1,4 dioxane and the dihalogens, Hassel concluded that size of the halogen atom has a direct relation with the strength of the X···O interaction.[8]

Table 1.2. Selected Bond Angles and Changes in the Bond Lengths (Å) of Donors and Acceptors in Charge Transfer Complexes

Compound	Charge transfer bond	Bond length	Sum of van der Waals radii	X-X bond length in complex	X-X bond length in free halogen	Donor-X-X angle
1,4 dioxane/Br_2	O···Br	2.71	3.35	2.31	2.28	180
1,4 dioxane/ICl	O···I	2.57	3.55	2.33	2.32	Approximately linear
1,4 dioxane/Cl_2	O···Cl	2.67	3.20	2.02	1.99	178
acetone/Br_2	O···Br	2.82	3.35	2.28	2.28	180
Benzyle sulphide/I_2	S···I	2.78	4.00	2.82	2.67	179
1,4 dithian/I_2	S···I	2.87	4.00	2.79	2.67	178
1,4 diselenan/I_2	Se···I	2.83	4.15	2.78	2.67	180

Another common type of X-bond encountered in the solid state is between a carbon halogen bond (C-X, X = Cl, Br, I) and the electronegative atom of nitrogen or oxygen. Allen et al[9]. discovered them by analyzing the crystal structures from the Cambridge Structural Database. They recognized that these X-bonds are highly directional and suggested that electrostatic effects play the main role in X…N or X…O interaction. The directionality of the interaction was related to the anisotropic charge distribution around the C-X bond.[9] Further studies by Metrangoloa et al[10].

showed that the C-I…N angle in different structures was about 175°. A similar trend was observed for C-I…I.$^{-}$[10]

Over the years, some semi-empirical rules have been developed to explain X-bond strength[30]. For example, an increase in the X-bond strength from oxygen to sulfur was explained previously by Pearson's rule of hard and soft acid and bases (HSAB).[11] This rule states that hard acids and soft acids bind more strongly to hard bases and soft bases, respectively. Iodine is a soft halogen (Lewis acid) so it binds more strongly to sulfur, a softer base, rather than oxygen. It also has been shown that the strength of an X-bond increases with the increasing polarizability of the electron deficient halogen atom. It follows the trend of F < Cl < Br < I, in which iodine is the most polarizable atom[12], thus, an iodine containing compound would be a good candidate for probing such X-bond interactions.

More recently, computational methods have been applied to investigate the nature of X-bond interactions, leading to some significant progress. The concept of the "sigma hole" was developed to explain the X-bond donor,[13] analogous to the H-bond donor. The sigma hole represents an area with positive electrostatic potential along the covalent R–X bond, where R can be F, Cl, Br, I, C, N, and so on. The sigma hole is the consequence of an anisotropic distribution of electron density along the same bond. This makes the radius of the halogen atom smaller along the covalent C–X bond but larger on the perpendicular direction. Politzer, Murray, and Clark[14] provided an atomic and molecular orbital view to demonstrate how the sigma hole is formed. Group VII atoms (halogens) have seven electrons in their p and s-orbitals of the valence shell, which creates an $s^2p_x^2p_y^2p_z^1$ configuration, where p_z is along the C–X bond to form a covalent bond with carbon. As a result, there is a depopulation of electron density at this p_z orbital due to the formation of a covalent bond with carbon, and a partial positive charge is created on the X atom. Since the electrons of the p_x and p_y are maintained around the C–X bond, an electron rich ring is created around the C–X bond.

There have been continuing discussions on the exact nature of X-bond interactions. For example, how dispersion interactions and the charge transfer influence the properties of the X-bond systems still is being debated. Symmetry-adapted perturbation theory and natural bond orbital (NBO) analysis have been used to explain how much different components contribute to the X-bond interaction[15], although the separation of different components is not unique and depends on the models applied.[15]

1.2 Applications of X-bond

The X-bond has played an important role in supramolecular chemistry, including crystal engineering and syntheses of nanomaterials and metal-organic frameworks and in medicinal chemistry. Some examples are given below, in which the same or similar halogen compounds investigated in this thesis are utilized.

The X-bond has been utilized to generate one-, two-, and three-dimensional crystal structures in crystal engineering. One-dimensional chains are formed if the donor and acceptor are both bidentate. Formation of more than one halogen bond by the same interacting species will form a two-dimensional structure. If the interacting species are tetradentate, three-dimensional structures will be formed. For example, Metrangolo and co-workers have reported one and two-dimensional structures, see Fig 1.2.[16]

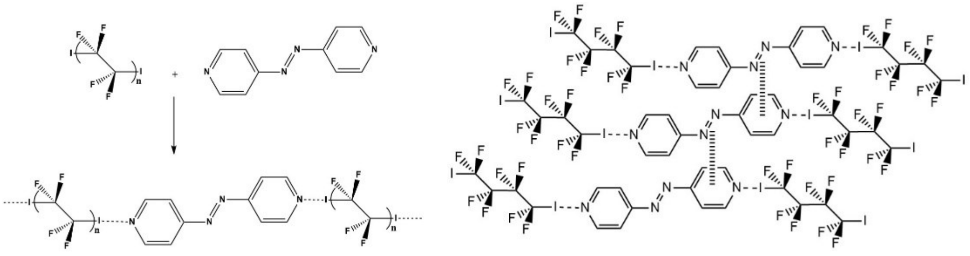

a b

Figure 1.2. Formation of 1D (a) and 2D (b) crystal structures between trans-4,4'-azobipyridine and 1,6-diiodoperfluorohexane.[16b]

As a supramolecular dynamics catalyst, Bryce and co-workers at Ottawa U. very recently showed that an X-bond can facilitate the rotation of methyl group in a series of supramolecular structures that contain 2,3,5,6-tetramethylpyrazine (TMP).[17] Using solid state NMR and density functional theory (DFT) calculations, the authors demonstrated that the methyl internal rotation activation energy drops from 7.31

kJ/mol in an isolated TMP gas phase molecule to only about 3–5 kJ/mol (Table 1.3) in a few supramolecular structures shown below (Figure 1.3).

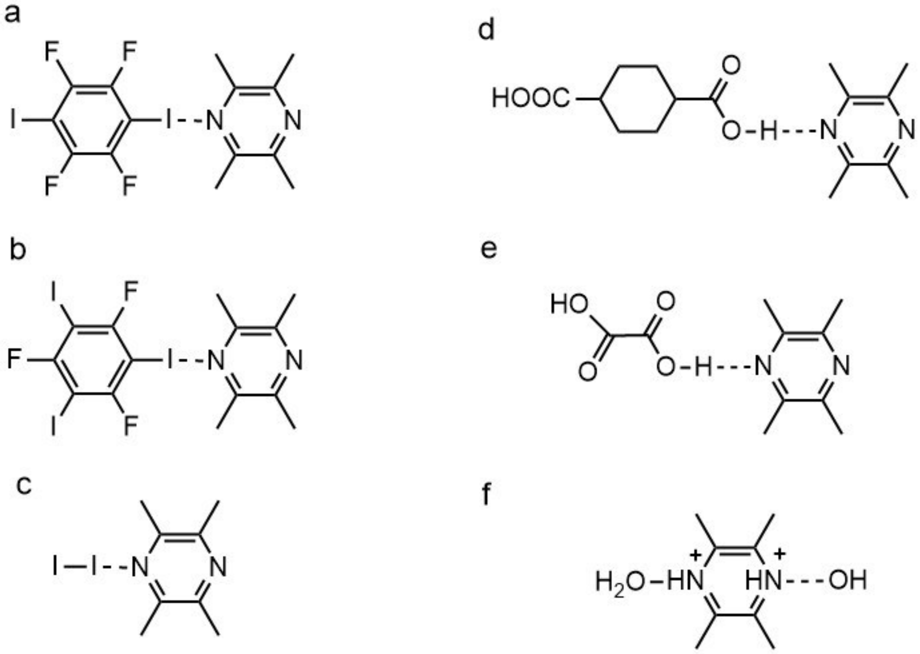

Figure 1.3. Molecular structures involving 2,3,5,6-tetramethylpyrazine (TMP). Dashed lines refer to the X-bonds (a,b,c) and the H-bonds (d,e,f). f exists as a salt with 2Cl anions (f.2HCl).[17]

Table 1.3. Methyl Group Rotational Activation Energies [17]

Compound	I···N/H···N bond length (Å)	Activation energy (kJ mol^{-1})	Note
a	3.0665(18)	2.84 ± 0.14	Halogen bonded
b	2.993(3)	2.84 ± 0.14	Halogen bonded
c	3.075(5)	3.62 ± 0.13	Halogen bonded
d	1.919	4.17 ± 0.09	Hydrogen bonded
e	1.809	5.02 ± 0.06	Hydrogen bonded
f.2HCl	n/a	6.81 ± 0.16	HCl salt

As can be seen in Table 1.3, in the case of an X-bond, this reduction is noticeably more than in the case of a H-bond[17]. It may be counter-intuitive that when TMP co-crystallizes with an X- or a H-bond interaction (Figure 1.3), the methyl internal rotation activation energy actually is reduced. A small reduction also was reported in the gas phase rotational spectroscopy studies before, for example, when the methyl glycidate monomer is H-bonded to water [31]. That was justified by the DFT calculations showing that the H-bond interactions preferentially stabilize the transition state more than the ground state structures, leading to a smaller activation energy than the methyl internal rotation activation energy. Similarly, although much more drastically in the solid state case, Bryce and co-workers used DFT calculations to show the observed catalytic activity of the X-bond, i.e., the reduction of the said activation energy, is due to the same kind of preferential stabilization of the transition state than the ground state structures of TMP in the solid.

Because of steric and polar properties of X-bond compounds, they can play important roles in biological systems to facilitate a drug reach its appropriate receptor. Davis et al. investigated the effect of halogenation on stability, lipophilicity, and enhanced in vitro blood-brain barrier permeability of a drug [18]. The chlorinated and brominated species showed an enhanced in vitro blood-brain barrier permeability.[18] Such medicinal chemistry application is also one motivation for the current thesis research to investigate X-bond interactions in solution at the molecular level.

1.3 Chiral Stereochemistry

Since I have utilized chiral molecules in all my thesis research projects, I discuss briefly about chirality here. According to Prelog,[19] "chirality is the property of an object to be non-superimposable on its mirror image by translation and rotation". Our left and right hands are not superimposable on one another; thus, they possess handedness or chirality. A pair of mirror-imaged molecules that are not superimposable onto one another are called enantiomers. A racemic mixture is the one where both enantiomers exist in equal amounts.

Chiral structural elements of a chiral molecule can be classified into three categories: center of chirality, axis of chirality, and plane of chirality[20], by which three different types of chirality, central, axial, and helical chirality, are defined. Central chirality is the case where four different groups are attached to a central carbon (or other) atom, called a stereogenic center. A stereogenic center could either be (R) or (S), based on the Cahn-Ingold-Prelog naming rule.[21] Axial chirality happens when four different groups occupy nonplanar positions on a chiral axis, as shown in Figure 1.4 a). Helical chirality is related to a structure having a helical geometry,[22] such as a double-stranded DNA structure. Helical chirality is labelled as P (plus) or Δ for a right-handed helix, or M (minus) or Λ for a left-handed helix.

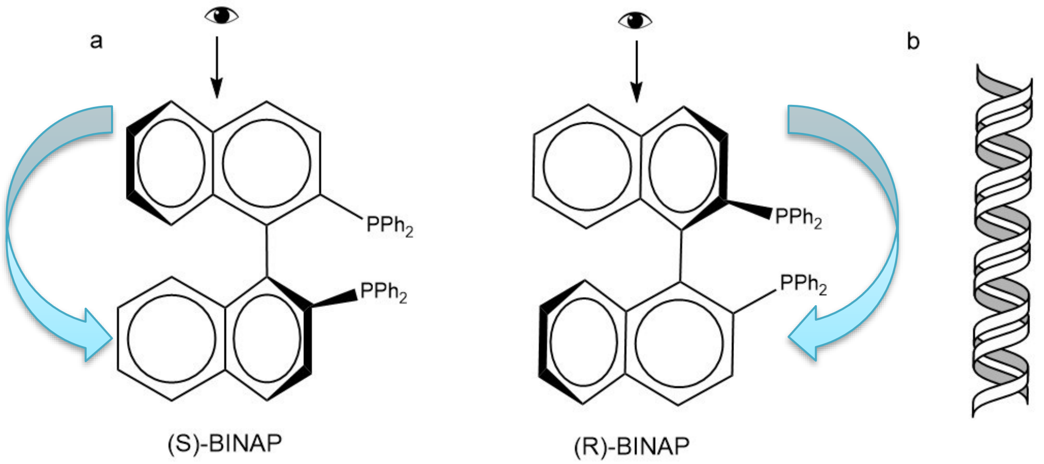

Figure 1.4. a) Axial chirality in (2,2′-bis(diphenylphosphino)-1,1′-binaphthyl) (BINAP). b) Helical chirality in a double-stranded DNA. [22]

1.4 Applying Vibrational Circular Dichroism to Study Chiral Species

It has been recognized that a pair of drug enantiomers may have drastically different medicinal properties. For example, (S) Ibuprofen has analgesic properties in contrast to the (R) configuration, which acts as an anti-inflammatory agent.[23] The need to know whether an enantiomer is (R) or (S), i.e., the absolute configuration, has led to the development of several relevant spectroscopic techniques.

One of the most common techniques used for determination of absolute configuration is single crystal X-ray diffraction (XRD).[24] For XRD, one would need a high-quality single crystal and often, preferably, an existence of a heavy atom in the crystal. Due to such restrictions, other methods, such as NMR with a chiral shift agent,[25] optical rotation, and electronic circular dichroism[26] (ECD) techniques also have been explored for the above purpose. ECD can be considered as the chiral version of UV/vis absorption spectroscopy. Here, circular dichroism (CD) is defined as the differential absorbance ($\Delta A = A_L - A_R$) between left and right circularly polarized light. Generally, a compound should have functionalities that absorb UV/vis radiation in order to obtain an ECD spectrum also. An ECD experiment is applicable directly in solution.

In the 70s, vibrational circular dichroism (VCD), a combination of chiral sensitivity of CD and structural precision of IR spectroscopy, was developed. First, theoretical studies were done in early 1970s, utilizing empirical methods to predict VCD spectra.[27] One of the earliest VCD measurements was demonstrated by Holzwart et al. in 1973.[28] In 1979 Nafie et al. developed the Fourier transform VCD technique and demonstrated the first measurment.[29] These VCD details will be discussed further in Chapter 2.

In general, UV/vis bands are quite broad because of the short life time of the electronic excited states in solution. In addition, it is typically much more difficult to predict the ECD spectral pattern well because of involvement of the excited electronic states. These two factors make it difficult to apply ECD for absolute configuration determination in some cases. In the IR region, on the other hand, often ten or more fundamental vibrational bands of a chiral molecule can be resolved easily from a solution directly. A pair of enantiomers will have identical or similar absorption patterns, whereas their VCD spectra are mirror images to each other. Theoretical simulations of IR and VCD spectra are also easier because only the ground electronic state is involved. These two reasons make VCD an attractive spectroscopic tool for absolute configuration determination.

1.5 Overview and Objectives of This Thesis

In comparison to H-bond interactions, X-bond interactions have been explored much less, despite their increasing importance in a wide range of research and application fields. Especially, X-bond interactions in solution have been investigated only sparsely. This situation is due to a number of factors. First, there are many non-covalent interactions in solution, for example, H-bonding interactions. Second, the spectral signatures are typically just a small shift in, for example, IR band shift, making it difficult to recognize conclusively. In this thesis, I apply both IR, VCD, and in some cases, UV-Vis, and ECD spectroscopies to examine X-bond interactions at the molecular level in combination with DFT calculations. VCD, in particular, often has the advantage of a distinctive VCD spectral pattern with positive and negative bands.

In this thesis, I focus my attention on a number of prototypical X-bond molecular systems, including complexes formed between these molecular systems, as shown in Figure 1.5.

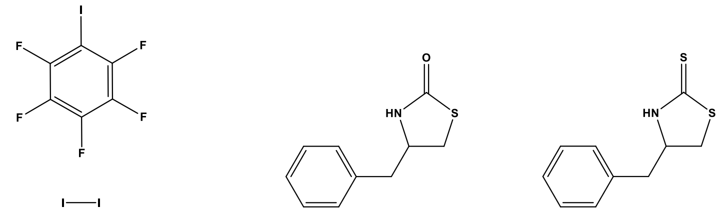

b

a. c. d.

Figure 1.5. Donors: a. I_2, b. pentafluoro-iodobenzene. Acceptors: c. 4-benzyl-1,3-thiazolidine-2-one d. 4-benzyl-1,3-thiazolidine-2-thione.

The main objectives of this thesis research are summarized below:

1. Obtain IR and VCD spectral signatures and also UV/vis and ECD spectra of several types of non-covalent interactions of the targeted chiral molecular species in solution. These species are capable of forming complexes among themselves and with solvent molecules bound together by X-bond and H-bond interactions.
2. Using some conformational search schemes and DFT theoretical calculations to identify possible structures of complexes formed with different targeted molecular species in solution and simulate their IR, VCD, UV/vis and ECD spectra.
3. Through comparisons of the experimental and theoretical spectra to identify what are the dominant non-covalent interactions in solution under varying experimental conditions.
4. Derive the most favorable geometries of the X-bond bonded species in solution and the X-bond donor and acceptor sites.

Six chapters are incorporated into this thesis. The first chapter is the introduction, which includes some background information on X-bonds. The second chapter will be on the subject of the experimental and theoretical methods used. In this chapter, I mainly will discuss some experimental and theoretical aspects of VCD spectroscopy, together with a brief review of IR, UV/vis, and NMR spectroscopic methods that have been used in this thesis to investigate the intermolecular interactions in solution. Some aspects of theoretical basics of the applied DFT calculations will also be discussed. Chapters 3, 4, 5 and 6 will be devoted to the experimental and theoretical results of interaction of the studied chiral halogen and hydrogen bond compounds with different species in the solution. The molecular systems and the goals of Chapters 3, 4, 5 and 6 are:

Chapter 3. In this chapter, halogen bonds between iodine and 4-benzyl-1,3-thiazolidine-2-one (NOS) will be studied by UV-vis, ^{1}H-NMR, IR, and vibrational circular dichroism (VCD) spectroscopy techniques.

Chapter 4. In this chapter, halogen bonds between iodine and and 4-benzyl-1,3-thiazolidine-2-thione (NSS) will be studied by UV-vis, ^{1}H-NMR, IR, and vibrational circular dichroism (VCD) spectroscopy techniques

Chapter 5. In this chapter, the balance between the formation of a halogen bond and an intermolecular hydrogen bond is explored between iodopentafluorobenzene (F_5BnI) and 4-benzyl-1,3-thiazolidine-2-one (NOS) by ^{1}H-NMR, ^{19}F-NMR, IR, and vibrational circular dichroism (VCD) spectroscopy techniques.

Chapter 6. In this chapter, the balance between the formation of a halogen bond and an intermolecular hydrogen bond is explored between iodopentafluorobenzene (F_5BnI) and 4-benzyl-1,3-thiazolidine-2-thione (NSS) by 1H-NMR, ^{19}F-NMR, IR, and vibrational circular dichroism (VCD) spectroscopy techniques.

Chapter 7 will be a conclusion chapter where the general outcome of the thesis research and future work in this research direction will be presented.

References

1. Guthrie, F., XXVIII.—On the iodide of iodammonium. *Journal of the Chemical Society* **1863,** *16* (0), 239-244.

2. Mulliken, R. S., Structures of Complexes Formed by Halogen Molecules with Aromatic and with Oxygenated Solvents. *J. Am. Chem. Soc.* **1950,** *72* (1), 600-608.

3. (a) Mulliken, R. S., Molecular Compounds and their Spectra. III. The Interaction of Electron Donors and Acceptors. *J. Phys. Chem.* **1952,** *56* (7), 801-822; (b) Mulliken, R. S., Molecular Compounds and their Spectra. II *J. Am. Chem. Soc.* **1952,** *74* (3), 811-824.

4. Hassel, O.; Hvoslef, J., The Structure of Bromine 1,4-Dioxanate. *Acta Chem. Scand.* **1954,** *8* (5), 873-873.

5. Eia, G.; Hassel, O., Structure of an Addition Compound Containing two Bromine Molecules and one Molecule of Hexamethylene Tetramine. *Acta Chem. Scand.* **1956,** *10* (1), 139-141.

6. (a) Hassel, O.; Stromme, K. O., Halogen-Molecule Bridges in Solid Addition Compounds. *Nature* **1958,** *182* (4643), 1155-1156; (b) Hassel, O.; Stromme, K. O., Crystal Structure of the 1:1 Addition Compound Formed by Acetone and Bromine. *Acta Chem. Scand.* **1959,** *13* (2), 275-280.

7. (a) Hassel, O.; Stromme, K. O., Crystal Structure of the Addition Compound 1,4-Dioxan-Chlorine. *Acta Chem. Scand.* **1959,** *13* (9), 1775-1780; (b) Hassel, O.; Hvoslef, J., Structure of an Addition Compound Containing two Molecules of Iodine Monochloride and One Molecule of 1,4-Dioxan. *Acta Chem. Scand.* **1956,** *10* (1), 138-139; (c) Hassel, O., The structure of addition compounds, especially those in which halogens act as electron-acceptors. *Proceedings of the Chemical Society of London* **1957,** (9), 250-255; (d) Hassel, O.; Romming, C., Crystal Structure of the 1:1 Molecular Compound 1,4-Dioxan, Sulphuric Acid. *Acta Chem. Scand.* **1960,** *14* (2), 398-406; (e) Romming, C., The Crystal Structure of the 1:1 Addition Compound Formed by Benzyl Sulphide and Iodine. *Acta Chem. Scand.* **1960,** *14* (10), 2145-2151; (f) Chao, G. Y.; McCullough, J. D., 1960-The refinement of the structure of the complex of iodine with 1,4 dithiane. $C_4H_8S_2.2I_2$. *Acta Crystallographica* **1960,** *13* (9), 727-732; (g) Chao, G. Y.; McCullough, J. D., 1961-The refinement of the structure of the complex of iodine with 1,4-diselenane. $C_4H_8S_2.2I_2$. *Acta Crystallographica* **1961,** *14* (9), 940-&; (h) McCullough, J. D., The structure of the compounds of iodine with 1,4 diselenane and 1,4 dithiane. *Acta Crystallographica* **1959,** *12* (10), 815-816.

8. Hassel, O., Structural Aspects of Interatomic Charge-Transfer Bonding. *Science* **1970,** *170* (3957), 497-&.

9. Lommerse, J. P. M.; Stone, A. J.; Taylor, R.; Allen, F. H., The nature and geometry of intermolecular interactions between halogens and oxygen or nitrogen. *J. Am. Chem. Soc.* **1996,** *118* (13), 3108-3116.

10. (a) Metrangolo, P.; Neukirch, H.; Pilati, T.; Resnati, G., Halogen bonding based recognition processes: A world parallel to hydrogen bonding. *Accounts Chem. Res.* **2005,** *38* (5), 386-395; (b) Rissanen, K., Halogen bonded supramolecular complexes and networks. *Crystengcomm* **2008,** *10* (9), 1107-1113.

11. Pearson, R. G., Hard and Soft Acids and Bases. *J. Am. Chem. Soc.* **1963,** *85* (22), 3533-&.

12. (a) Cametti, M.; Crousse, B.; Metrangolo, P.; Milani, R.; Resnati, G., The fluorous effect in biomolecular applications. *Chem. Soc. Rev.* **2012,** *41* (1), 31-42; (b) Cardillo, P.; Corradi, E.; Lunghi, A.; Meille, S. V.; Messina, M. T.; Metrangolo, P.; Resnati, G., The N center dot center dot center dot I intermolecular interaction as a general protocol for the formation of perfluorocarbon-hydrocarbon supramolecular architectures. *Tetrahedron* **2000,** *56* (30), 5535-5550; (c) Gilday, L. C.; Robinson, S. W.; Barendt, T. A.; Langton, M. J.; Mullaney, B. R.; Beer, P. D., Halogen Bonding in Supramolecular Chemistry. *Chem. Rev.* **2015,** *115* (15), 7118-7195; (d) Metrangolo, P.; Murray, J. S.; Pilati, T.; Politzer, P.; Resnati, G.; Terraneo, G., Fluorine-Centered Halogen Bonding: A Factor in Recognition Phenomena and Reactivity. *Cryst. Growth Des.* **2011,** *11* (9), 4238-4246; (e) Parisini, E.; Metrangolo, P.; Pilati, T.; Resnati, G.; Terraneo, G., Halogen bonding in halocarbon-protein complexes: a structural survey. *Chem. Soc. Rev.* **2011,** *40* (5), 2267-2278; (f) Politzer, P.; Murray, J. S.; Clark, T., Halogen bonding: an electrostatically-driven highly directional noncovalent interaction. *Phys. Chem. Chem. Phys.* **2010,** *12* (28), 7748-7757.

13. Politzer, P.; Lane, P.; Concha, M. C.; Ma, Y. G.; Murray, J. S., An overview of halogen bonding. *J. Mol. Model.* **2007,** *13* (2), 305-311.

14. (a) Clark, T.; Hennemann, M.; Murray, J. S.; Politzer, P., Halogen bonding: the sigma-hole. *J. Mol. Model.* **2007,** *13* (2), 291-296; (b) Politzer, P.; Murray, J. S.;

Lane, P., sigma-hole bonding and hydrogen bonding: Competitive interactions. *Int. J. Quantum Chem.* **2007,** *107* (15), 3046-3052.

15. (a) Riley, K. E.; Hobza, P., Investigations into the nature of halogen bonding including symmetry adapted perturbation theory analyses. *J. Chem. Theory Comput.* **2008,** *4* (2), 232-242; (b) Wu, J. Y.; Zhang, J. C.; Wang, Z. X.; Cao, W. L., Theoretical study on intermolecular interactions in BrF/HnX adducts. *Chem. Phys.* **2007,** *338* (1), 69-74; (c) Riley, K. E.; Hobza, P., Strength and Character of Halogen Bonds in Protein-Ligand Complexes. *Cryst. Growth Des.* **2011,** *11* (10), 4272-4278; (d) Lu, Y. X.; Zou, J. W.; Wang, Y. H.; Jiang, Y. J.; Yu, Q. S., Ab initio investigation of the complexes between bromobenzene and several electron donors: Some insights into the magnitude and nature of halogen bonding interactions. *J. Phys. Chem. A* **2007,** *111* (42), 10781-10788; (e) Murray, J. S.; Riley, K. E.; Politzer, P.; Clark, T., Directional Weak Intermolecular Interactions: sigma-Hole Bonding. *Aust. J. Chem.* **2010,** *63* (12), 1598-1607.

16. (a) Metrangolo, P.; Meyer, F.; Pilati, T.; Resnati, G.; Terraneo, G., Halogen bonding in supramolecular chemistry. *Angew. Chem.-Int. Edit.* **2008,** *47* (33), 6114-6127; (b) Fox, D.; Metrangolo, P.; Pasini, D.; Pilati, T.; Resnati, G.; Terraneo, G., Site-selective supramolecular synthesis of halogen-bonded cocrystals incorporating the photoactive azo group. *Crystengcomm* **2008,** *10* (9), 1132-1136.

17. Szell, P. M. J.; Zablotny, S.; Bryce, D. L., Halogen bonding as a supramolecular dynamics catalyst. *Nat. Commun.* **2019,** *10*, 8.

18. Gentry, C. L.; Egleton, R. D.; Gillespie, T.; Abbruscato, T. J.; Bechowski, H. B.; Hruby, V. J.; Davis, T. P., The effect of halogenation on blood-brain barrier permeability of a novel peptide drug. *Peptides* **1999,** *20* (10), 1229-1238.

19. Prelog, V., Problems in chemical topology. *Chem. Br.* **1968,** *4* (9), 382-&.

20. Sokolov, V. I., Stereochemistry of optically active compounds. Problems and prospects. *Russ. Chem. Bull.* **2001,** *50* (8), 1339-1355.

21. Cahn, R. S.; Ingold, C.; Prelog, V., Specification of Molecular Chirality. *Angew. Chem.-Int. Edit.* **1966,** *5* (4), 385-415.

22. Moss, G. P., Basic terminology of stereochemistry. *Pure Appl. Chem.* **1996,** *68* (12), 2193-2222.

23. Adams, S. S.; Bresloff, P.; Mason, C. G., Pharmacological Differences between optical isomers of Ibuprofen - Evidence for metabollic Inversion of (-)-isomer. *J. Pharm. Pharmacol.* **1976,** *28* (3), 256-257.

24. Flack, H. D.; Bernardinelli, G., Absolute structure and absolute configuration. *Acta Crystallogr. Sect. A* **1999,** *55*, 908-915.

25. Hoye, T. R.; Hamad, A. S. S.; Koltun, D. O.; Tennakoon, M. A., An NMR method for determination of configuration of beta-substituted carboxylic acids. *Tetrahedron Lett.* **2000,** *41* (14), 2289-2293.

26. Uray, G.; Verdino, P.; Belaj, F.; Kappe, C. O.; Fabian, W. M. F., Absolute configuration in 4-alkyl- and 4-aryl-3,4-dihydro-2(1H)-pyrimidones: A combined theoretical and experimental investigation. *J. Org. Chem.* **2001,** *66* (20), 6685-6694.

27. (a) Bouman, T. D.; Moscowitz, A., Optical activity of saturated ketones. *J. Chem. Phys.* **1968,** *48* (7), 3115-+; (b) Schellman, J. A., Vibrational optical-activity. *J. Chem. Phys.* **1973,** *58* (7), 2882-2886; (c) Stigter, D.; Schellman, J. A., Approximation in one-electron theory of optical rotation. *J. Chem. Phys.* **1969,** *51* (8), 3397-+; (d) Holzwart.G; Chabay, I., Optical activity of vibrational transitions: A coupled oscillator model. *J. Chem. Phys.* **1972,** *57* (4), 1632-&; (e) Faulkner, T. R.; Moscowit.A; Holzwart.G; Hsu, E. C.; Mosher, H. S., Infrared circular dichroism of carbon-hydrogen and carbon-deuterium stretching modes. Calculations. *J. Am. Chem. Soc.* **1974,** *96* (1), 252-253.

28. Holzwart.G; Hsu, E. C.; Mosher, H. S.; Faulkner, T. R.; Moscowit.A, Infrared circular dichroism of carbon-hydrogen and carbon-deuterium stretching modes. Observations. *J. Am. Chem. Soc.* **1974,** *96* (1), 251-252.

29. (a) Lipp, E. D.; Nafie, L. A., Fourier-transform infrared vibrational circular-dichroism - improvements in methodology and mid-infrared spectral results. *Appl. Spectrosc.* **1984,** *38* (1), 20-26; (b) Lipp, E. D.; Zimba, C. G.; Nafie, L. A., Vibrational circular-dichroism in the mid-infrared using fourier-transform spectroscopy. *Chem. Phys. Lett.* **1982,** *90* (1), 1-5; (c) Nafie, L. A.; Diem, M., Theory

of high-frequency differential interferometry - application to the measurement of infrared circular and linear dichroism via fourier-transform spectroscopy. *Appl. Spectrosc.* **1979,** *33* (2), 130-135; (d) Nafie, L. A.; Diem, M.; Vidrine, D. W., Fourier transform infrared vibrational circular dichroism. *J. Am. Chem. Soc.* **1979,** *101* (2), 496-498.

30. Rezac, R., Description of Halogen Bonding in SemiempiricalQuantum-Mechanical and Self-Consistent ChargeDensity-Functional Tight-Binding Methods. *J. Comput. Chem*. **2019**, 40, 1633–1642.

31. Jason T. A. Gall, Javix, T., Fan, X, Zhibo, W., Jäger, W, Xu, Y,. Rotational spectroscopy of the methyl glycidate–water complex: conformation and water and methyl rotor tunneling motions, *Phys. Chem. Chem. Phys*., **2017**, *19,* 29508–29515

CHAPTER 2

Methods

2.1 VCD Basis

Vibrational circular dichroism (VCD) is used to determine the absolute configuration of chiral molecules.[1] These molecules show vibrational optical activity (VOA). Infrared vibrational circular dichroism,[2] or VCD, and vibrational Raman optical activity,[3] or ROA, are the two forms of VOA.

Vibrational circular dichroism (VCD) is defined as the difference in absorption of the circularly polarized IR light by a chiral structure.

$$\Delta A = A_\mathrm{L} - A_\mathrm{R} \tag{2.1}$$

A_L and A_R are the corresponding absorbances of left circularly polarized (LCP) and right circularly polarized (RCP) infrared radiation.

Infrared (IR) electromagnetic radiation induces vibrational transitions in molecules. When a molecule is exposed to IR light, such a vibrational transition could happen if the energy of light matches the energy gap between the initial (Ψ_1) and final (Ψ_2) vibrational states, and there is a net change of the dipole moment as the molecule vibrates (nonzero electric transition dipole moment μ_elec).[4]

$$\mu_{elec,12} = <\Psi_1 \mid \mu_{elec} \mid \Psi_2|> \tag{2.2}$$

Ψ_1 and Ψ_2 are the wave functions related to the initial and final vibrational states (ground state g and excited state e). μ_elec represents the operator for the electric dipole moment, and μ_elec itself is the sum of the dipole moments of electrons ($\mu^\mathrm{e}_\mathrm{elec}$) and nucleus ($\mu^\mathrm{n}_\mathrm{elec}$).

$$\mu_{elec} = (\mu^e_{elec} + \mu^n_{elec}) \tag{2.3}$$

The dipole strength is the square of the transition dipole moment ($\mu_\mathrm{elec,12}$) and is denoted as $|\mu_\mathrm{elec,12}|$.[2]

$$|\mu_{elec,12}|^2 = |<\Psi_1 \mid \mu_{elec} \mid \Psi_2|>|^2 \tag{2.4}$$

The infrared absorbance of a molecule (intensity of an IR or VCD band) is directly proportional to the molar extinction coefficient ε, or the differential molar extinction coefficient Δε of the transition, where Δε and ε are dependent on dipole strength D and rotational strength R of the transition.[5]

$$D(g \rightarrow e) = <g|\mu_{\mathrm{elec}}|g> * <g|\mu_{\mathrm{elec}}|g> \qquad (2.5)$$

$$R(g \rightarrow e) = -i<g|\mu_{\mathrm{elec}}|g> * <g|\mu_{\mathrm{mag}}|g> \qquad (2.6)$$

μ_{elec} and μ_{mag} are electric and magnetic dipole moments, and μ_{mag} is also the sum of the dipole moments of electrons ($\mu^{\mathrm{e}}_{\mathrm{mag}}$) and nucleus ($\mu^{\mathrm{n}}_{\mathrm{mag}}$).

$$\mu_{mag} = (\mu^{e}_{\mathrm{mag}} + \mu^{n}_{\mathrm{mag}}) \qquad (2.7)$$

Determination of the dipole strength of a vibrational transition is performed by evaluation of the electric transition dipole moment. Determination of the rotational strength of a vibrational transition requires the determination of both the electric and magnetic transition dipole moments. Vibrational electric transition dipole moment is calculated with the Born Oppenheimer (BO) approximation and the electronic contribution of the vibrational magnetic transition dipole moment gets the value of zero,[6] which happens because the electronic contribution of the vibrational magnetic transition dipole moment is generated only by the velocities of nuclei.

However, according to the BO approximation, the velocity of a nucleus does not have any dependency on the electronic variables. Consequently, the electronic contribution of the vibrational magnetic transition dipole moment does not exist in the BO approximation. As a result, several theoretical approaches have been developed to account for the aforementioned consequence and evaluate the vibrational magnetic transition dipole moment more accurately. Some of these approaches are the fixed partial charge (FPC) model,[7] the coupled oscillator (CO) model,[8] the dynamic polarization (DP) model,[9] the localized molecular orbital model,[10] the nuclear electric shielding tensor model,[11] the vibronic coupling model,[4c] and the the magnetic field perturbation (MFP) model.[12]

2.2 Theoretical Spectra

The prediction of vibrational absorption spectra is done by choosing a geometry for the molecule and a reliable theoretical level; in this project, it is the density functional method with different basis sets. A simulation of the vibrational spectra of a chiral structure can be performed by knowing the dipole and rotational strengths. These spectra can be obtained for each conformer, and the weight of each conformer will be accounted, using the Boltzmann population distribution to acquire the final IR and VCD for a chiral compound. Having a close agreement between the simulated spectrum and the experimental one allows us to find out the absolute configuration of the chemical structure used in the experimental measurements. In general, if the majority of the measured bands and calculated ones show a relative agreement in sign and magnitude, the absolute configuration of the structure used in the simulation is the same as the structure of the measured sample. However, if the magnitudes show a relative agreement, but the signs are opposite, then the absolute configuration of the measured sample is the opposite of the chosen structure for the simulation.

An initial comparison of the IR and VCD spectra of each conformer with the measured spectra results in the identification of the one or two most contributing conformers, and these conformers are usually at the lowest calculated energy levels. Subsequently, the calculated frequencies need to be scaled by a factor of 0.96- 0.98, depending on the functional and basis set used for calculation [24]. This is due to the fact that the calculated frequencies are based on a harmonic force field, but the observed frequencies are actually anharmonic force fields. Experimental measurements are done in the solution phase, thus, the solvent causes more shifting in the observed frequencies. In the Gaussian program [25], a solvent effect can be included in the process of geometry optimization. By numbering the normal modes from low to high, frequencies of the simulated IR spectrum will be assigned to the frequencies of the measured IR spectrum, based on the relative intensities and locations of the bands. In an IR spectrum all bands are positive, and so the assignments can be done relatively quickly. However, in a VCD spectrum, where there is a reduction or intensity cancellation due to the existence of peaks with opposite signs and also a change the location of spectral peaks due to the same reason, the assigning process would be more difficult. Assigning the VCD normal modes can be done, using the similar correlation used to assign the IR peaks, and this will allow us to find out the absolute configuration of the measured sample by comparing it with the simulated spectrum. In the projects presented in this thesis, where the two were not the same, a dimerization effect and improved basis sets were utilized.

2.3 Instrumentation

There are dispersive mid-IR spectrometers and FTIR spectrometers. In the dispersive instrument, where polychromatic light from the source is dispersed by using a grating, there is significant light loss both at the entrance and exit slits of the monochromator. There is no light loss in FTIR instruments, therefore, they have a higher throughput. Besides, the measurement time is shorter in FTIR instruments because the detection of light at all wavelengths happens simultaneously; this is known as spectral multiplexing.[2b, 13] Thus, the majority of VCD instruments are Fourier transform (FT) VCD machines, with some exceptions where scanning dispersive VCD spectrometers are used.[14] Nafie in 1979 used a Nicolet 7199 FTIR machine and established the FT-VCD method for the first time.[13] He used a ZnSe photoelastic modulator (PEM) and placed that before the sample in the FTIR spectrometer to modulate the polarization of the infrared light to the LCP and RCP states. He has developed a dual-PEM device for baseline corrected spectra and to reduce artifacts.[15] All spectra were measured by an FTIR-VCD instrument, consisting of an FTIR spectrophotometer (Vertex 70, Bruker) and a VCD module (PMA 50, Bruker). The block diagram of the FTIR-VCD instrument is shown in Figure 2.1.

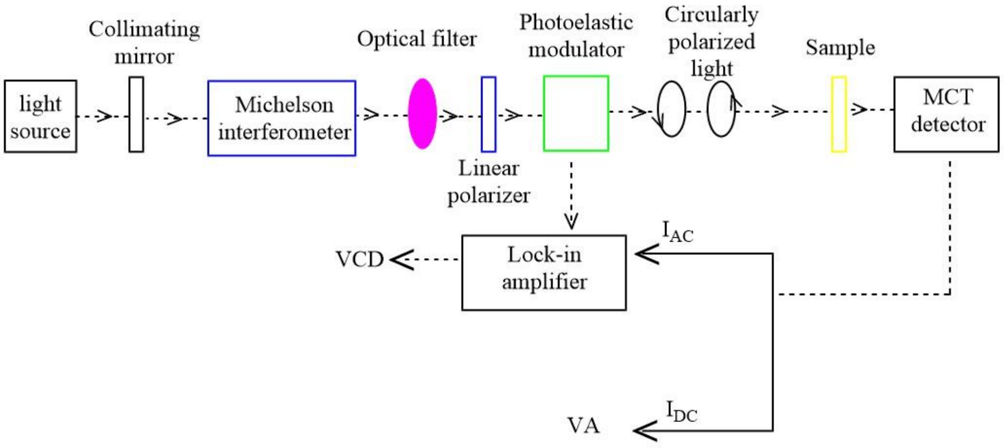

Figure 2.1. The block diagram of FTIR-VCD instrument.

IR radiation from the Globar source (silicon carbide SiC) is directed toward the center of the Michelson interferometer by a collimating mirror. The radiation from the interferometer passes through an optical filter, then is linearly polarized to constitute a single plate of polarization at an angle of 45°. The optical filter has an adjustable cut off to narrow down to the range of the VCD of interest. In this study, the upper cut off is at 1800 cm^{-1}. This beam then passes through the photoelastic modulator (PEM), which modulates the polarization between left and right circularly polarized light. The frequency of this modulation is 50 kHz to distinguish the signal and noise. The PEM of the FT-VCD machine in the lab is composed of a transparent silica bar (optical bar) attached horizontally to a piezoelectric (i.e., electricity caused by pressure) transducer that when squeezed by pressure converts this energy into voltage. The transducer is connected to a 50 kHz alternating current (AC) source. The job of the piezoelectric transducer is to establish stress in the silica bar by compressing or stretching the bar. As a result of this stress, the silica bar becomes birefringent. The polarized beam that was going to pass through the photoelastic modulator (PEM) would be either parallel or perpendicular to the modulator axis. Due to the birefringent character of the silica bar, the two directions of the beam will have different speeds through the silica bar (Figure 2.2).

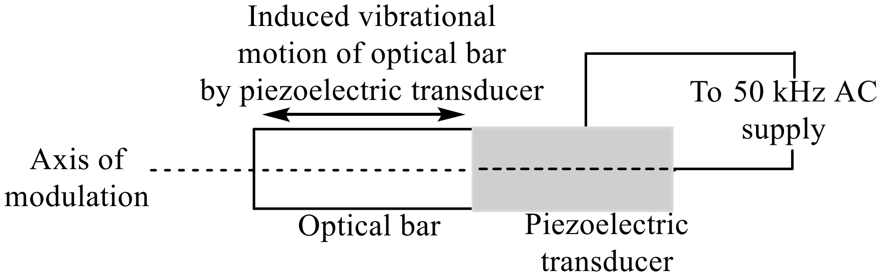

Figure 2.2. Schematic of the photoelastic modulator (PEM) used in the FT-VCD instrument.

The two directions of the beam then pass through the sample. Then, the beam intensity is converted to an electrical signal by the MCT (HgCdTe) detector that needs to be cooled down by liquid nitrogen. There are two electronic pathways at this point. One is for the measurement of the IR spectrum, and the other one has a lock-in amplifier tuned to the PEM frequency. The latter one demodulates the spectral data at that frequency and yields the VCD spectrum.[16]

In order to have a VCD spectrum with good quality, several factors need to be considered while doing the IR measurement. They are: choice of the solvent to avoid interference in the finger print region; choice of the window to avoid interaction with the solvent and to have the desired low and high cut-off region; choice of path length and sample concentration to avoid a saturation effect where the typical desired IR absorbance intensity is between 0.2–0.9 to yield a good VCD signal. This means that VCD intensities are usually four orders smaller than their parent IR intensities. Thus, absorbance intensities that approach 1.0 or above result in high VCD noise levels, and the VCD measurement will not be considered reliable. However, despite the FT-VCD set up, artifacts are common in VCD measurements and originate from birefringence in the IR lenses and applied windows and affect the outcome of LCP and RCP beams. Artifacts typically are observed in two locations, in which one is deviations of the baseline from zero and the other is the appearance of fake VCD absorption bands, even in a nonchiral or racemic environment or in the absence of the sample. Artifacts in the baseline can be removed by doing a blank VCD measurement, where only solvent and window are available. Fake VCD absorption bands are done by running the VCD on the opposite enantiomer or racemic mixture under the same condition and subtracting them from the desired VCD measurement. Nafie has utilized a dual-PEM device for a baseline correction and reduction of the artifacts.[15] The second PEM is placed after the sample, with axes parallel to the first PEM. The modulation frequency of the second PEM is set to be slightly different from that of the first PEM. The first PEM measures the VCD of the sample, which includes the initial birefringence baseline artifact, and the second PEM measures the entire birefringence artifact in the spectrum. As a result, the signal will have two PEM modulated intensities. In this design, the two PEM signals are demodulated by separate lock-in amplifiers and subtracted from each other to remove artifacts from the VCD spectrum.

2.4 Other Techniques

^{1}HNMR and UV-vis have been used widely in this thesis to assist the recognition of possible interactions between the donor and acceptor species.

Nuclear magnetic resonance (NMR) is a phenomenon in which the nuclei absorb energy in a magnetic field. NMR spectroscopy is useful to investigate intramolecular interactions in various systems[17] and is used widely in this thesis. Nuclei with an odd mass or odd atomic number have a nuclear spin, possess a magnetic moment (such as ^{1}H, or ^{13}C), and behave like tiny magnets. When these nuclei are placed in a magnetic field, they start to precess like a spinning top (Figure 2.3).

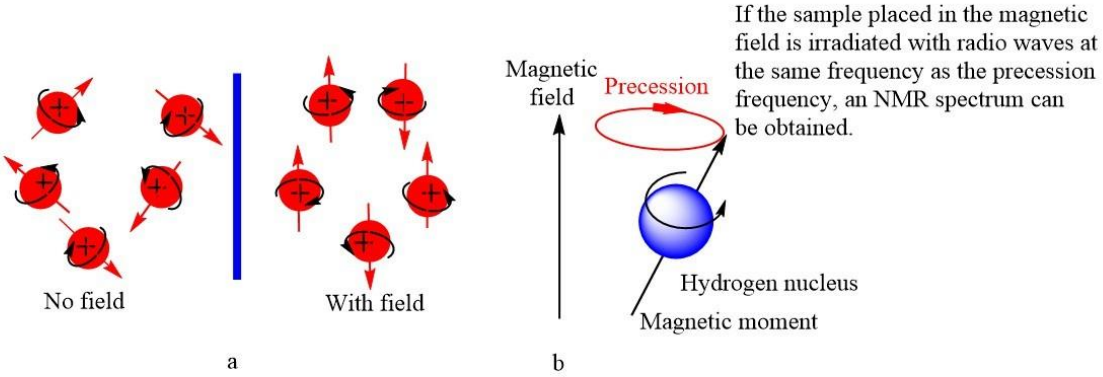

Figure 2.3. a. Nuclei line up parallel to the applied field with either spin aligned or opposite to the external magnetic field..[18] b. Precession of the ^{1}H nuclei in an external magnetic field.

The chemical shift of a nucleus contains information about the environment and availability of interactions surrounding the nucleus. The chemical shift is the frequency of the resonance of a nucleus with respect to a standard compound, which is defined to be at 0 ppm. As a result, the positions of the resonances (peaks) in an NMR spectrum are expressed relatively. For example, a peak at a chemical shift, δ, of 8 ppm is considered downfield or deshielded with respect to a peak at 3 ppm. Similarly, one could say that the peak at 3 ppm is upfield or shielded with respect to the peak at 8 ppm[19] (Figure 2.4).

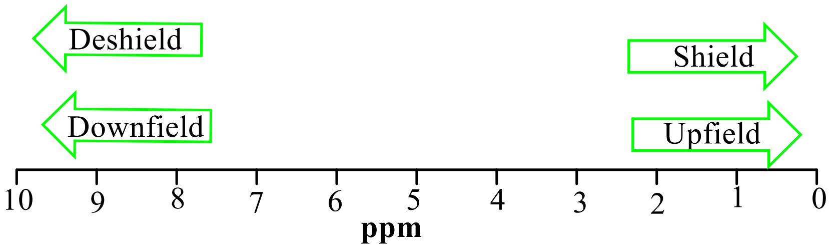

Figure 2.4. Comparison of shielding (downfield) and deshielding (upfield concepts).[18]

H-protons that are involved in hydrogen or halogen bonding typically are deshielded and appear at relatively higher chemical shift values, depending on the strength of the interaction they are involved in. But in general, the more ^{1}H becomes involved in inter- or intra-molecular interactions, the more the proton will be deshielded, and it will appear at higher chemical shifts. Relative chemical shifts of the donor and acceptor species will be studied throughout this thesis when applicable.

Since both halogen and hydrogen bonding are involved with the relative displacement of electronic charge, UV-vis spectroscopy is utilized in this work to monitor the possible effect of such displacement on electronic transitions before and after each species is involved in inter- or intra-molecular interactions. UV-vis spectroscopy is based on the absorption of ultraviolet light or visible light by chemical compounds. Upon the absorption of light, electrons move from a ground state to an excited state. The difference in the energies of the ground and the excited states is equal to the energy of the UV-vis radiation absorbed by the molecule[20] (Figure 2.5).

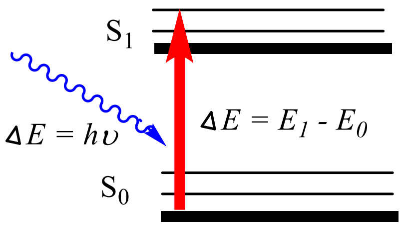

Figure 2.5. Excitation of an electron from the ground state (S_0) to the excited state (S_1).[21]

The Beer–Lambert law, which measures the transmittance of light through a sample is especially useful for obtaining information on the species, such as the relative comparison of energy gap between ground and excited states.

$$A = \varepsilon L c = \log (I_0/I) = \log (I_0/T) = -\log T \tag{2.8}$$

I_0 is intensity of the incident light, I the intensity of the transmitted light, c the sample's concentration, ε the molar absorptivity, and L the cuvette path length. The main components of a UV-vis spectrophotometer are shown in Figure 2.6.

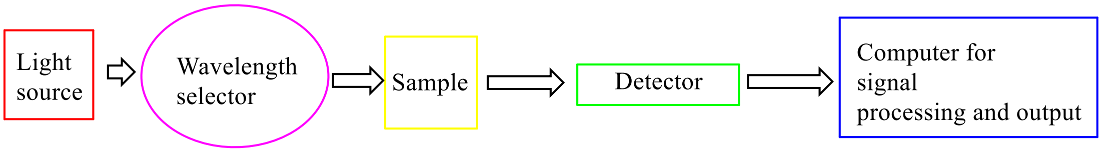

Figure 2.6. Schematic of the main components of a UV-vis spectrophotometer.[21]

In all measurements, quartz sample holders were used because they are transparent to the majority of UV light and are transparent in the range of 220 nm to 500 nm. UV-vis spectroscopy of halogens show variations in different environments and can be used to study the type of intra-molecular interactions in the solution. In general, formation of halogen bonds is accompanied by red shifts of the stretching frequencies of a dihalogen, which are due to the movement of the charge density.[22] In this study, UV-vis spectra of iodine will be studied under different conditions.

The UV-vis spectrum of I_2 has a similar pattern to that of Br_2 since they belong to the same group. The ground state in which the orbitals are filled up to the π* level will be the highest occupied molecular orbital (HOMO). The lowest energy electronic transition involves the excitation of one electron from the HOMO to the σ* lowest unoccupied molecular orbital (LUMO). The three commonly observed states are referred to as the A, B, and C states. Due to spin orbit coupling, electronic excited states will split, and several transitions would happen (Figure 2.7).[23]

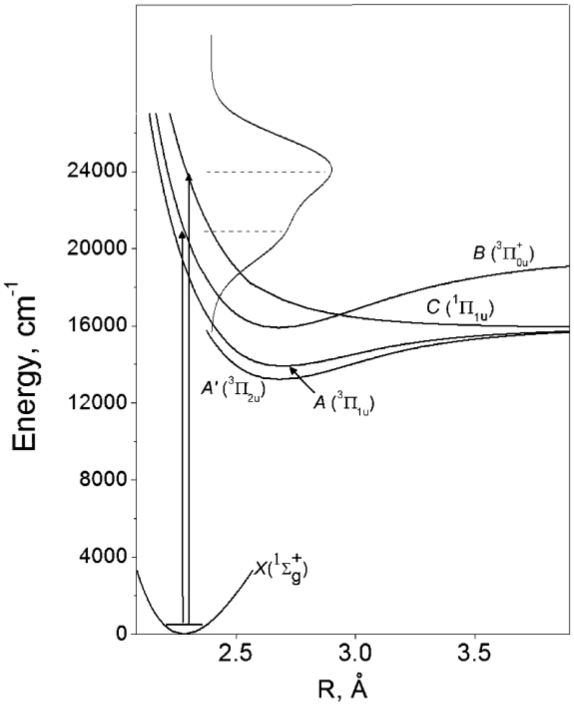

Figure 2.7. Potential energy curves for five electronic states of Br_2. [23]

As a result, two transitions were observed to B and C states. The B and C states have close energy levels. This will result in overlapping spectra. Since the B state is a triplet, the X→B transition is allowed due to spin–orbit coupling. As a result, this transition will be weak. The X→B transition will be at lower energies compared to X→C. The X→A transition would be very weak compared to the other two transitions. The peak of the bromine absorption is in the near UV range, resulting in its red color. Cl_2 shows a stronger X→C transition, mostly in the UV range, which is responsible for the pale yellow color of chlorine. I_2 blends the two transitions, appear mainly in the visible area, and are responsible for the dark purple color of iodine. Solvents can shift the shape of the halogen peaks by interacting with the excited electronic states. In this work, charge transfer complexes of I_2 will be studied for the availability of possible shifts due to the donor–acceptor interaction in charge transfer species. [23]

References

1. Nafie, L. A., Infrared and Raman vibrational optical activity: Theoretical and experimental aspects. *Annu. Rev. Phys. Chem.* **1997,** *48*, 357-386.

2. (a) Freedman, T. B.; Cao, X. L.; Dukor, R. K.; Nafie, L. A., Absolute configuration determination of chiral molecules in the solution state using vibrational circular dichroism. *Chirality* **2003,** *15* (9), 743-758; (b) Polavarapu, P. L.; He, J. T., Chiral analysis using Mid-IR vibrational CD spectroscopy. *Analytical Chemistry* **2004,** *76* (3), 61A-67A.

3. Polavarapu, P. L., The absolute configuration of bromochlorofluoromethane. *Angew. Chem.-Int. Edit.* **2002,** *41* (23), 4544-+.

4. (a) Stephens, P. J.; Lowe, M. A., Vibrational circular dichroism. *Annu. Rev. Phys. Chem.* **1985,** *36*, 213-241; (b) Stephens, P. J., Theory of vibrational circular dichroism. *J. Phys. Chem.* **1985,** *89* (5), 748-752; (c) Nafie, L. A.; Freedman, T. B., Vibronic coupling theory of infrared vibrational transitions. *J. Chem. Phys.* **1983,** *78* (12), 7108-7116; (d) Craig, D. P.; Thirunamachandran, T., A theory of vibrational circular dichroism in terms of vibronic interactions. *Mol. Phys.* **1978,** *35* (3), 825-840.

5. Schellman, J. A., Circular dichroism and optical rotation. *Chem. Rev.* **1975,** *75* (3), 323-331.

6. Faulkner, T. R.; Marcott, C.; Moscowitz, A.; Overend, J., Anharmonic effects in vibrational circular dichroism. *J. Am. Chem. Soc.* **1977,** *99* (25), 8160-8168.

7. Schellman, J. A., Vibrational optical-activity. *J. Chem. Phys.* **1973,** *58* (7), 2882-2886.

8. Holzwart.G; Chabay, I., Optical activity of vibrational transitions: A coupled oscillator model. *J. Chem. Phys.* **1972,** *57* (4), 1632-&.

9. Barnett, C. J.; Drake, A. F.; Kuroda, R.; Mason, S. F., A dynamic polarization model for vibrational optical activity and the infrared circular dichroism of a dihydro[5]helicene. *Mol. Phys.* **1980,** *41* (2), 455-468.

10. (a) Nafie, L. A.; Walnut, T. H., Vibrational circular-dichroism theory - localized molecular-orbital model. *Chem. Phys. Lett.* **1977,** *49* (3), 441-446; (b)

Walnut, T. H.; Nafie, L. A., IR absorption and Born-Oppenheimer approximation .2. vibrational circular-dichroism. *J. Chem. Phys.* **1977,** *67* (4), 1501-1510.

11. Hunt, K. L. C.; Harris, R. A., Vibrational circular dichroism and electric-field shielding tensors: A new physical interpretation based on nonlocal susceptibility densities. *J. Chem. Phys.* **1991,** *94* (11), 6995-7002.

12. (a) Stephens, P. J., Gauge dependence of vibrational magnetic dipole transition moments and rotational strengths. *J. Phys. Chem.* **1987,** *91* (7), 1712-1715; (b) Buckingham, A. D.; Fowler, P. W.; Galwas, P. A., Velocity-dependent property surfaces and the theory of vibrational circular dichroism. *Chem. Phys.* **1987,** *112* (1), 1-14.

13. Nafie, L. A.; Diem, M.; Vidrine, D. W., Fourier transform infrared vibrational circular dichroism. *J. Am. Chem. Soc.* **1979,** *101* (2), 496-498.

14. Keiderling, T. A.; Stephens, P. J., Vibrational circular dichroism of overtone and combination bands. *Chem. Phys. Lett.* **1976,** *41* (1), 46-48.

15. Nafie, L. A., Dual polarization modulation: A real-time, spectral-multiplex separation of circular dichroism from linear birefringence spectral intensities. *Appl. Spectrosc.* **2000,** *54* (11), 1634-1645.

16. Busch, K. W. B. M. A., Chiral Analysis: Instrumental aspects of chiroptical detection. **2006**.

17. Gunther, H., *NMR spectroscopy: basic principles, concepts, and applications in chemistry*. **2013**; Vol. 3rd.

18. Keeler, J,. Understanding NMR Spectroscopy. **2010**.

19. Zerbe, O. J., S., *Applied NMR spectroscopy for chemists and life scientists*. Wiley-VCH: Weinheim: 2014.

20. Skoog, D. A. H., F. James; Crouch, Stanley R., *Principles of Instrumental Analysis*. Belmont, CA: Thomson Brooks/Cole: 2007.

21. Goldenberg, D, P,. Principles of NMR Spectroscopy: An Illustrated Guide. **2016.**

22. Alkorta, I.; Rozas, I.; Elguero, J., Charge-transfer complexes between dihalogen compounds and electron donors. *J. Phys. Chem. A* **1998,** *102* (46), 9278-9285.

23. Kerenskaya, G.; Goldschleger, I. U.; Apkarian, V. A.; Janda, K. C., Spectroscopic signatures of halogens in clathrate hydrate cages. 1. Bromine. *J. Phys. Chem. A* **2006,** *110* (51), 13792-13798.

24. Palafox, MA,. The prediction of vibrational spectra: the use of scale factors. *Recent Research Developments in Physical Chemistry*. **1998**, 2 (12), 213-232.

25. M. J. F., G. W. Trucks, H. B. Schlegel, G. E. Scuseria, M. A. Robb, J. R. Cheeseman, G. Scalmani, V. Barone, B. Mennucci, G. A. Petersson, H. Nakatsuji, M. Caricato, X. Li, H. P. Hratchian, A. F. Izmaylov, J. Bloino, G. Zheng, J. L. Sonnenberg, M. Hada, M. Ehara, K. Toyo-ta, R. Fukuda, J. Hasegawa, M. Ishida, T. Nakajima, Y. Honda, O. Kitao, H. Nakai, T. Vreven, J. A. Montgomery, Jr., J. E. Peralta, F. Ogliaro, M. Bearpark, J. J. Heyd, E. Brothers, K. N. Kudin, V. N. Staroverov, R. Kobayashi, J. Normand, K. Raghavachari, A. Rendell, J. C. Burant, S. S. Iyengar, J. Tomasi, M. Cossi, N. Rega, J. M. Millam, M. Klene, J. E. Knox, J. B. Cross, V. Bakken, C. Adamo, J. Jaramillo, R. Gomperts, R. E. Stratmann, O. Yazyev, A. J. Austin, R. Cammi, C. Pomelli, J. W. Ochterski, R. L. Mar-tin, K. Morokuma, V. G. Zakrzewski, G. A. Voth, P. Sal-vador, J. J. Dannenberg, S. Dapprich, A. D. Daniels, Ö. Farkas, J. B. Foresman, J. V. Ortiz, J. Cioslowski, and D. J. Fox, Gaussian 09, Revision D.01. Gaussian, I., Wallingford CT, Ed. 2009.

CHAPTER 3

Interactions of Iodine with 4-benzyl-1,3-thiazolidine-2-one in Solution

3.1 Introduction

Intermolecular interactions have important roles in biological processes, such as proteins and their interactions with DNA and ligands[1] and in chemical reactions.[2] Such interactions have been studied by various tools, such as NMR,[3] fluorescence spectroscopy,[3b] X-ray,[4] Infrared spectroscopy,[5] vibrational circular dichroism spectroscopy (VCD),[6] and quantum chemical calculations.[7] Such interactions are considered to be non-covalent and are different from covalent interactions.[8] They are responsible for the rise in versatility of chemical structures.[8] According to Pauling,[8] the main difference between the two is that strong attraction forces in covalent bonding causes atoms to overcome the repulsion between positive nuclei and share their electrons to be attracted by the involved nuclei. Non-covalent interactions, on the other hand, can be viewed as electrostatic interactions between species that possess permanent and/or temporary charges. However, there are always other components contributing to this effect, without which non-covalent interactions would be deficient. They are induction between a permanent charge and an induced charge, repulsion between electron densities, and dispersion between induced dipoles on polarizable species.[2a] Such components are responsible for hydrogen bonding, halogen bonding, Van der Waals forces, and steric repulsions that are categorized as non-covalent interactions.

Hydrogen bonding, which is prevalent in biological systems[9] occurs among different molecular species. Wang et al. in 2016 found out that hydrogen bonding to carbonyl of nitrogen-pyramidalized bicyclic beta-proline derivatives would switch the nitrogen-pyramidalization direction and consequently make it detectable by VCD spectroscopy.[10]

Vibrational circular dichroism (VCD) is defined as the difference in absorption of the left and right circularly polarized IR light by a chiral structure and is sensitive to conformational changes, such as one caused by hydrogen bonding.[11] The VCD spectra of such systems, which are sensitive to structural dynamics are affected by the temperature and anharmonicity effects.[12] Xia et al. have used the Generalized Coupled Oscillator (GCO) model to study the rotational strength of vibrational transitions to reach a higher agreement between the experimental and the simulated spectra in the study of inter- and intra-hydrogen bond interactions in benzyl α-hydroxysilane.[12] Molecular dynamics is the other approach to account for this structural dynamics and the quest for the proper conformers.[13]

Xu et al. proposed that water bonds to the chiral glycidol through hydrogen bonding in a series of insertion conformers and becomes optically active.[14] Sugeta et al. found out that most of the molecules of a solution of 1,2-diols and -methoxyalcohols are involved in the intramolecular hydrogen bonding.[15] A pevious study on 2,2-dimethyl-1,3-dioxolane-4-methanol revealed that lower temperatures of 10 °C and 3 °C would be preferable for the observation of intra- and inter-molecular hydrogen bonds in this molecule, and as the temperature increased to 50 °C and 60 °C the intermolecular hydrogen bond peak almost disappeared in the O-H stretching region of the infrared spectrum.[16] Various systems for the formation of hydrogen bonds made IUPAC to propose a definition for hydrogen bonding in 2011.[17] "The hydrogen bond is an attractive interaction between a hydrogen atom from a molecule or a molecular fragment X–H, in which X is more electronegative than H, and an atom or a group of atoms in the same or a different molecule, in which there is evidence of bond formation."[17] As such, a hydrogen bond should be depicted as X–H...Y–Z. The three dots denote that the hydrogen bond, X–H, is the hydrogen bond donor and the Y that is bonded to Z represents the acceptor; it could be an atom, an anion, a fragment, or a molecule. Electrostatic and dispersion forces are considered the sole components of this type of interaction.

A halogen bond is represented as XB and denoted as R–X...Y. R–X is the halogen bond donor (Lewis acid), such as I_2 and Br_2, Y is the halogen bond acceptor (Lewis base); it could be an anion (halides or oxyanions), a system (double or triple bonds), or neutral (amine or pyridine). X is any electron deficient halogen atom, and R is an atom or a group covalently bonded to X. As a result, two distinctive electrostatic regions appear around the R–X bond:[18] a negatively charged belt orthogonal to the R–X bond and a depleted electron density cap on the elongation of R–X bond[19] on the halogen atom. Politzer named the electron deficient area the σ-hole.[18a] Politzer and his co-workers performed a B3LYP natural bond analysis on CF_3Cl, CF_3Br, and CF_3I. Their results show that the electronic configuration of Cl, Br, and I were $s^2p_x^2p_y^2p_z^1$. The electrons in $s^2p_x^2p_y^2$ surround the R–X bond with a negative electrostatic charge. The outer region of the R–X bond has a diminished electron density and is denoted as σ-hole. Nyburg and Faerman[20] used the Cambridge Structural Database to study the van der Waals atomic radii of N, O, F, S, Cl, Se, Br (R), and I bonded to carbon. They found out that in all cases, except for N and O, van de Waals shapes were spheroidal, with the shorter length along the R–C bond. They described this effect as "polar flattening". This anisotropic distribution of electron density forms a nucleophilic and an electrophilic region around the halogen atom[19] (Figure3.1).

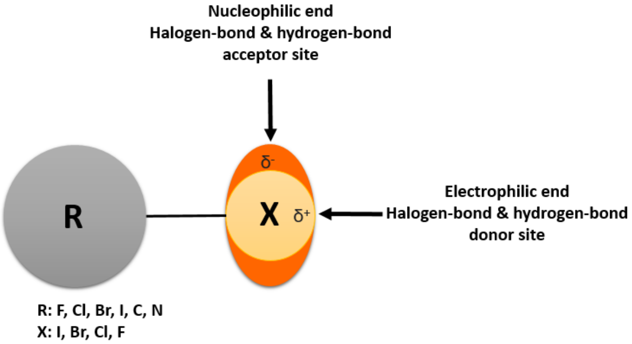

Figure 3.1. Anisotropic distribution of electron density around halogen atom.

Herein we cautiously have chosen a system in which halogen bonding, hydrogen bonding, and π bonding sites would be able to compete in solution together. The purpose of such a study is to evaluate the strength and the possibility of formation of halogen bonds from different acceptor sites in the relevant molecules. Such a study provides valuable insights into the intra-molecular interactions involving a dihalide and a carbonyl electron rich site of 4-benzyl-1,3-thiazolidine-2-one, abbreviated as NOS (Figure2.2).

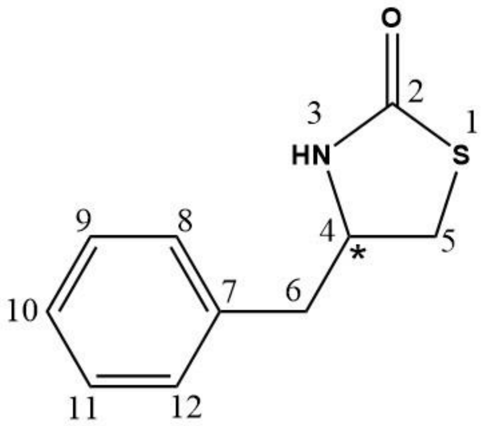

Figure 3.2. Chemical structure of 4-benzyl-1,3-thiazolidine-2-one (NOS).

4-benzyl-1,3-thiazolidine-2-one has two π bond systems that could be the σ-hole acceptor in the interaction with molecular iodine. 4-benzyl-1,3-thiazolidine-2-one can form hydrogen bonds in the solution so we would be able to compare the strength of the halogen with hydrogen bond in the solution. To reduce the interference with the solvents, chloroform and carbon tetrachloride have been chosen as the solvent throughout the study. This system, due to its size, would be suitable for ab-initio and DFT studies. In order to measure the VCD signals one must use one enantiomeric form of the analyte only. Thus throughout all the measurements only enantio-pure forms of NOS was utilized.

3.2 Experimental and Theoretical Details

4-benzyl-1,3-thiazolidine-2-one was purchased from Astatech. ^{1}H-NMR spectra of this compound were recorded on a Bruker (400 MHz) spectrometer to confirm the purity of reagents. VA and VCD spectra were measured using a Bruker FTIR (Vertex 70) spectrometer equipped with a PMA 50 module for VCD measurements.[21] The data were collected at 4 cm^{-1} resolution in the wavenumber region of 1700–1100 cm^{-1}, using a liquid nitrogen cooled MCT detector for a period of 5 h (~4300 scans per hour). Solutions of 0.258 M enantio-pure S-NOS in $CDCl_3$, 0.096 M of NOS in $CDCl_3$ (this solution existed as a mixture with I_2), were used for the VA and VCD measurements. The solution samples were placed between a pair of BaF_2 windows with a path-length of 0.1 mm. A solution with the same concentration is used to carry out the UV-vis measurements. UV-vis measurements were carried out on a Hewlett Packard 8453 spectrometer with a 1 mm cell. The Gaussian 09 program package[22] was used for all geometrical searches and optimizations, harmonic frequency calculations, and VA and VCD intensity predictions using density functional theory (DFT).[23] A Becke three parameters, Lee-Yang-Parr, functional (B3LYP)[23] and 6-311++G(d,p)[24] was used for the calculations. The polarizable continuum model (PCM) was used to account for the bulk solvent environment[25] of $CDCl_3$. A Lorentzian line shape with a half-width at half-height of 4 cm^{-1} was used for the simulations of VA and VCD spectra.

3.3 Results and Discussions

3.3.1 Conformers of the NOS

Rotation of the phenyl ring around the axis of C_6-C_7 bond, rotation of the 5-membered ring around the axis of C_4-C_6 bond and scanning the dihedral angle of N-C_4-C_6-C_7 yielded three conformers gauche-, gauche+ and syn. This rotation was in a relaxed mode and no other angles were fixed. Figure 3.3 illustrates the Newman projection of the obtained conformers. These conformers are different in terms of the types of gauche interactions with C_7.

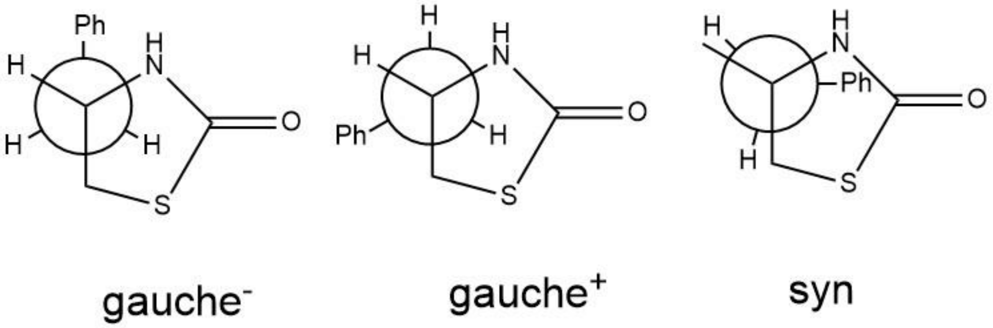

Figure 3.3. Newman projection of conformers of 4-benzyl-1,3-thiazolidine-2-one (NOS).

The volume of groups in the gauche interactions account for the relative stability of the conformers (Figure 3.4).

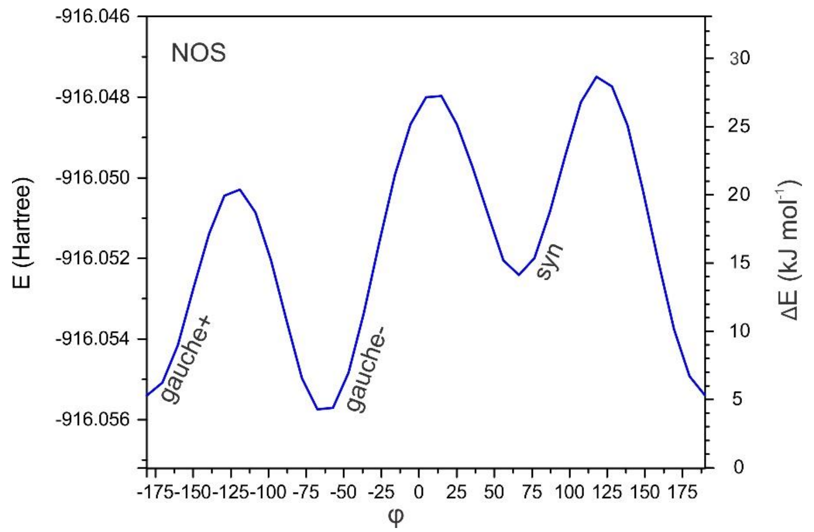

Figure 3.4. Chemical relative stability of conformers of NOS in kJ.mol^{-1} NOS and in Hartrees. φ is the dihedral angle of N-C_4-C_6-C_7 scanned over 360°. Energy of the conformer with the lowest energy is defined as zero.

The gauche- conformer is 1.2 kJ mol^{-1} and 9.9 kJ .mol^{-1} more stable than the gauche+ and syn conformers, respectively. Such an energy gap has made gauche- conformer with the highest Boltzmann population (Table 3.1).

Table 3.1 Relative Energies and Boltzmann Distribution of Conformers of NOS

Conformer	ΔE (kJ .mol^{-1})	%Boltzmann Distribution (298 K)
gauche-	0	64.8
gauche+	1.2	34.2
syn	9.9	0.1

3.3.2 ^{1}H-NMR and UV-vis Study of NOS Interacting with I_2

To evaluate the interactions between I_2 and NOS, we first carried out UV-vis and ^{1}H-NMR titrations. Since NOS can be dissolved well in $CDCl_3$, while I_2 dissolves only moderately,[26] we performed the titration by adding the I_2 in $CDCl_3$ solution to the concentrated 0.258 M NOS in $CDCl_3$ solutions dropwise. ^{1}H-NMR data showed that the proton attached to nitrogen underwent shielding from 6.1 ppm to 5.8 ppm upon increasing the concentration of iodine solution. The UV-vis titration experiments, on the other hand, exhibit a much different behavior for the two systems. In the UV-vis titration of NOS with iodine (Figure 3.5) the iodine $\pi_g^* \rightarrow \sigma_u^*$ transition at 512 nm shows no change in its position at all.

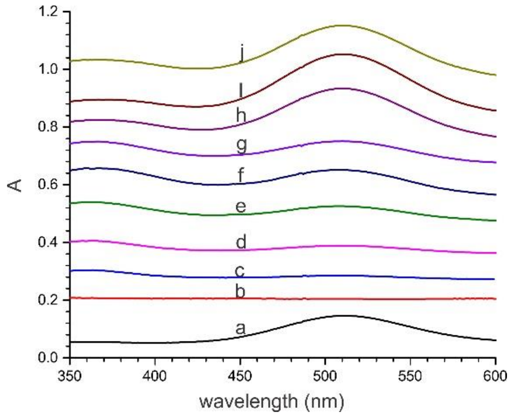

Figure 3.5. Iodine absorption band in titration of NOS with I_2 in $CDCl_3$. a: I_2 b: NOS c: $[I_2]$ = 1/6[NOS] d: $[I_2]$ =1/5[NOS] e: $[I_2]$ =1/4[NOS] f: $[I_2]$ =1/3[NOS] g: $[I_2]$ =1/2[NOS] h: $[I_2]$ =[NOS] i: $[I_2]$ =1.5[NOS] j: $[I_2]$ = 2[NOS] = 0.516 M. [] refers to the relative concentration of each species in the bracket.

To understand what exactly is going on in such mixed solutions with NOS and I_2 in $CDCl_3$, we decided to examine their IR and VCD spectra, aided with ab initio calculations.

Iodine, being a halogen-bond donor, acts as an electron acceptor. Under no such Lewis acid/base interaction, iodine shows its $\pi_g^* \rightarrow \sigma_u^*$ transition at 512 nm in $CDCl_3$. Upon interaction with a halogen-bond acceptor (Lewis base) this transition will show a blue shift due to the increase gap between σ^* and π^* orbitals. Greenwood and Earnshaw[27] suggested that, without any coordinating agent, the energy gap between HOMO (π_g^*) and LUMO (σ_u^*) remains unchanged. However, a halogen bond acceptor (Lewis base) can donate an electron to σ_u^* and cause a blue shift in the electronic transition (Figure 3.6).

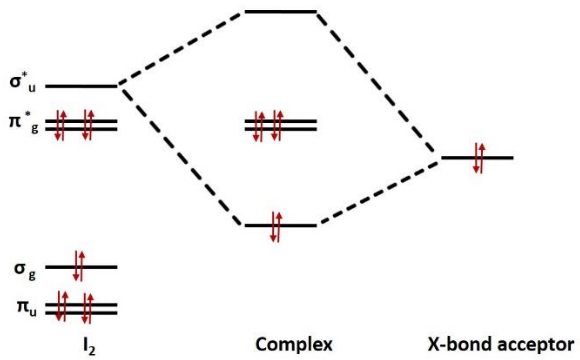

Figure 3.6. Schematic molecular orbital energy diagram of iodine formed from 5P orbitals (π_u, σ_g, π_g^*, σ_u^*) and the effect of a halogen bond interaction on the $\pi_g^* \rightarrow \sigma_u^*$ transition. The energy gap between π_g^* and σ_u^* increases after halogen bond interaction.[27]

3.3.3 IR Study of NOS-iodine Interaction

IR titration spectra of NOS with iodine in $CDCl_3$ are summarized in Figure 3.7 and Figure 3.8 for the carbonyl stretching frequency (1620 cm^{-1}–740 cm^{-1}) and the NH stretching frequency (3150 cm^{-1}–3450 cm^{-1}), respectively. Stepwise addition of iodine to the NOS solution demonstrates a blue shift of carbonyl stretching frequency from 1681 cm^{-1} to 1684 cm^{-1}. Simultaneously, in the NH stretching region, two bands are observed as a result of N-H being/not being involved in the hydrogen bonding. These are a broader band around 3225 cm^{-1} and a narrower band at 3410 cm^{-1}. As one added more drops by I_2 in $CDCl_3$, the broad peak at 3225 cm^{-1} seems to diminish in solution I.

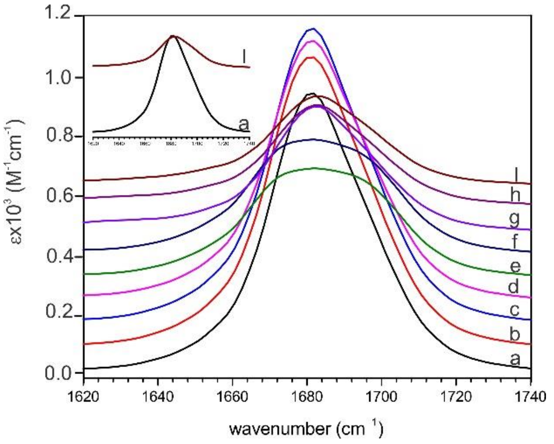

Figure 3.7. Gradual shift in the carbonyl stretching frequency upon stepwise addition of iodine to NOS solution in $CDCl_3$. a: NOS b: $[I_2] = 1/6[NOS]$ c: $[I_2] = 1/5[NOS]$ d: $[I_2] = 1/4[NOS]$ e: $[I_2] = 1/3[NOS]$

f: [I_2] = 1/2[NOS] g: [I_2] = [NOS] h: [I_2] = 1.5[NOS] i: [I_2] = 2[NOS]. [NOS]$_a$ = 0.258M [NOS]$_I$ = 0.096.

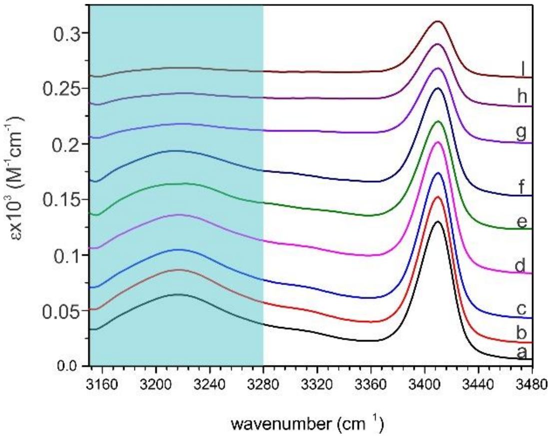

Figure 3.8. Gradual NH stretching region of NOS. At higher concentrations of iodine solution monomeric form of NOS is preferred. a: NOS b: [I_2] = 1/6[NOS] c: [I_2] = 1/5[NOS] d: [I_2] = 1/4[NOS] e: [I2] =1/3[NOS] f: [I_2] = 1/2[NOS] g: [I_2]= [NOS] h: [I_2] 1.5[NOS] i: [I_2] = 2[NOS]. [NOS]$_a$= 0.258M. [NOS]$_I$ = 0.096.

Since the broad band at 3225 cm^{-1} strongly resembles those reported for the H-bonded NH stretching band before,[28] direction dilution experiments also were carried out without iodine under the same condition as before. Interestingly, the stretching frequency of carbonyl group showed the same value of blue shift upon diluting the solution from 0.258M to 0.096M. This slight blue shift is the result of partial charge transfer from carbonyl π^* orbital to antibonding orbital of N-H moiety on NOS molecule. The broad peak at N-H stretching frequency region also disappeared upon diluting the system under the same condition. This broad peak now can be attributed to the formation of a dimer between two NOS units (Figure 3.9).

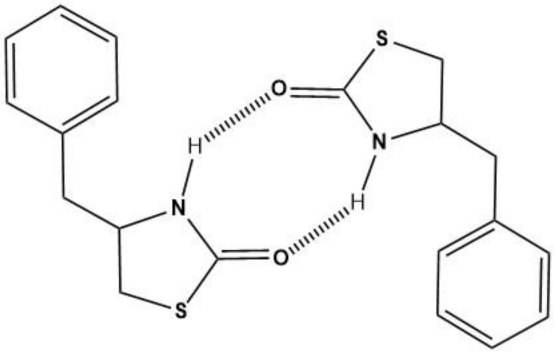

Figure 3.9. Structure of the dimer of NOS.

The relative location of the N-H stretching frequencies of the monomer and dimer was confirmed further by the calculated infrared spectra of each optimized structure (Figure 3.10).

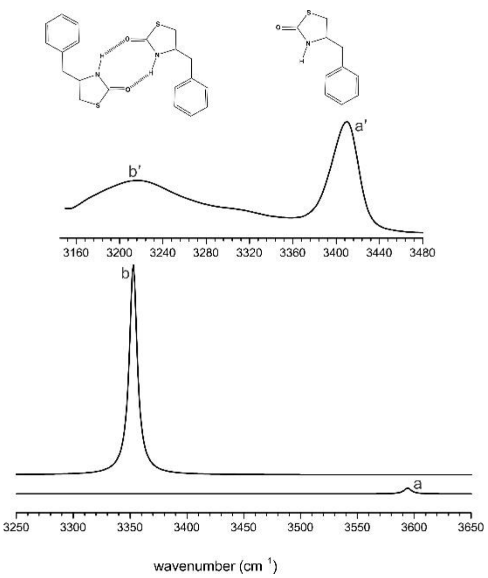

Figure 3.10. N-H stretching frequencies of monomer (a) and dimer (b) of gauche - acquired via B3LYP 6-311++G(d,p) and their experimental counterparts b' and a' respectively.

3.3.4 VCD Study of NOS

A relative VCD study of NOS-iodine was done at the same level of concentration as the NOS. Figure 3.11 shows the infrared and VCD spectrum of NOS and NOS-iodine solution.

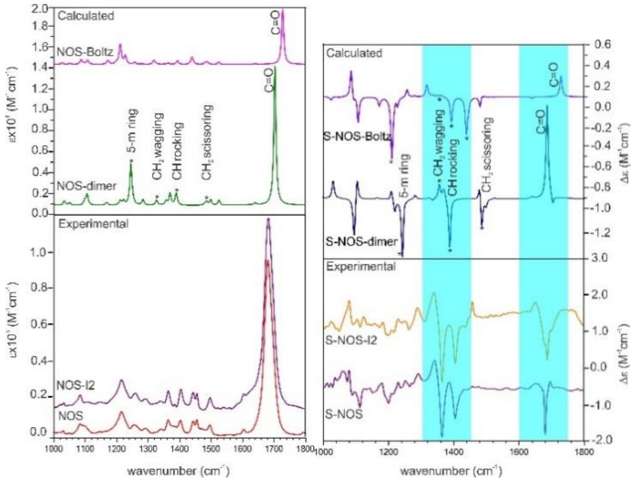

Figure 3.11. N- Superimposed experimental and calculated IR (left) and VCD (right) of NOS and NOS-iodine showing selected functionalities involved in the range of 1000 cm^{-1}-1800 cm^{-1}.

Since iodine and NOS do not have a significant interaction, we would not expect a drastic change between the IR spectra of NOS before and after adding iodine. Knowing the identity of the IR bands allows us to find out which are active in VCD experiments. Some of these peaks are shown in the IR spectrum of Figure 3.11. Due to the insignificant interaction between iodine and NOS, the VCD of NOS does not differ comparably after adding iodine. However, some of the IR and VCD such as CH_2 wagging, CH rocking, and vibrational modes involving the 5-membered ring were produced successfully in the calculated data.

The energy of interaction of formation of dimer for NOS molecule and the formation of a halogen bond interaction between NOS and iodine also is calculated (Table 3.2).

Table 3.2 Energy of Interaction of Formation of Dimer for Two NOS Molecules and Formation of Halogen Bond Interaction Between NOS and Iodine

Species	E_{int} (KJ mol^{-1})
$(g\text{-}NOS)_2$	-37.3 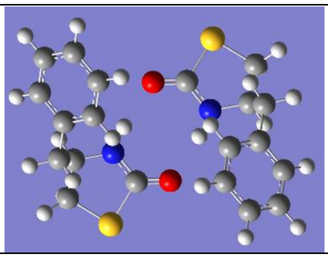
$(g\text{-}NOS)\text{-}I_2$	-28.2 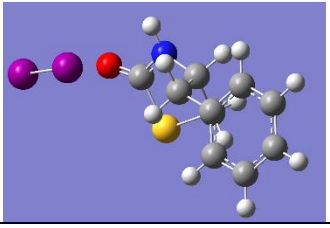

3.4 Conclusion

Based on the experimental UV-vis and IR studies of NOS with iodine, it was observed that formation of a halogen bond is not significant between NOS and iodine. Instead, formation of a dimer by a hydrogen bond is dominant to the halogen bond interaction.

The outcome of such competition is also proven by our calculated data (Table 3.2). The lower value of the energy of interaction of the NOS dimer shows the relative stability of this structure compared to NOS-I_2.

3.5 References

1. (a) Bruinsma, R. F., Physics of protein-DNA interaction. *Physica A* **2002,** *313* (1-2), 211-237; (b) Degennes, P. G., Interactions between polymers and surfactants. *J. Phys. Chem.* **1990,** *94* (22), 8407-8413; (c) Cabane, B.; Duplessix, R., Decoration of semidilute polymer solutions with surfactant micelles. *Journal De Physique* **1987,** *48* (4), 651-662; (d) Cabane, B.; Duplessix, R., Organization of surfactant micelles adsorbed on a polymer molecule in water : a neutron scattering study. *Journal De Physique* **1982,** *43* (10), 1529-1542; (e) Kekicheff, P.; Cabane, B.; Rawiso, M., Macromolecules dissolved in a lamellar lyotropic mesophase. *Journal of Colloid and Interface Science* **1984,** *102* (1), 51-70.

2. (a) Hunter, C. A., Quantifying intermolecular interactions: Guidelines for the molecular recognition toolbox. *Angew. Chem.-Int. Edit.* **2004,** *43* (40), 5310-5324; (b) Singh, R. N.; Baboo, V.; Rawat, P.; Gupta, V. P., Studies on molecular weaker interactions, spectroscopic analysis and chemical reactivity of synthesized ethyl 3,5-dimethyl-4- 3-(2-nitro-phenyl)-acryloyl -1H-pyrrole-2-carboxylate through experimental and quantum chemical approaches. *J. Mol. Struct.* **2013,** *1037*, 338-351.

3. (a) Parks, J. S.; Cistola, D. P.; Small, D. M.; Hamilton, J. A., Interactions of the carboxyl group of oleic-acid with bovine serum-albumin - a c-13 nmr-study. *J. Biol. Chem.* **1983,** *258* (15), 9262-9269; (b) Sahu, P. K.; Nanda, R.; Seth, S.; Ghosh, A.; Sarkar, M., Nuclear magnetic resonance, fluorescence correlation spectroscopy and time-resolved fluorescence anisotropy studies of intermolecular interactions in bis(1-methyl-1H-imidazol-3-ium-3-yl)dihydroborate bis (trifluoromethylsulfonyl)amide and its mixtures with various cosolvents. *Chem. Phys. Lett.* **2016,** *661*, 100-106; (c) Sethio, D.; Raggi, G.; Lindh, R.; Erdelyi, M., Halogen Bond of Halonium Ions: Benchmarking DFT Methods for the Description of NMR Chemical Shifts. *J. Chem. Theory Comput.* **2020,** *16* (12), 7690-7701; (d) von der Heiden, D.; Vanderkooy, A.; Erdelyi, M.,

Halogen bonding in solution: NMR spectroscopic approaches. *Coordination Chemistry Reviews* **2020,** *407*; (e) Bryce, D. L., Preparation Strategies and Solid-State NMR Characterization of Supramolecular Architectures based on Halogen Bonds, Chalcogen Bonds, and Pnictogen Bonds. *Acta Crystallographica a-Foundation and Advances* **2021,** *77*, C252-C252.

4. Gavezzotti, A., Comparing the strength of covalent bonds, intermolecular hydrogen bonds and other intermolecular interactions for organic molecules: X-ray diffraction data and quantum chemical calculations. *New J. Chem.* **2016,** *40* (8), 6848-6853.

5. Tsai, C. E.; Hwang, B. J., Intermolecular interactions between methanol/water molecules and Nafion (TM) membrane: An infrared spectroscopy study. *Fuel Cells* **2007,** *7* (5), 408-416.

6. Mazzeo, G.; Abbate, S.; Longhi, G.; Castiglioni, E.; Villani, C., Vibrational Circular Dichroism (VCD) Reveals Subtle Conformational Aspects and Intermolecular Interactions in the Carnitine Family. *Chirality* **2015,** *27* (12), 907-913.

7. Lewis, G. N., The atom and the molecule. *J. Am. Chem. Soc.* **1916,** *38*, 762-785.

8. Pauling, L., *The Nature of the Chemical Bond and the Structure of Molecules and Crystals: An Introduction to Modern Struc-tural Chemistry*. Cornell University Press: 1960.

9. (a) Hobza, P.; Zahradnik, R., Intermolecular interactions between medium-sized systems. Nonempirical and empirical calculations of interaction energies. Successes and failures. *Chem. Rev.* **1988,** *88* (6), 871-897; (b) Jeffrey, G. A.; Saenger, W., *Hydrogen bonding in biological structures*. 1991; p XIV+569P-XIV+569P.

10. Wang, S.; Taniguchi, T.; Monde, K.; Kawahata, M.; Yamaguchi, K.; Otani, Y.; Ohwada, T., Hydrogen bonding to carbonyl oxygen of nitrogen-pyramidalized amide - detection of pyramidalization direction preference by vibrational circular dichroism spectroscopy. *Chem. Commun.* **2016,** *52* (21), 4018-4021.

11. (a) Magyarfalvi, G.; Tarczay, G.; Vass, E., Vibrational circular dichroism. *Wiley Interdiscip. Rev.-Comput. Mol. Sci.* **2011,** *1* (3), 403-425; (b) Gobi, S.; Vass, E.;

Magyarfalvi, G.; Tarczay, G., Effects of strong and weak hydrogen bond formation on VCD spectra: a case study of 2-chloropropionic acid. *Phys. Chem. Chem. Phys.* **2011,** *13* (31), 13972-13984.

12. Xia, Y. Y.; Koenis, M. A. J.; Collados, J. F.; Ortiz, P.; Harutyunyan, S. R.; Visscher, L.; Buma, W. J.; Nicu, V. P., Regional Susceptibility in VCD Spectra to Dynamic Molecular Motions: The Case of a Benzyl -Hydroxysilane. *ChemPhysChem* **2018,** *19* (5), 561-565.

13. Kwac, K.; Lee, K. K.; Han, J. B.; Oh, K. I.; Cho, M., Classical and quantum mechanical/molecular mechanical molecular dynamics simulations of alanine dipeptide in water: Comparisons with IR and vibrational circular dichroism spectra. *J. Chem. Phys.* **2008,** *128* (10), 13.

14. Yang, G. C.; Xua, Y. J., Probing chiral solute-water hydrogen bonding networks by chirality transfer effects: A vibrational circular dichroism study of glycidol in water. *J. Chem. Phys.* **2009,** *130* (16), 9.

15. Yamamoto, K.; Nakao, Y.; Kyogoku, Y.; Sugeta, H., Vibrational circular dichroism in hydrogen bond systems: Part III. Vibrational circular dichroism of the OH stretching vibrations of 1,2-diols and β-methoxyalcohols. *J. Mol. Struct.* **1991,** *242*, 75-86.

16. Nakao, Y.; Kyogoku, Y.; Sugeta, H., Vibrational circular-dichroism in hydrogen-bond systems .2. vibrational circular-dichroism of the oh stretching vibration in 2,2-dimethyl-1,3-dioxolane-4-methanol. *J. Mol. Struct.* **1986,** *146*, 85-90.

17. (a) Arunan, E.; Desiraju, G. R.; Klein, R. A.; Sadlej, J.; Scheiner, S.; Alkorta, I.; Clary, D. C.; Crabtree, R. H.; Dannenberg, J. J.; Hobza, P.; Kjaergaard, H. G.; Legon, A. C.; Mennucci, B.; Nesbitt, D. J., Definition of the hydrogen bond (IUPAC Recommendations 2011). *Pure Appl. Chem.* **2011,** *83* (8), 1637-1641; (b) Arunan, E.; Desiraju, G. R.; Klein, R. A.; Sadlej, J.; Scheiner, S.; Alkorta, I.; Clary, D. C.; Crabtree, R. H.; Dannenberg, J. J.; Hobza, P.; Kjaergaard, H. G.; Legon, A. C.; Mennucci, B.; Nesbitt, D. J., Defining the hydrogen bond: An account (IUPAC Technical Report). *Pure Appl. Chem.* **2011,** *83* (8), 1619-1636.

18. (a) Clark, T.; Hennemann, M.; Murray, J. S.; Politzer, P., Halogen bonding: the sigma-hole. *J. Mol. Model.* **2007,** *13* (2), 291-296; (b) Murray, J. S.; Lane, P.; Politzer, P., Expansion of the sigma-hole concept. *J. Mol. Model.* **2009,** *15* (6), 723-729; (c) Politzer, P.; Murray, J. S.; Clark, T., Halogen bonding and other sigma-hole interactions: a perspective. *Phys. Chem. Chem. Phys.* **2013,** *15* (27), 11178-11189.

19. Cavallo, G.; Metrangolo, P.; Milani, R.; Pilati, T.; Priimagi, A.; Resnati, G.; Terraneo, G., The Halogen Bond. *Chem. Rev.* **2016,** *116* (4), 2478-2601.

20. Nyburg, S. C.; Faerman, C. H., A revision of van der Waals atomic radii for molecular crystals: N, O, F, S, Cl, Se, Br and I bonded to carbon. *Acta Crystallographica Section B-Structural Science* **1985,** *41* (AUG), 274-279.

21. Losada, M.; Xu, Y., Chirality transfer through hydrogen-bonding: Experimental and ab initio analyses of vibrational circular dichroism spectra of methyl lactate in water. *Phys. Chem. Chem. Phys.* **2007,** *9* (24), 3127-3135.

22. M. J. Frisch., G. W. Trucks, H. B. Schlegel, G. E. Scuseria, M. A. Robb, J. R. Cheeseman, G. Scalmani, V. Barone, B. Mennucci, G. A. Petersson, H. Nakatsuji, M. Caricato, X. Li, H. P. Hratchian, A. F. Izmaylov, J. Bloino, G. Zheng, J. L. Sonnenberg, M. Hada, M. Ehara, K. Toyota, R. Fukuda, J. Hasegawa, M. Ishida, T. Nakajima, Y. Honda, O. Kitao, H. Nakai, T. Vreven, J. A. Montgomery, Jr., J. E. Peralta, F. Ogliaro, M. Bearpark, J. J. Heyd, E. Brothers, K. N. Kudin, V. N. Staroverov, R. Kobayashi, J. Normand, K. Raghavachari, A. Rendell, J. C. Burant, S. S. Iyengar, J. Tomasi, M. Cossi, N. Rega, J. M. Millam, M. Klene, J. E. Knox, J. B. Cross, V. Bakken, C. Adamo, J. Jaramillo, R. Gomperts, R. E. Stratmann, O. Yazyev, A. J. Austin, R. Cammi, C. Pomelli, J. W. Ochterski, R. L. Martin, K. Morokuma, V. G. Zakrzewski, G. A. Voth, P. Salvador, J. J. Dannenberg, S. Dapprich, A. D. Daniels, Ö. Farkas, J. B. Foresman, J. V. Ortiz, J. Cioslowski, and D. J. Fox, Gaussian 09, Revision D.01. Gaussian, I., Wallingford CT, Ed. 2009.

23. (a) Becke, A. D., Density-functional thermochemistry. III. The role of exact exchange. *J. Chem. Phys.* **1993,** *98* (7), 5648-5652; (b) Becke, A. D., Density-functional exchange-energy approximation with correct asymptotic behavior. *Physical Review A* **1988,** *38* (6), 3098-3100; (c) Lee, C. T.; Yang, W. T.; Parr, R. G.,

Development of the Colle-Salvetti correlation-energy formula into a functional of the electron density. *Physical Review B* **1988,** *37* (2), 785-789.

24. Harihara, P. C,.; Pople, J. A., The influence of polarization functions on molecular orbital hydrogenation energies. *Theoretica Chimica Acta* **1973,** *28* (3), 213-222.

25. Tomasi, J.; Mennucci, B.; Cammi, R., Quantum mechanical continuum solvation models. *Chem. Rev.* **2005,** *105* (8), 2999-3093.

26. Seidell, A., *Solubilities of inorganic and metal organic compounds*. 3 ed.; New York: D. Van Nostrand Company: 1940; Vol. 1.

27. Greenwood, N. N,. Earnshaw, A,. *Chemistry of the Elements*. Butterworth-Heinemann: 1997.

28. Hansen, P, E,. Vakili, M,. Kamounah, F, S,. Spanget-Larsen, J,. NH Stretching Frequencies of Intramolecularly Hydrogen-Bonded Systems: An Experimental and Theoretical Study. *Molecules*. **2021**. 26 (24), 7651-7669

CHAPTER 4

Interactions of Iodine with 4-Benzyl-1,3-thiazolidine-2-thione in Solution

4.1 Introduction

As discussed in the previous chapter about the halogen bonds, polar flattening and the anisotropic distribution of electron density forms a nucleophilic and an electrophilic region around the halogen atom[1] (Figure 4.1).

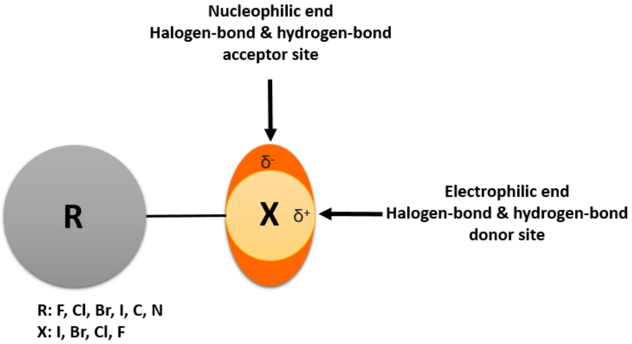

Figure 4.1. Anisotropic distribution of electron density around halogen atom.

Halogen bonding, which has numerous application in biochemistry,[2] also has been successful in demanding a unique definition from IUPAC. “A halogen bond occurs when there is evidence of a net attractive interaction between an electrophilic region associated with a halogen atom in a molecular entity and a nucleophilic region in another, or the same, molecular entity”.[3] These bonds are particularly interesting because they can be orthogonal to hydrogen bonds in a sense that they can be independently added or removed in chemical reactions,[4] or they can introduce a specific conformational change in biomolecules even when in competition with a hydrogen bond in the same environment.[5] It is noteworthy to mention that halogen bonds can play a significant role to design one, two, or three dimensional molecular crystals,[6] and some crystal designs show elastic behaviors (displacement of atoms from the equilibrium positions in the crystal lattice).[7] Solvent affects the stability and also the symmetry of the halogen bond.[8] A symmetric 3-center–4-electron iodine bond [I---I---I]$^-$ is preferred over an [I-I---I]$^-$ bond in polar aprotic solvents, such as acetonitrile.[8] Halogen bonds have been studied quantum chemically,[9] and surprisingly, it has been shown that a good estimation of the geometry and energy components will be acquired even without considering the dispersion corrections.[10] M06-2X, ωB97XD, and double hybrids are considered suitable DFT methods to study halogen bond interactions.[10] As a result, it is understood that electrostatic forces initiate the interaction; however, a charge transfer component will enhance the strength of the interaction greatly.

The R of an R–X bond in a halogen bond, XB, should be sufficiently electronegative to avoid the neutralization of a σ-hole[3] by the halogen atom and would provide two sites for electrophilic and nucleophilic attacks. The first one is perpendicular to R–X and is called the halogen bond, and the latter one is along the R–X bond on the side of the halogen atom that is not considered as the halogen bond according to IUPAC definition (Figure 4.2).

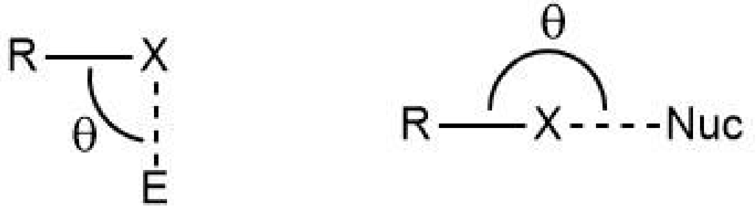

Figure 4.2. Nucleophilic (left) and electrophilic (right) sites of R–X bond. [3]

This shows that the halogen bond is directional. Desiraju and Parthasarathy in 1989 proposed two classifications of interaction with an R–X bond[11] (Figure 4.3). A type I contact is merely the consequence of close packing and is not considered a halogen bond. Type II is the net interaction between electrophilic and nucleophilic areas and is considered a halogen bond (Figure 4.3).

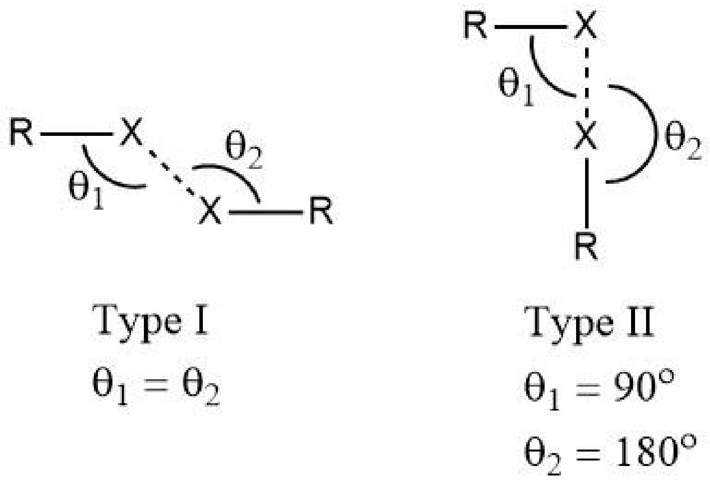

Type I
$\theta_1 = \theta_2$

Type II
$\theta_1 = 90°$
$\theta_2 = 180°$

Figure 4.3. Type I and type II halogen…halogen short contacts. [11]

A type II interaction also is known as “charge transfer” or “electron-donor-acceptor” or generally as a halogen bond due to its similarity to a hydrogen bond.[12] Established crystal data from the Cambridge Structural Database shows that Θ_2 is close to 180° for many of halogen bonded complexes (Figure 4.4).

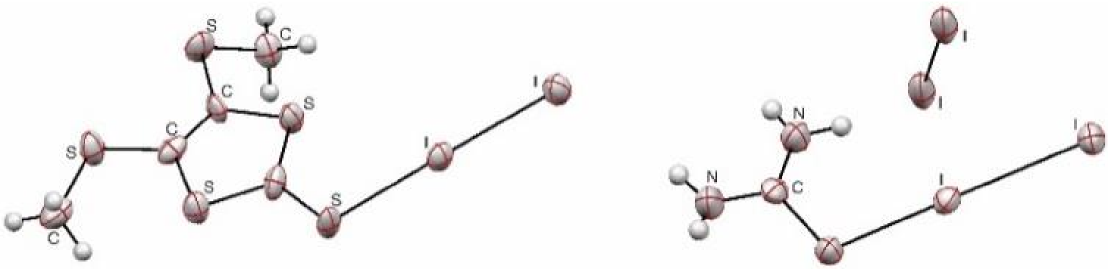

Figure 4.4. X-ray structures of diiodine complexes of urea and thiourea. (Data from the from the Cambridge Structural Database).

Θ_2 is close to 90° for pentaiodobenzoic acid (PIBA) and N,N′-dimethylformamide.[13] (Figure 4.5).

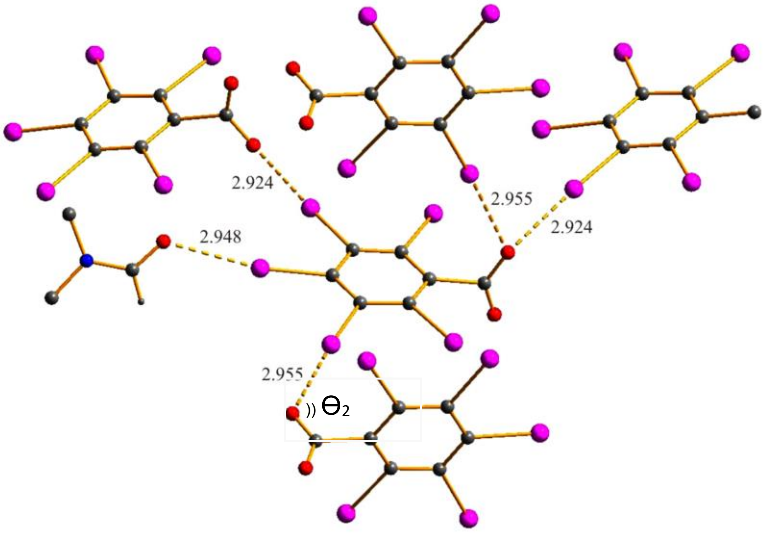

Figure 4.5. Formation of halogen bond between pentaiodobenzoic acid (PIBA) and N,N′-dimethylformamide. [13]

The chosen system of study, 4-benzyl-1,3-thiazolidine-2-thione, abbreviated as NSS (Figure 4.6) enables halogen bonding, hydrogen bonding, and pi bonding sites to compete in solution together over the halogen bond formation. Thus, it provides an experimental tool to look into and compare the extent of interaction between an electron deficient site (iodine) and an electron rich site (thiocarbonyl) and reveals the effect of such interaction on the absolute configuration of the electron rich molecules.

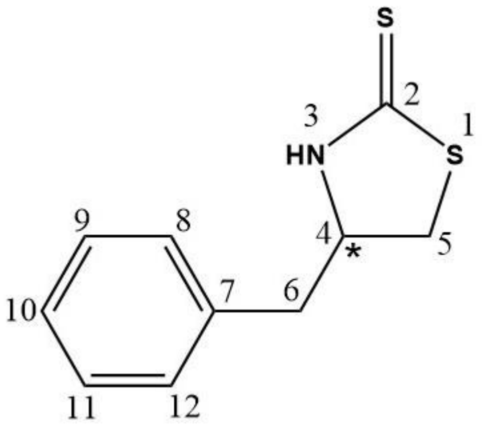

Figure 4.6. Chemical structures of 4-benzyl-1,3-thiazolidine-2-thione (NSS).

Here, we will evaluate the possibility of formation of halogen bonds from different acceptor sites in the NSS molecules to acquire an insight into the intra-molecular interactions involving a dihalide and a thiocarbonyl electron rich site. 4-Benzyl-1,3-thiazolidine-2-thione provides two π bond systems as the σ-hole acceptor sites. 4-Benzyl-1,3-thiazolidine-2-thione would be able to form hydrogen bonds in the solution to indicate the competition between the halogen with the hydrogen bond in the solution. To reduce the interference with the solvent, chloroform and carbon tetrachloride have been chosen as the solvents throughout the study. This system, due to its size, would be suitable for ab-initio and DFT studies. . In order to measure the VCD signals one must use one enantiomeric form of the analyte only. Thus throughout all the measurements only enantio-pure forms of S-NSS was utilized.

4.2 Experimental and Theoretical Details

4-Benzyl-1,3-thiazolidine-2-thione was purchased from Astatech. ^{1}H-NMR spectra of this compound were recorded on a Bruker (400 MHz) spectrometer to confirm the purity of reagents. VA and VCD spectra were measured, using a Bruker FTIR (Vertex 70) spectrometer equipped with a PMA 50 module for VCD measurements.[14] The data were collected at 4 cm^{-1} resolution in the wavenumber region of 1700–1100 cm^{-1}, using a liquid nitrogen cooled MCT detector for a period of 5 h (~4300 scans per hour). Solutions of 0.238 M NSS in $CDCl_3$ and 0.093 M of the mixture of NSS and I_2 in $CDCl_3$ were used for the VA and VCD measurements. The solution samples were placed between a pair of BaF_2 windows with a path-length of 0.1 mm. A solution with the same concentration is used to carry out the UV-vis measurements. UV-vis measurements were carried out on a Hewlett Packard 8453 spectrometer with a 1 mm cell. The Gaussian 09 program package[15] was used for all geometrical searches and optimizations, harmonic frequency calculations, and VA and VCD intensity predictions, using density functional theory (DFT)[16]. A Becke three parameters, Lee-Yang-Parr, functional (B3LYP)[16] and 6-311++G(d,p)[17] was used for the calculations. The polarizable continuum model (PCM) was used to account for the bulk solvent environment[18] of $CDCl_3$. A Lorentzian line shape with a half-width at half-height of 4 cm^{-1} was used for the simulations of VA and VCD spectra.

4.3 Results and Discussions

4.3.1 Conformers of the NOS

Rotation of the phenyl ring around the axis of a C_6-C_7 bond, rotation of the 5-membered ring around the axis of a C_4-C_6 bond, and scanning the dihedral angle of N-C_4-C_6-C_7 yielded three conformers, gauche-, gauche+, and syn. This rotation was in a relaxed mode and no other angles were fixed. Figure 4.7 illustrates the Newman projection of the obtained conformers. These conformers are different in terms of the types of gauche interactions with C_7.

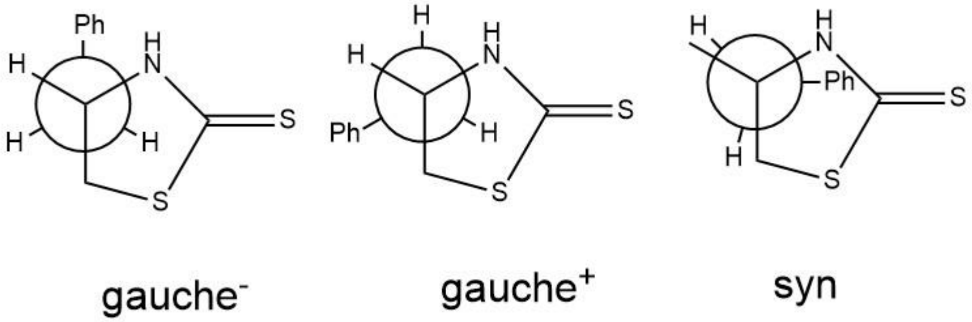

Figure 4.7. Newman projection of conformers of 4-benzyl-1,3-thiazolidine-2-thione (NSS).

The volume of groups in the gauche interactions account for the relative stability of the conformers. Figure 4.8 merely demonstrates the relative stability of conformers with respect to each other. Exact values are provided in Table 4.8.

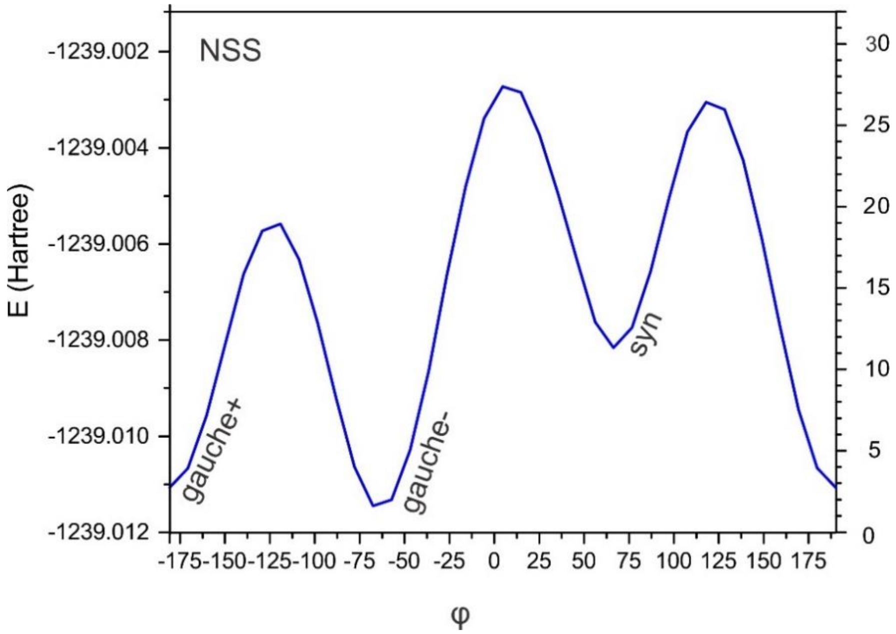

Figure 4.8. Chemical relative stability of conformers of NSS in kJ.mol^{-1} NSS and in Hartrees. φ is the dihedral angle of N-C_4-C_6-C_7 scanned over 360°. Energy of the conformer with the lowest energy is defined as zero.

The gauche- conformer is 1.3 kJ mol^{-1} and 9.5 kJ .mol^{-1} more stable than the gauche+ and syn conformers, respectively. Thus, the gauche- conformer has the highest Boltzmann population (Table 4.1).

Table 4.1 Relative Energies and Boltzmann Distribution of Conformers of NSS

Conformer	ΔE (kJ .mol^{-1})	%Boltzmann Distribution (298 K)
gauche-	0	67
gauche+	1.3	32.2
syn	9.5	0.8

4.3.2 ^{1}H-NMR and UV-vis Study of NSS Interacting with I_2

To evaluate the interactions between I_2 and NSS, we first carried out UV-vis and ^{1}H-NMR titrations. Since NSS can be dissolved well in $CDCl_3$, while I_2 dissolves only moderately,[19] we performed the titration by adding the I_2 in $CDCl_3$ solution to the concentrated 0.238 M NSS in $CDCl_3$ solutions dropwise. ^{1}H-NMR data showed that the proton attached to nitrogen underwent shielding from 7.8 ppm to 7.6 ppm upon increasing the concentration of iodine solution. The UV-vis titration experiments, on the other hand, exhibit a much different behavior compared to the NOS system. The UV-Vis titration of NSS with I_2, in contrast, shows a sizable blue shift from 512 nm to 420 nm after introducing iodine to the solution (Figure 4.9).

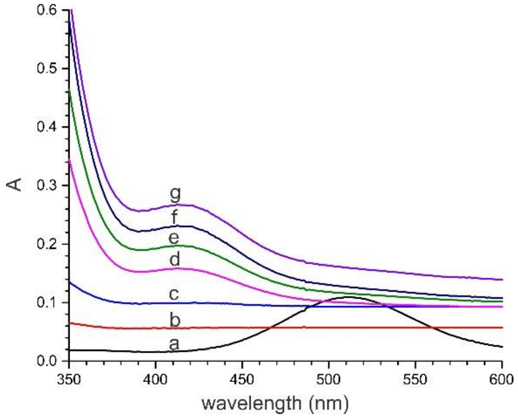

Figure 4.9. Iodine absorption band in titration of NSS with I_2 in $CDCl_3$. a: I_2 b: NSS c: $[I_2] = 1/4[NSS]$ d: $[I_2] = 1/2[NSS]$ e: $[I_2] = [NSS]$ f: $[I_2] = 1.5[NSS]$ g: $[I_2] = 2[NSS]$.

To further understand the identity of the interactions, we decided to examine their IR and VCD spectra, aided with ab initio calculations.

Iodine, acts as the halogen-bond donor and is an electron acceptor. Without any interaction, iodine shows its $\pi_g^* \rightarrow \sigma_u^*$ transition at 512 nm in $CDCl_3$. Interaction with a halogen-bond acceptor (Lewis base) increases the gap between σ^* and π^* orbitals and, consequently, a blue shift due is observed. Greenwood and Earnshaw[20] suggested that, without any coordinating agent, the energy gap between π_g^* and σ_u^* remains unchanged. However, a Lewis base can donate an electron to σ_u^* and cause a blue shift (Figure 4.10).

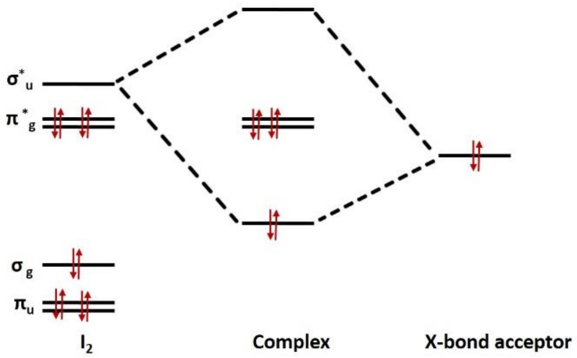

Figure 4.10 Schematic molecular orbital energy diagram of iodine formed from 5P orbitals (π_u, σ_g, π_g^*, σ_u^*) and the effect of a halogen bond interaction on the $\pi_g^* \rightarrow \sigma_u^*$ transition. The energy gap between π_g^* and σ_u^* increases after halogen bond interaction. [20]

4.3.3 IR Study of NSS-iodine Interaction

The stretching frequency of the NH region, 3050cm^{-1}–3450cm^{-1}, at lower concentrations of iodine consists of two bands around 3140 cm^{-1} and 3390 cm^{-1}. At higher ratios of [I_2]/[NSS] concentrations a new band appears at around 3310 cm^{-1} (Figure 4.11).

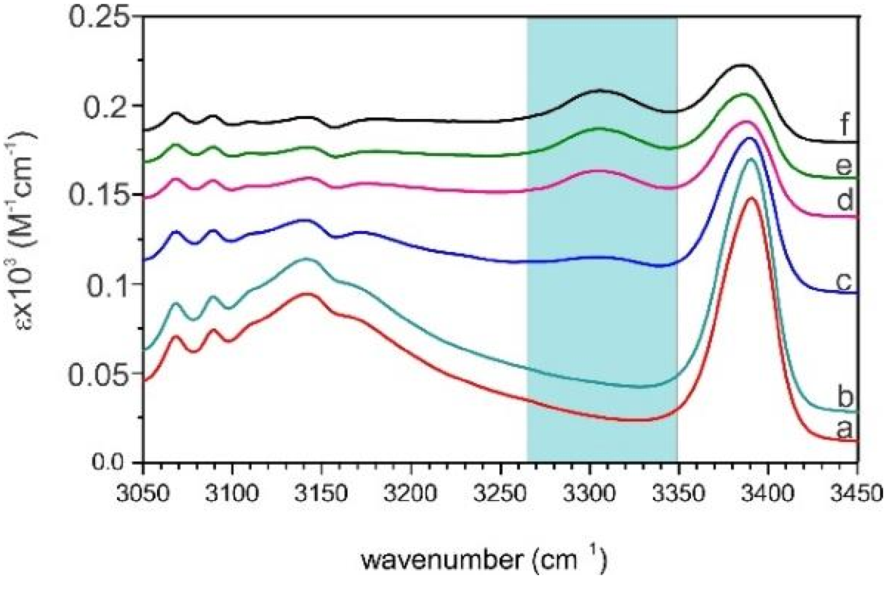

Figure 4.11. Titration with iodine. NH stretching region of NSS. Formation of the new band at 3310 cm^{-1} is more prominent when excess of iodine introduced to the solution. a: NSS b: [I_2] = 1/4[NSS] c: [I_2] = 1/2[NSS] d: [I_2] = [NSS] e: [I_2] = 1.5[NSS] f: [I_2] = 2[NSS]. $[NSS]_a = 0.238M$. $[NSS]_I = 0.093$. 360°

In order to approach the characterization of this band, a series of dilution experiments were done to watch the occurrence of such peak at different concentration levels without introduction of iodine to the solution. Upon dilution of the NSS solution to the 2nd, 3rd, and higher levels, the new band did not show up; hence, it was confirmed due to the interaction with iodine (Figure 4.12).

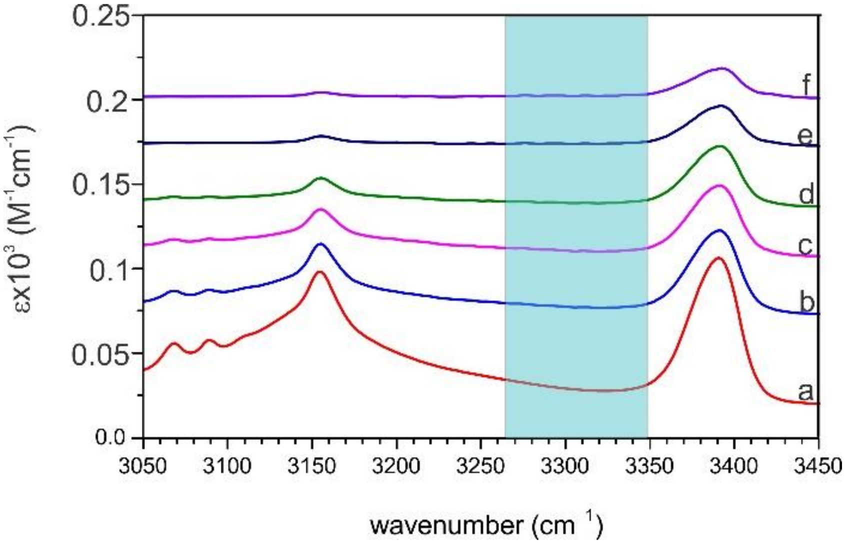

Figure 4.12. Dilution experiment. Concentration of NSS decreases from a to f. NH stretching region of NSS shows formation of no new band at around 3310 cm^{-1}. The bands at around 3150 cm^{-1} and 3390 cm^{-1} are due to the dimer and the monomer respectively. $[NSS]_a$= 0.238M. $[NSS]_I$ = 0.093.

Infrared analysis of the optimized structures of NSS, (g-NSS)$_2$, and (g-NSS)-I$_2$ reveals that the new band as a result of interaction of iodine with NSS appears between the N-H stretching frequencies of the monomer and dimer (Figure 4.13).

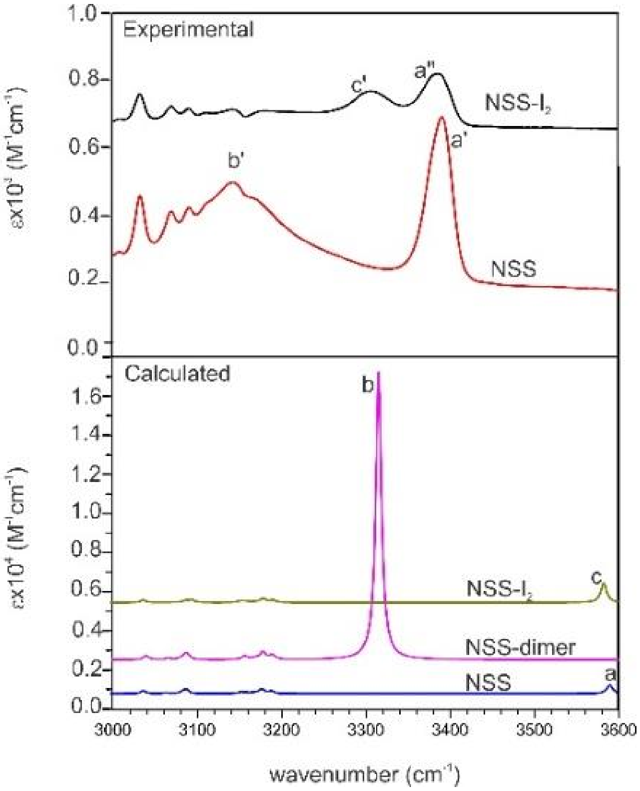

Figure 4.13. Optimization of the NSS structure in monomer (NSS), dimer (NSS-dimer), and iodine complex (NSS-I_2) shows that N-H stretching frequency (3584 cm^{-1}) is between the values of the monomer (3592 cm^{-1}) and the dimer (3316 cm^{-1}) as was observed for the experimental data. a' and a", are the experimental counterparts of the calculated N-H stretching frequency in the experimental data. b' is the experimental counterpart of b and c' is the N-H stretching frequency as a result of interaction of iodine with NSS.

In the IR spectrum thiocarbonyl stretching frequency was involved with several overlaps, and it was not possible to follow the changes of this functionality in the experimental data. Thus, by knowing that the interaction of iodine with NSS includes the NH moiety, we were interested to look into the bending region of this group. The optimized structure of the monomer of NSS shows two bands next to one another between 1480 cm^{-1} and 1520 cm^{-1} (Figure 4.14 marked with a_1 and a_2). The dimer shows the same bending bands between 1520cm^{-1} and 1580 cm^{-1} (Figure 4.14 marked with b_1 and b_2). Both of the spectroscopic features of the monomer and dimer were observed in the N-H bending region in the acquired spectra (Figure 4.14. a'_1, a'_2, b'_1 and b'_2 counterparts in the experimental spectra). The structure of the iodine-NSS complex was optimized and it was found that the new N-H bending mode appeared between the monomer and dimer counterparts (Figure 4.14 marked with c). By introducing iodine to the solution and monitoring the changes in the N-H bending region, it was observed that the new N-H bending mode appeared similarly between that of the monomer and the dimer (Figure 4.14 c' counterpart in the experimental spectra).

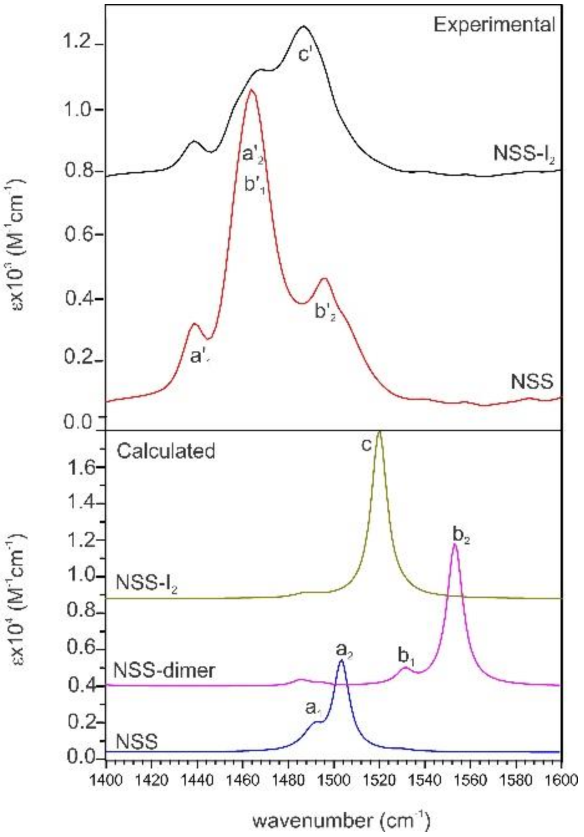

Figure 4.14. Bending region of N-H in the calculated spectra (a_1, a_2, b_1, b_2, and c) and their experimental counterparts (a'_1, a'_2, b'_1, b'_2, and c') in the measured spectra. The new band in the iodine-NSS complex is denoted as c in the optimized structure and c' in the measured spectrum.

The optimized structure of the NSS-I_2 complex shows the simultaneous formation of the halogen bond and the hydrogen bond with an NSS molecule Figure 4.15).

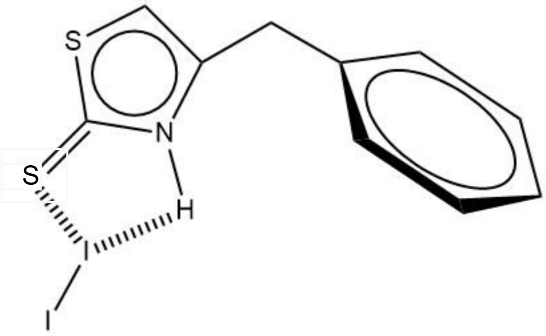

Figure 4.15. Formation of halogen and hydrogen bond with iodine.

Directionality[11] is a major criterion for the formation of such charge transfer complexes and cannot happen by other bonding patterns[21] (Figure 4.16).

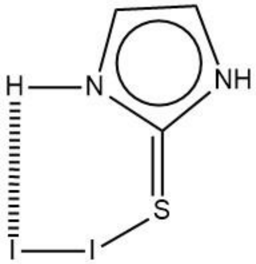

Figure 4.16. Charge transfer complex formed between an 1,3-imidazolidine-2-thione and iodine. Such structure is not consistent with the directionality of charge transfer.

Table 4.2 shows the major bond lengths before and after interaction of iodine with NSS molecule.

Table 4.2 Change of the Bond Length is More Dominant in Iodine as It Is Involved in Both a Halogen and a Hydrogen Bond, but Less Prominent in An N-H Bond Involved in a Relatively Weaker Hydrogen Bond

Bond length Bond type	Monomer	I_2-NSS
I-I	2.86 Å	3.04 Å
N-H	1.01 Å	1.01 Å
C=O	1.66 Å	1.69 Å

Iodine is involved in both the halogen bond and the hydrogen bond. Consequently, a σ_u^* orbital carries more electron density and the I-I bond shows a larger lengthening compared to other covalent bonds involved in this interaction.

4.3.4 VCD Study of NSS

A study of the VCD of the NSS was done with the selected functional frequencies. A study of the calculated and experimental IR spectra showed the sensitivity of the N-H bending motion to the interaction of this moiety with iodine (Figure 4-17). The calculated spectra of NSS in monomeric and dimeric interaction showed the relative sensitivity of this group in different environments. Thus, VCD measurements were carried out to study these two regions (Figure 4.17).

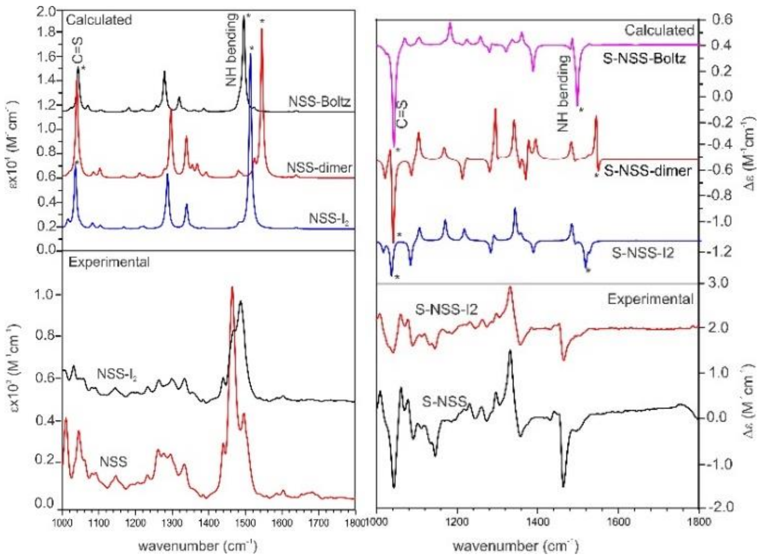

Figure 4.17. Superimposed experimental and calculated IR (left) and VCD (right) of NSS and NSS-iodine showing some main functionalities involved in the range of 1000 cm^{-1}–1800 cm^{-1}.

It was observed that formation of a halogen bond with iodine did not change the VCD spectrum of NSS-iodine compared with NSS significantly in either of the aforementioned regions. However, several features of both IR and VCD spectra of NSS and NSS-iodine complex were produced successfully for the study.

Table 4.3 shows the energy of interaction of formation of a dimer for an NSS molecule and the formation of a halogen bond interaction between NSS and iodine also is calculated.

Table 4.3 Energy of Interaction of Formation of a Dimer for Two g-NSS Molecules and Formation of Halogen Bond Interaction between NSS and Iodine

Species	E_{int} (KJ mol^{-1})
$(NSS)_2$	-30.3
NSS-I_2	-61.2

4.4 Conclusion

NSS proves to be a good halogen bond acceptor for the iodine molecule. The calculated data for the energy of interaction also confirms this finding (Table 4.3).

A UV-vis study of the interaction of NSS with iodine showed an increase in the energy gap between the HOMO and LUMO orbitals of an iodine molecule, caused by charge transfer component from NSS molecule to iodine, and this was demonstrated by the blue shift in the $\pi_g^* \rightarrow \sigma_u^*$ transition in iodine molecule. IR titration of NSS with iodine, and a comparison with calculated data showed the effect of halogen bond interaction on the N-H bending motion and N-H stretching vibration. The IR spectrum in such an environment shows features of formation of an NSS-iodine complex as well as an NSS dimer.

4.5 References

1. Cavallo, G.; Metrangolo, P.; Milani, R.; Pilati, T.; Priimagi, A.; Resnati, G.; Terraneo, G., The Halogen Bond. *Chem. Rev.* **2016,** *116* (4), 2478-2601.

2. (a) Auffinger, P.; Hays, F. A.; Westhof, E.; Ho, P. S., Halogen bonds in biological molecules. *Proc. Natl. Acad. Sci. U. S. A.* **2004,** *101* (48), 16789-16794; (b) Hardegger, L. A.; Kuhn, B.; Spinnler, B.; Anselm, L.; Ecabert, R.; Stihle, M.; Gsell, B.; Thoma, R.; Diez, J.; Benz, J.; Plancher, J.-M.; Hartmann, G.; Banner, D. W.; Haap, W.; Diederich, F., Systematic Investigation of Halogen Bonding in Protein-Ligand Interactions. *Angew. Chem.-Int. Edit.* **2011,** *50* (1), 314-318.

3. Clark, T.; Hennemann, M.; Murray, J. S.; Politzer, P., Halogen bonding: the sigma-hole. *J. Mol. Model.* **2007,** *13* (2), 291-296.

4. Voth, A. R.; Khuu, P.; Oishi, K.; Ho, P. S., Halogen bonds as orthogonal molecular interactions to hydrogen bonds. *Nat. Chem.* **2009,** *1* (1), 74-79.

5. Voth, A. R.; Hays, F. A.; Ho, P. S., Directing macromolecular conformation through halogen bonds. *Proc. Natl. Acad. Sci. U. S. A.* **2007,** *104* (15), 6188-6193.

6. Aakeroy, C. B.; Panikkattu, S.; Chopade, P. D.; Desper, J., Competing hydrogen-bond and halogen-bond donors in crystal engineering. *Crystengcomm* **2013,** *15* (16), 3125-3136.

7. Mukherjee, A.; Desiraju, G. R., Halogen bonds in some dihalogenated phenols: applications to crystal engineering. *IUCrJ* **2014,** *1*, 49-60.

8. Carlsson, A. C. C.; Uhrbom, M.; Karim, A.; Brath, U.; Grafenstein, J.; Erdelyi, M., Solvent effects on halogen bond symmetry. *Crystengcomm* **2013,** *15* (16), 3087-3092.

9. (a) Tsuzuki, S.; Wakisaka, A.; Ono, T.; Sonoda, T., Magnitude and Origin of the Attraction and Directionality of the Halogen Bonds of the Complexes of C_6F_5X and C_6H_5X (X=I, Br, Cl and F) with Pyridine. *Chem.-Eur. J.* **2012,** *18* (3), 951-960; (b) Pinter, B.; Nagels, N.; Herrebout, W. A.; De Proft, F., Halogen Bonding from a Hard and Soft Acids and Bases Perspective: Investigation by Using Density Functional Theory Reactivity Indices. *Chem.-Eur. J.* **2013,** *19* (2), 518-529.

10. Kozuch, S.; Martin, J. M. L., Halogen Bonds: Benchmarks and Theoretical Analysis. *J. Chem. Theory Comput.* **2013,** *9* (4), 1918-1931.

11. Desiraju, G. R.; Parthasarathy, R., The nature of halogen...halogen interactions: are short halogen contacts due to specific attractive forces or due to close packing of nonspherical atoms? *J. Am. Chem. Soc.* **1989,** *111* (23), 8725-8726.

12. Dumas, J. M., Gomel, M. & Guerin, M., *The Chemistry of Functional Groups*. Wiley: 1983.

13. Bondarenko, M. A.; Novikov, A. S.; Chernova, K. V.; Sokolov, M. N.; Adonin, S. A., 2-methylpyridinium salt of pentaiodobenzoic acid: role of the halogen bond in the formation of a crystal packing. *Journal of Structural Chemistry* **2021,** *62* (8), 1237-1242.

14. Losada, M.; Xu, Y., Chirality transfer through hydrogen-bonding: Experimental and ab initio analyses of vibrational circular dichroism spectra of methyl lactate in water. *Phys. Chem. Chem. Phys.* **2007,** *9* (24), 3127-3135.

15. M. J. Frisch., G. W. Trucks, H. B. Schlegel, G. E. Scuseria, M. A. Robb, J. R. Cheeseman, G. Scalmani, V. Barone, B. Mennucci, G. A. Petersson, H. Nakatsuji, M. Caricato, X. Li, H. P. Hratchian, A. F. Izmaylov, J. Bloino, G. Zheng, J. L. Sonnenberg, M. Hada, M. Ehara, K. Toyota, R. Fukuda, J. Hasegawa, M. Ishida, T. Nakajima, Y. Honda, O. Kitao, H. Nakai, T. Vreven, J. A. Montgomery, Jr., J. E. Peralta, F. Ogliaro, M. Bearpark, J. J. Heyd, E. Brothers, K. N. Kudin, V. N. Staroverov, R. Kobayashi, J. Normand, K. Raghavachari, A. Rendell, J. C. Burant, S. S. Iyengar, J. Tomasi, M. Cossi, N. Rega, J. M. Millam, M. Klene, J. E. Knox, J. B. Cross, V. Bakken, C. Adamo, J. Jaramillo, R. Gomperts, R. E. Stratmann, O. Yazyev, A. J. Austin, R. Cammi, C. Pomelli, J. W. Ochterski, R. L. Martin, K. Morokuma, V. G. Zakrzewski, G. A. Voth, P. Salvador, J. J. Dannenberg, S. Dapprich, A. D. Daniels, Ö. Farkas, J. B. Foresman, J. V. Ortiz, J. Cioslowski, and D. J. Fox, Gaussian 09, Revision D.01. Gaussian, I., Wallingford CT, Ed. 2009.

16. (a) Becke, A. D., Density-functional thermochemistry. III. The role of exact exchange. *J. Chem. Phys.* **1993,** *98* (7), 5648-5652; (b) Becke, A. D., Density-functional exchange-energy approximation with correct asymptotic behavior. *Physical Review A* **1988,** *38* (6), 3098-3100; (c) Lee, C. T.; Yang, W. T.; Parr, R. G., Development of the Colle-Salvetti correlation-energy formula into a functional of the electron density. *Physical Review B* **1988,** *37* (2), 785-789.

17. Harihara.Pc; Pople, J. A., The influence of polarization functions on molecular orbital hydrogenation energies. *Theoretica Chimica Acta* **1973,** *28* (3), 213-222.

18. Tomasi, J.; Mennucci, B.; Cammi, R., Quantum mechanical continuum solvation models. *Chem. Rev.* **2005,** *105* (8), 2999-3093.

19. Seidell, A., *Solubilities of inorganic and metal organic compounds*. 3 ed.; New York: D. Van Nostrand Company: 1940; Vol. 1.

20. Greenwood, N. N,. Earnshaw, A,.; *Chemistry of the Elements*. Butterworth-Heinemann: 1997.

21. Devillanova, F. A.; Verani, G., Charge transfer complexes between I_2 and 1,3-imidazolidine-2-thione and its n-mono- and n,n'-di-substituted derivatives. *Tetrahedron* **1979,** *35* (4), 511-514.

CHAPTER 5

Interactions of Iodopentafluorobenzene with 4-benzyl-1,3-thiazolidine-2-one in Solution

5.1 Introduction

Lewis bases have the tendency to interact with elements from group 14-17 which are covalently bonded to electron deficient species. As a result of these interactions four types of bonding are observed and are called tetrel, pnictogen, chalcogen, and halogen bonding respectively (Figure5.1).

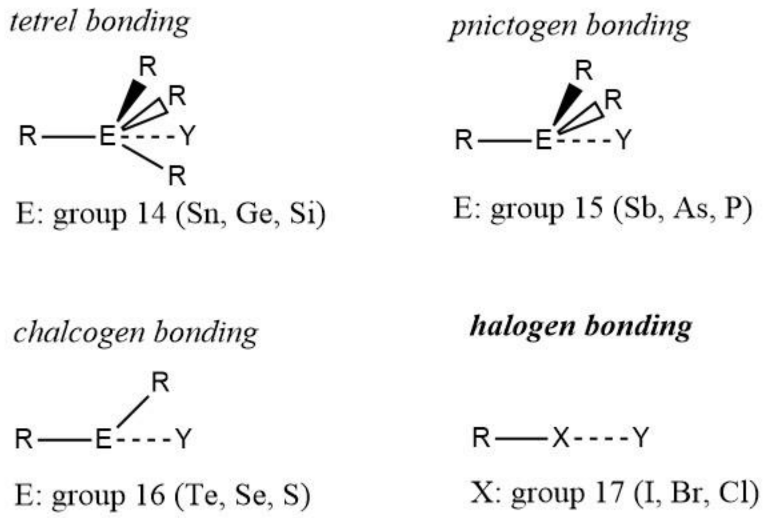

Figure 5.1. Depiction of tetrel, pnictogen, chalcogen, and halogen bonding.

Halogen bonding occurs between an electron deficient halogen compound and a Lewis base. Halogenated compounds are able to be involved in two different kinds of noncovalent interactions. Due to the high electronegativity of the halogen atoms, they could act as hydrogen bond acceptors and thus interact with electron-deficient sites in other molecules, such as the C atoms of carbonyl groups. Besides, certain halogenated compounds show a tendency to be involved in noncovalent interactions with Lewis basic moieties. This behavior cannot be explained based on their electronegativities. Such interactions which have been observed in various halogenated species are known as halogen bonds. Halogen bond (X-bond) can be broadly defined as non-covalent interactions between an electron deficient X-bond donor and an electron rich X-bond acceptor, in a similar fashion as a hydrogen bond (H-bond). One of the early studies of X-bond was by Guthrie[1] in 1863 when he added iodine powder to a solution of ammonia to form the complex which he then suggested to be $I_2 \cdots NH_3$ and named it "iodide of iodammonium". Guthrie found that this complex decomposed upon treating with water and turned water into reddish-brown color, and produced a residue which exploded spontaneously under water. "A halogen bond occurs when there is evidence of a net attractive interaction between an electrophilic region associated with a halogen atom in a molecular entity and a nucleophilic region in another, or the same, molecular entity".[2] Solvent affects the stability and also the symmetry of the halogen bond[3]. Halogen bonds have been quantum chemically studied[4] and surprisingly it has been shown that a good estimation of the geometry and energy components will be acquired even without considering the dispersion corrections.[5] M06-2X, ωB97XD and double hybrids are considered suitable DFT methods to study halogen bond interactions[5]. Halogen bond is represented as XB and denoted as R–X...Y. R–X is the halogen bond donor (Lewis acid) such as I_2 and Br_2, Y is the halogen bond acceptor (Lewis base) that could be an anion (halides or oxyanions), a system (double or triple bonds), or neutral (amine or pyridine). X is any electron deficient halogen atom, and R is an atom or a group covalently bonded to X. As a result, two distinctive electrostatic regions appear around R–X bond.[2, 6] This anisotropic distribution of electron density forms a nucleophilic and an electrophilic region around the halogen atom[7] (Figure5.2). The strength of the halogen bond increases with the electronegativity of the R group.

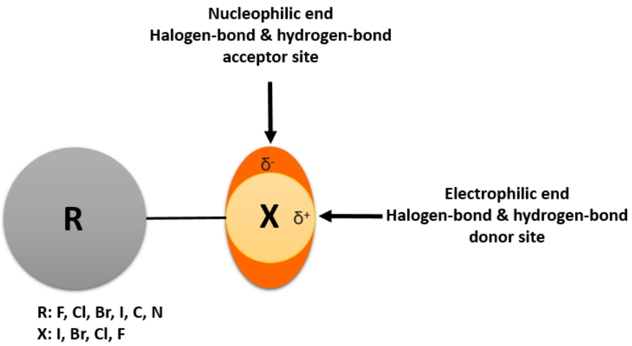

Figure 5.2. Anisotropic distribution of electron density around halogen atom.

Nuclear magnetic resonance (NMR) has been used to study structural dynamics of the molecules and is applicable to liquid, solid state and gas phase. This technique is sensitive to non-covalent interactions such as hydrogen bond[8] and halogen bond using ^{1}H-NMR and ^{19}F-NMR techniques.[9] Chemical shifts of fluorine in different halogen bonded complexes are dependent on the strength and orientation of the respective bond. The halogen bond donor ability of iodoperfluoroalkanes and iodoperfluoroarenes were discovered about sixty years ago.[9a, 10] Larsen and Allred were able to determine the K_a values for the complex formed between CF_3I and 2,4,6-trimethylpyridine in cyclopentane using ^{19}F-NMR spectroscopy.[9a, 10] The enthalpy of interaction between these two species was calculated as -21 KJ. mol^{-1}. The change in ^{19}F-NMR chemical shift ($\Delta\sigma$) can be used as a measure of the strength of halogen bond interaction between a halogenated molecule and the solvent. Metrangolo and Panzeri measured this change between a haloperflourocarbon and a particular solvent (donor solvent) relative to cyclohexane (non-donor solvent).[7] Heavy halogen atoms showed a higher values of $\Delta\sigma$ as CF_2I> CF_2Br> CF_2Cl for primary iodoperflourocarbon and $(CF_3)_2CFI$> $CF_3CF_2CF_2I$ for secondary iodoperflourocarbons.[9h] Perutz and Brammer have provided more insight into the thermodynamics of the halogen bond interactions of the perfluorinated halogen bond donors in organic solvents. They studied the interaction of C_6F_5I with group 10 metal fluoride complexes in toluene.[11]

Considering all the possibilities and competitions, we have carefully chosen a system where halogen bonding, hydrogen bonding and π bonding sites would be able to compete in the solution together. The purpose of such study is to evaluate the strength and the possibility of formation of halogen bond from different acceptor sites in the relevant molecule. Such a study provides an experimental tool to look into and compares the extent of interaction between an electron deficient site (iodine of Iodopentafluorobenzene) and an electron rich site (carbonyl) and reveals the effect of such interaction on the absolute configuration of the electron rich molecules. Thus, for this part of the study we introduce 4-benzyl-1,3-thiazolidine-2-one, abbreviated as NOS and study its interaction with Iodopentafluorobenzene (F_5BnI) (Figure 5.3).

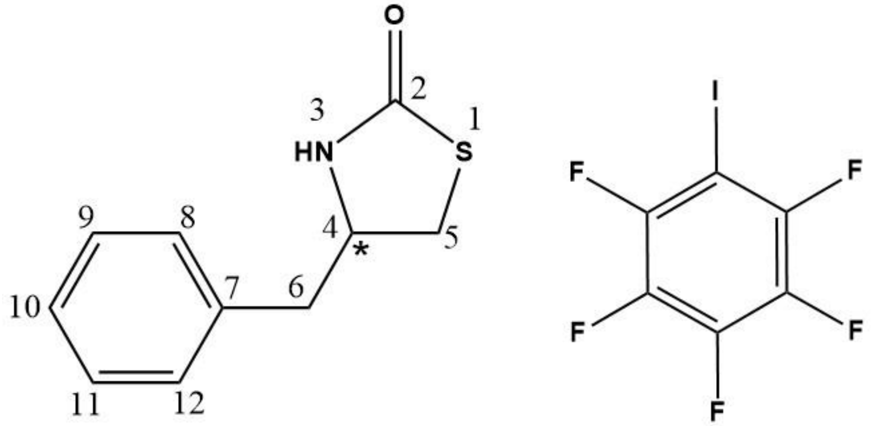

Figure 5.3. Chemical structures of 4-benzyl-1,3-thiazolidine-2-one (NOS) (left) and Iodopentafluorobenzene (F_5BnI) (right).

4-benzyl-1,3-thiazolidine-2-one has a delocalized π bond systems and a carbonyl functionality. Each of the three π systems can act as the acceptor site in the interaction with Iodopentafluorobenzene. 4-benzyl-1,3-thiazolidine-2-one molecules can form hydrogen bonds in the solution so we would be able to compare the strength of the halogen with hydrogen bond in the solution. To reduce the interference with the solvent, chloroform and carbon tetrachloride have been chosen as the solvent throughout the study. This system, due to its size, would be suitable for ab-initio and DFT studies.

5.2 Experimental and Theoretical Details

4-benzyl-1,3-thiazolidine-2-one was purchased from Astatech. F_5BnI was purchased from Sigma-Aldrich. ^{1}H-NMR and ^{19}F-NMR spectra of the compounds were recorded on a Bruker (400 MHz) spectrometer to confirm the purity of reagents. VA and VCD spectra were measured using a Bruker FTIR (Vertex 70) spectrometer equipped with a PMA 50 module for VCD measurements. The data were collected at 4 cm^{-1} resolution in the wavenumber region of 1700-1100 cm^{-1} using a liquid nitrogen cooled MCT detector for a period of 5 hours (~4300 scans per hour). A range of solutions were used for the VA and VCD measurements. The solution samples were placed between a pair of BaF_2 windows with a path-length of 0.1 mm, 0.015mm and 0.005mm. The Gaussian 09 program package[12] was used for all geometrical searches and optimizations, harmonic frequency calculations, and VA and VCD intensity predictions using density functional theory (DFT).[13] Becke three parameters, Lee-Yang-Parr, functional (B3LYP)[13] and 6-311++G(d,p)[14] was used for the calculations. Polarizable continuum model (PCM) using the universal force field radii was used to account for the bulk solvent environment[15] of $CDCl_3$. A Lorentzian line shape with a half-width at half-height of 4 cm^{-1} was used for the simulations of VA and VCD spectra VCD spectra.

5.3 Results and Discussions

5.3.1 Dispersion effect and the relative stability of conformers of NOS

Previous study (see chapter 3) of the conformers of the 4-benzyl-1,3-thiazolidine-2-one yielded three conformers gauche-, gauche+ and syn (Figure 5.4).

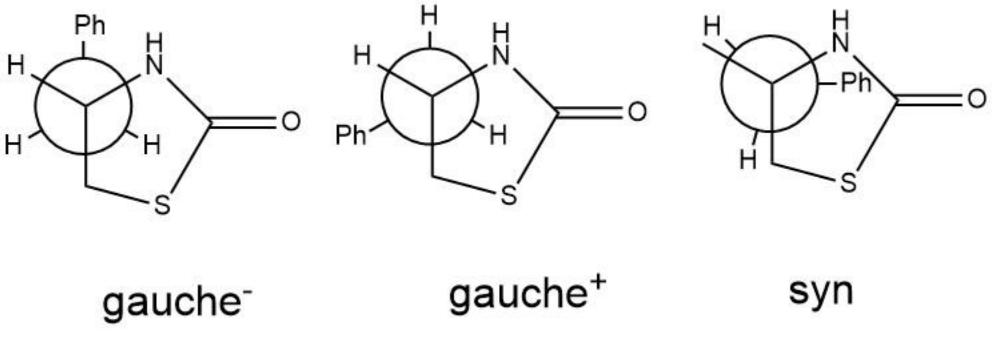

Figure 5.4. Newman projection of conformers of 4-benzyl-1,3-thiazolidine-2-one (NOS).

Volume of the groups participating in the gauche interaction with C_7 are responsible for the relative stability of the conformers. Herein empirical dispersion correction D3BJ[17] was introduced and affected the relative stability of the conformers.

Figure 5.5 demonstrates the relative energies but the exact values are shown in Table 5.1.

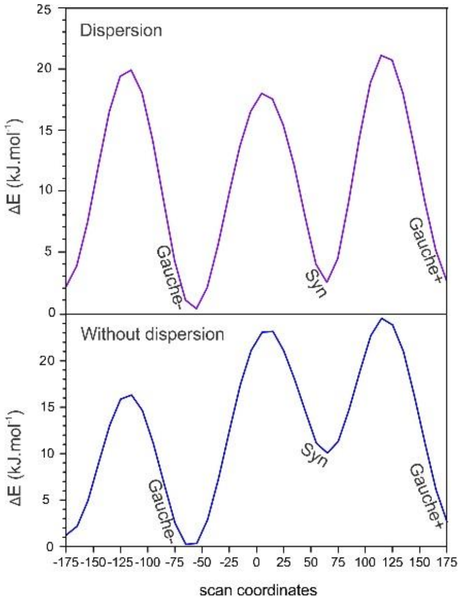

Figure 5.5. Relative stability of conformers of NOS in kJ.mol^{-1}. Scan coordinates is the dihedral angle of N-C_4-C_6-C_7 scanned over 360°. Energy of the conformer with the lowest energy is defined as zero.

The gauche- conformer is 3.2 kJ mol^{-1} and 2.5 kJ. mol^{-1} with the dispersion effect more stable than the gauche+ and syn conformers, respectively. Such an energy gap has made gauche- conformer with the highest Boltzmann population (Table 5.1).

Table 5.1 Comparison of the relative energies and Boltzmann distribution of conformers of NOS

Conformer	ΔE (kJ. mol^{-1}) With||Without dispersion	%Boltzmann Distribution With||Without Dispersion (298 K)
gauche-	0||0	78.6||64.8
gauche+	3.2||1.2	21.4||34.2
syn	2.5||9.9	0.0||0.1

5.3.2 ^{1}H-NMR and ^{19}F-NMR Study of NOS

To evaluate the interaction between F_5BnI and 4-benzyl-1,3-thiazolidine-2-one ^{1}H-NMR and ^{19}F-NMR titrations were carried out in $CDCl_3$. ^{1}H-NMR data showed the proton attached to nitrogen of NOS underwent shielding from 6.1 ppm to 5.35 ppm upon increasing the concentration of F_5BnI in the solution. Figure 5.6 shows the trend.

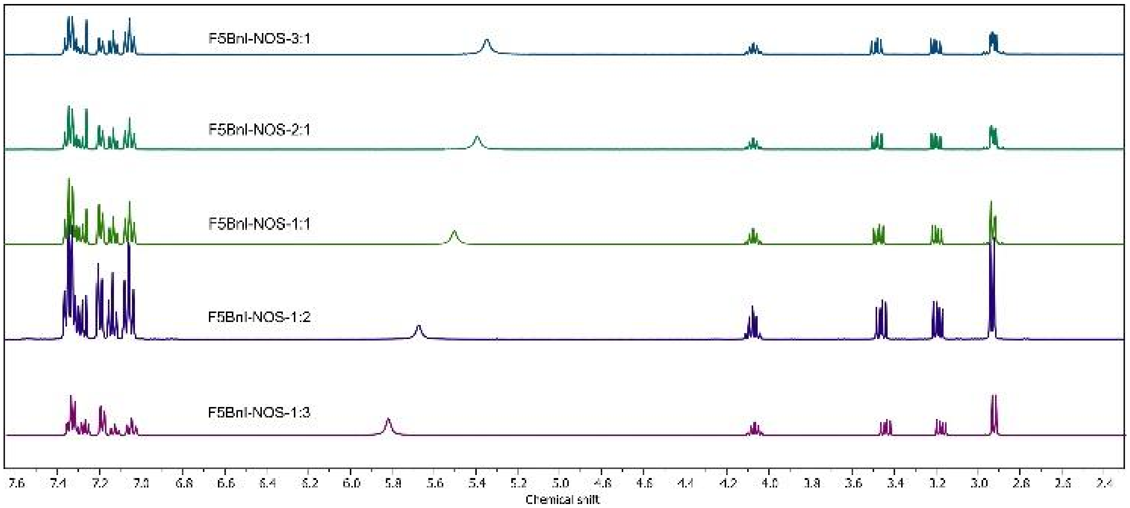

Figure 5.6. Shielding effect on N-H proton of NOS upon interacting with various concentrations of F_5BnI. Ratios from the bottom are F_5BnI/NOS:1/3; F_5BnI/NOS:1/2; F_5BnI/NOS:1; F_5BnI/NOS:2; F_5BnI/NOS:3.

^{19}F-NMR data allows to monitor the changes of the electron density around each of the fluorine atoms. Para fluorine was monitored during the titration experiments. Para-F appeared at -152.05 ppm in the F_5BnI molecule. Ratios of F_5BnI/NOS varied among 1/3, 1/2, 1, 2, and 3 values and the respective para-F shifts were -152.07, -152.06, -152.04, -152.03, and -152.03 respectively as illustrated in Figure 5.7.

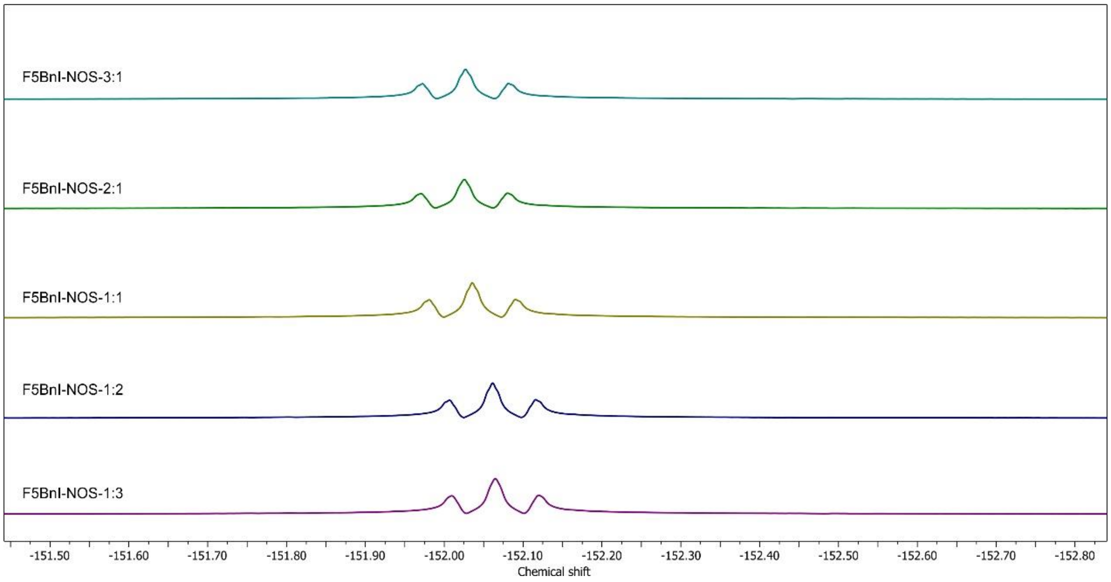

Figure 5.7. Changes in the chemical shifts of Para-F of NOS upon interacting with various concentrations of F_5BnI. Ratios from the bottom are F_5BnI/NOS:1/3; F_5BnI/NOS:1/2; F_5BnI/NOS:1; F_5BnI/NOS:2; F_5BnI/NOS:3.

Downfield shift of the fluorine atoms adjacent to iodo substituent is not unprecedented upon increasing the concentration of the acceptor species. Sarwar, Dragisic and coworkers studied the interaction of different Lewis bases with fluorinated iodoalkenes and iodoarenes.[9k] They recorded the ^{19}F-NMR spectra of the halogen bond donors upon interaction with the halogen bond acceptor (Lewis base). This study was performed for several para-substituted iodotetrafluorobenzenes as donors and tri-n-butylephosphine oxide acceptor where in all cases there was a downfield shift of the ^{19}F-NMR signal upon complexation. Other cases have also been observed in the literature where ^{19}F-NMR signal shows an upfield change on the fluorine substituted species. Chudzinski and his coworkers studied a series of urea-based halogen bond acceptors through ^{1}H-NMR and ^{19}F-NMR spectroscopy (Figure 5.8).[16]

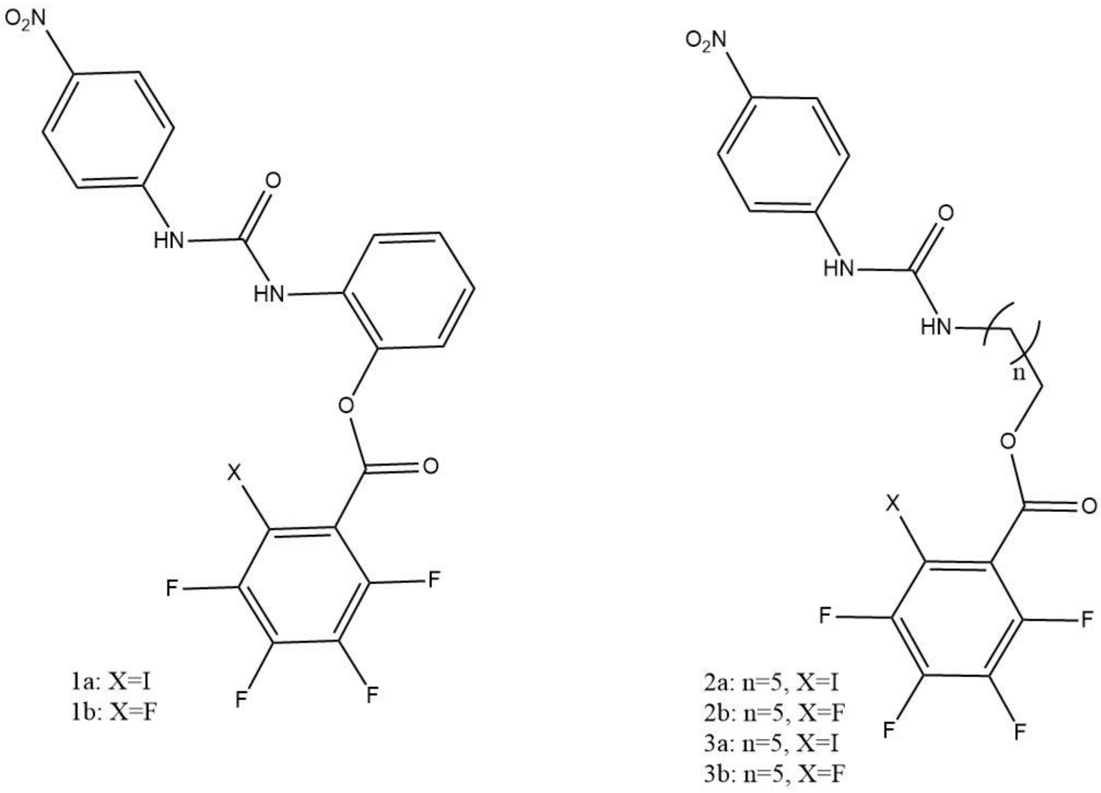

1a: X=I
1b: X=F

2a: n=5, X=I
2b: n=5, X=F
3a: n=5, X=I
3b: n=5, X=F

Figure 5.8. Structures of the halogen bond acceptors.

Addition of halide anions (n-Bu_4N^+ cation and Cl^-, Br^-, I^- anions) to the above donors, or in other words increasing the concentration of the halogen bond acceptor, resulted in the change of the ^{19}F-NMR chemical shifts. This upfield change in the chemical shift ($\Delta\sigma$) for the case of 1a acceptor was involved with a range of concentration of 0M to $6.0*10^{-3}$ M of Br^-. The observed $\Delta\sigma$ was from zero to ~1.1 ppm for the ^{19}F-NMR signals. It is noteworthy to mention that this trend in the change in the chemical shift of the ^{19}F-NMR is consistent with the measured data where a down field shift was observed upon increasing the concentration of the halogen bond acceptor NOS.

5.3.3 IR Study of NOS-F_5BnI Interaction

IR study of NOS with various concentration ratios of F_5BnI in $CDCl_3$ showed a distinct region for stretching frequency of the NH that is 3180cm^{-1} – 3490cm^{-1}. This region includes a broader band around 3217 cm^{-1}, distinctive of NOS dimer, and another one around 3414 cm^{-1} referring to the monomeric form of NOS. Yet by increasing the concentration of F5BnI in the solution no changes were observed at either of the location of the peaks (Figure 5.9)

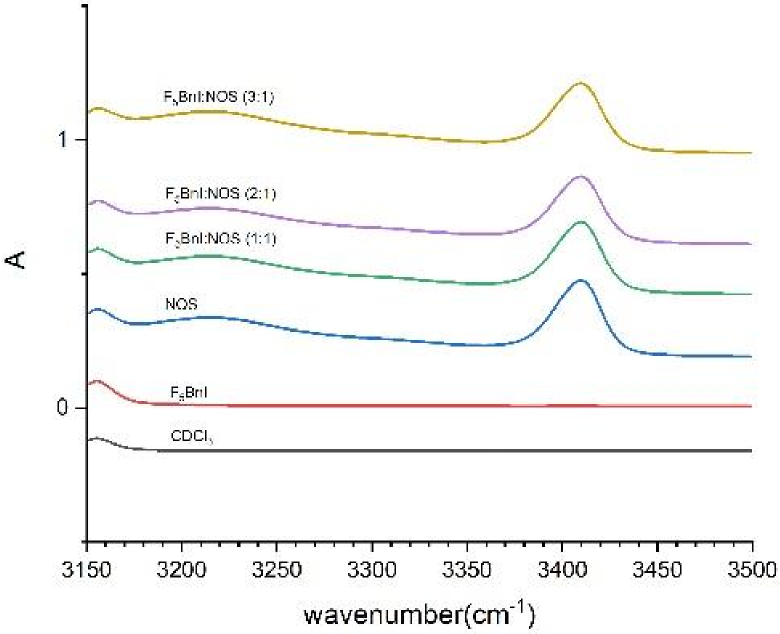

Figure 5.9. NH stretching region of NOS. At higher concentrations of F5BnI solution no changes happen to monomeric or dimeric forms of NOS moieties.

The broad peak at the N-H region confirms the formation of $(NOS)_2$ at lower and higher concentrations of F5BnI in the solution. A similar trend was also observed for the carbonyl region that was ~1620 cm^{-1}. This peak did not show a shift upon addition of the F5BnI to the solution (Figure 5.10).

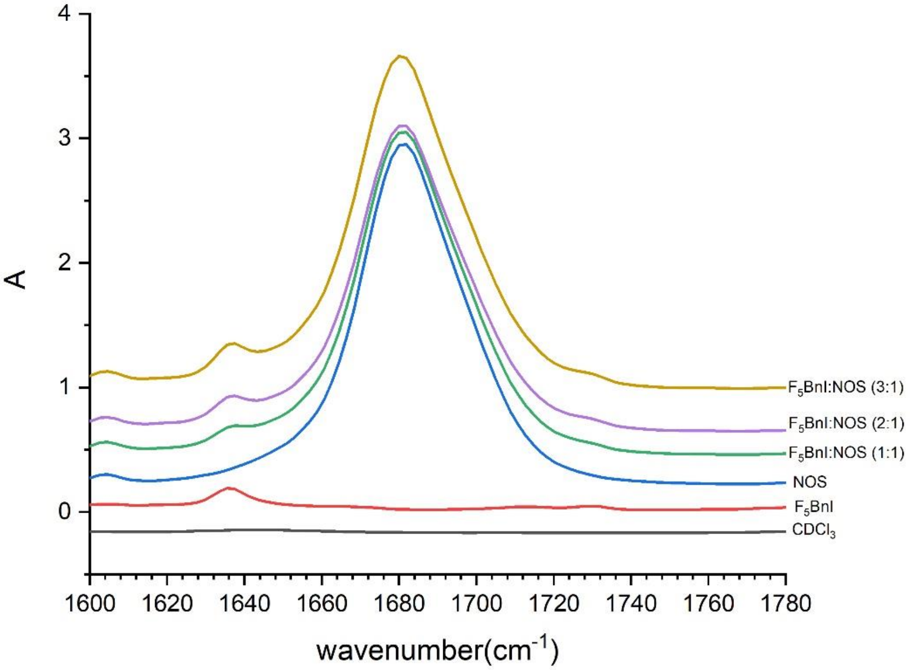

Figure 5.10. Carbonyl stretching region of NOS. At higher concentrations of F_5BnI solution no shift was observed.

This shows that the partial charge transfer from carbonyl π^* orbital to antibonding orbital of N-H moiety on NOS molecule is not being affected by the introduction of the F_5BnI to the solution containing the $(NOS)_2$ dimer. The lack of disappearance of the broad peak at N-H stretching frequency region under the same condition also confirms this observation.

Relative locations of the N-H stretching frequencies of the monomer and different dimer combinations were also studied and confirmed by comparison of the experimental data with the calculated infrared spectra of the optimized structures. (Figure 5.11).

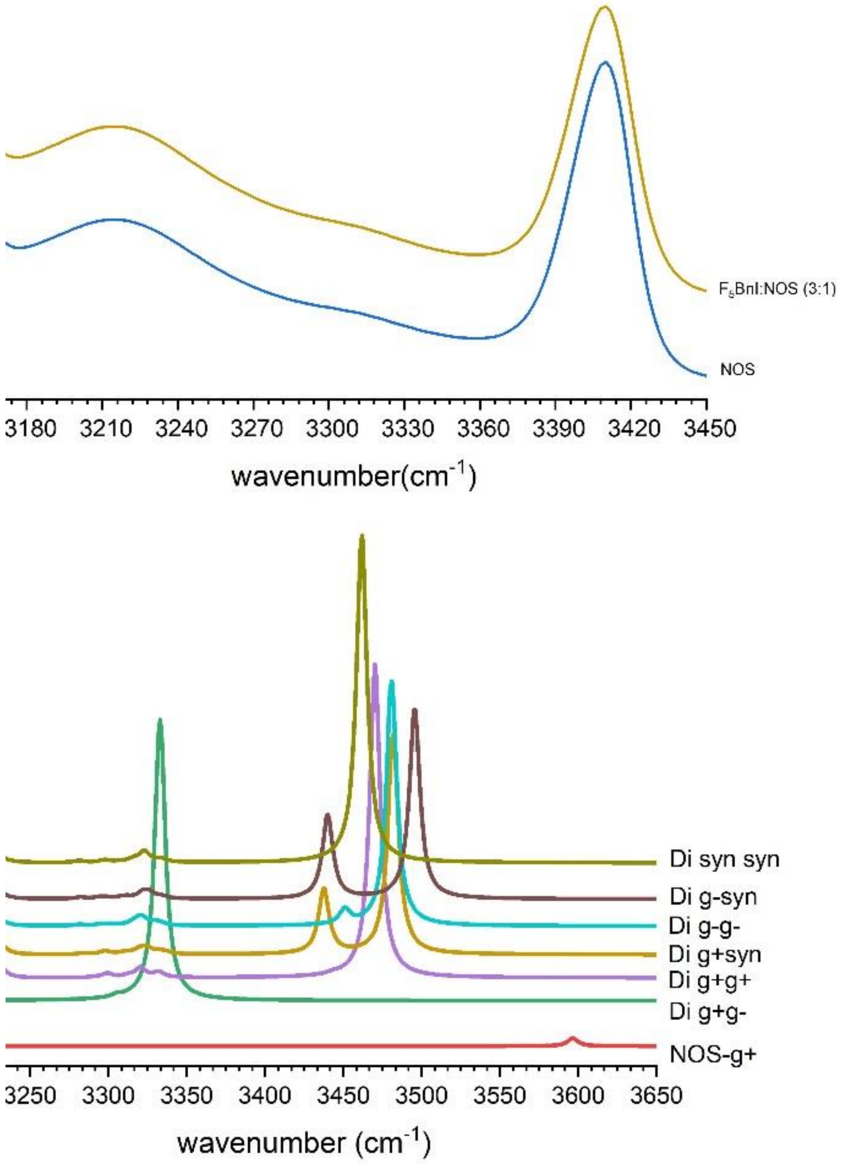

Figure 5.11. N-H stretching frequencies of monomer and possible dimer combinations and their experimental counterparts.

The closest frequency of the dimer to the experimental value was reproduced by the g+g- dimer. Table 5.2 shows the relative values of the energetics of different conformational dimeric structures. This dimer conformer is one of the most abundant ones among the possible structures acquired after optimization of each conformer twins with and without the dispersion effect.

Table 5.2 Relative energies and Boltzmann distribution of NOS dimers formed from different conformers

Conformer	ΔE (kJ .mol^{-1}) With||Without dispersion	%Boltzmann Distribution With||Without dispersion
g-g-	0||6.68	27.85||3.11
g+g-	0.05||0.005	27.24||46.11
g+g+	1.64||0	14.31||46.20
g+syn	1.65||6.08	14.30||3.96
g-syn	2.87||10.93	8.73||0.56
synsyn	3.23||17.26	7.54||0.04

5.3.4 VCD Study

VCD study of NOS-F$_5$BnI was done at the same level of concentration as the NOS. Figure 5.12 shows the VCD spectrum of NOS- F$_5$BnI solution.

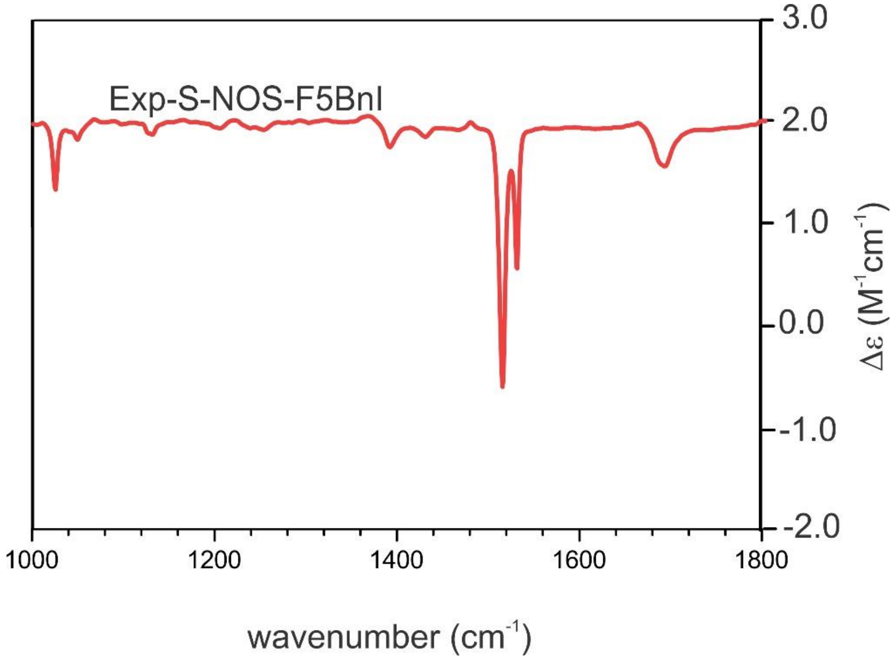

Figure 5.12. VCD of of S-NOS-F5BnI in 1000 cm^{-1}- 1800 cm^{-1}.

Comparison between the acquired VCD spectra and the simulated data provides insight about the dominant conformer of the NOS molecule during the course of interaction with each other. As such here we propose the gauche- as the dominant conformer to interact with the F_5BnI molecule. By comparison of the theoretical and experimental spectra it was observed that gauche- was able to produce similar features in the experimental spectra (Figure 5.13).

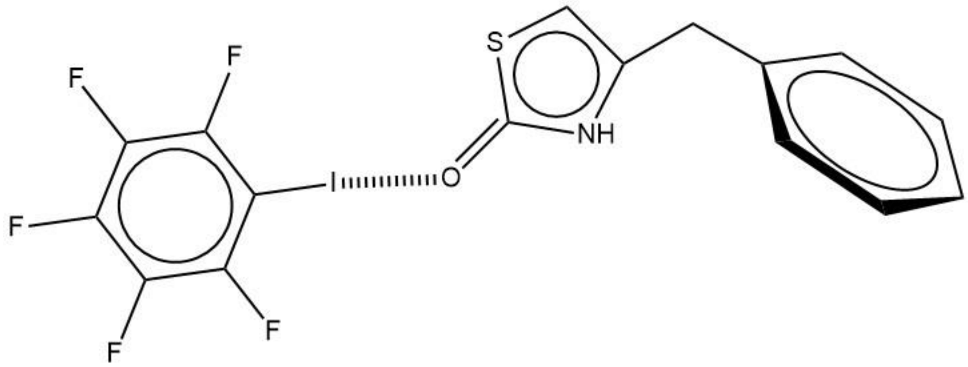

Figure 5.13. Structures and special positions of the gauche- NOS and F_5BnI during the process of the halogen bond interaction.

Study of interaction between available conformers and the F_5BnI was carried out to find out the structures of interacting species. For this reason, two sites on interaction for each conformer were studied. These two sites which incorporate different steric and electronic properties are *cis* and *trans* defined for each conformer. Cis interaction includes interaction of F_5BnI approaching from N-H side to the 4-benzyl-1,3-thiazolidine-2-one molecule. This site has possibility of interaction with the hydrogen of N-H functionality as well as the carbonyl group. Such interaction was confirmed previously. Trans interaction includes interaction of F_5BnI approaching from the opposite side of the molecules that is away from the N-H functionality. Generation of a negative VCD signal around 1700 cm^{-1} for the S enantiomer could only be derived from either the monomer form of NOS or the gauche – conformer with F_5BnI at the trans position (Figure 5.14).

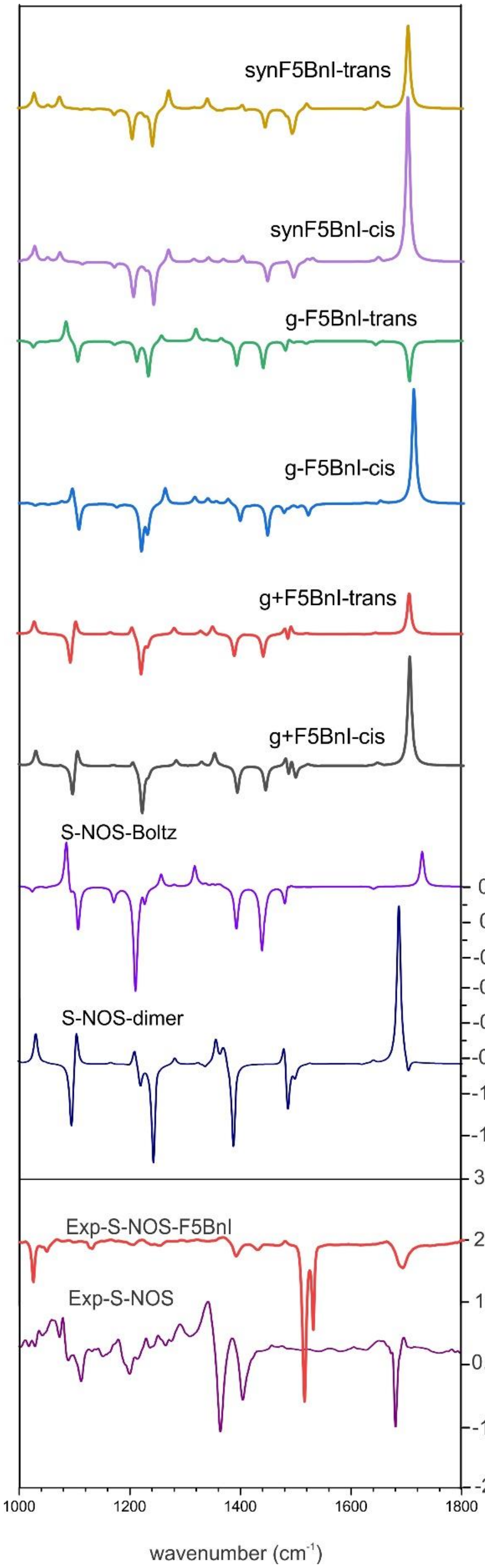

Figure 5.14. Comparison of the experimental and calculated VCD of of NOS and NOS-F5BnI in 1000 cm^{-1}- 1800 cm^{-1}. S-NOS dimer refers to the g- dimer.

5.4 Conclusion

The interaction between NOS as the halogen bond donor and F_5BnI as the halogen bond acceptor did not show a meaningful shift in the infrared spectroscopy of the titration of these moieties. The shielding of the N-H proton in the ^{1}H-NMR signals also was similar to what was observed for interaction between the NOS and iodine. ^{19}F-NMR showed a slight deshielding effect upon addition of the F_5BnI to the solution. However with the aid of the VCD spectroscopy and the calculations we could find out the most probable structure which is responsible for the interaction between the donor and acceptor species.

5.5 References

1. Guthrie, F., XXVIII.—On the iodide of iodammonium. *Journal of the Chemical Society* **1863,** *16* (0), 239-244.

2. Clark, T.; Hennemann, M.; Murray, J. S.; Politzer, P., Halogen bonding: the sigma-hole. *J. Mol. Model.* **2007,** *13* (2), 291-296.

3. Carlsson, A. C. C.; Uhrbom, M.; Karim, A.; Brath, U.; Grafenstein, J.; Erdelyi, M., Solvent effects on halogen bond symmetry. *Crystengcomm* **2013,** *15* (16), 3087-3092.

4. (a) Tsuzuki, S.; Wakisaka, A.; Ono, T.; Sonoda, T., Magnitude and Origin of the Attraction and Directionality of the Halogen Bonds of the Complexes of C_6F_5X and C_6H_5X (X=I, Br, Cl and F) with Pyridine. *Chem.-Eur. J.* **2012,** *18* (3), 951-960; (b) Pinter, B.; Nagels, N.; Herrebout, W. A.; De Proft, F., Halogen Bonding from a Hard and Soft Acids and Bases Perspective: Investigation by Using Density Functional Theory Reactivity Indices. *Chem.-Eur. J.* **2013,** *19* (2), 518-529.

5. Kozuch, S.; Martin, J. M. L., Halogen Bonds: Benchmarks and Theoretical Analysis. *J. Chem. Theory Comput.* **2013,** *9* (4), 1918-1931.

6. (a) Murray, J. S.; Lane, P.; Politzer, P., Expansion of the sigma-hole concept. *J. Mol. Model.* **2009,** *15* (6), 723-729; (b) Politzer, P.; Murray, J. S.; Clark, T., Halogen

bonding and other sigma-hole interactions: a perspective. *Phys. Chem. Chem. Phys.* **2013,** *15* (27), 11178-11189.

7. Cavallo, G.; Metrangolo, P.; Milani, R.; Pilati, T.; Priimagi, A.; Resnati, G.; Terraneo, G., The Halogen Bond. *Chem. Rev.* **2016,** *116* (4), 2478-2601.

8. (a) Alkorta, I.; Elguero, J.; Denisov, G. S., A review with comprehensive data on experimental indirect scalar NMR spin-spin coupling constants across hydrogen bonds. *Magnetic Resonance in Chemistry* **2008,** *46* (7), 599-624; (b) Aliev, A. E.; Harris, K. D. M., Probing hydrogen bonding in solids using solid state NMR spectroscopy. In *Supramolecular Assembly Via Hydrogen Bonds I*, Mingos, D. M. P., Ed. 2004; Vol. 108, pp 1-53; (c) Brunner, E.; Sternberg, U., Solid-state NMR investigations on the nature of hydrogen bonds. *Progress in Nuclear Magnetic Resonance Spectroscopy* **1998,** *32*, 21-57; (d) Wu, G.; Freure, C. J.; Verdurand, E., Proton chemical shift tensors and hydrogen bond geometry: A H-1-H-2 dipolar NMR study of the water molecule in crystalline hydrates. *J. Am. Chem. Soc.* **1998,** *120* (50), 13187-13193.

9. (a) Larsen, D. W.; Allred, A. L., Halogen Complexes. III. The Association of 2,4,6-Trimethylpyridine and Trifluoroiodomethane. *J. Phys. Chem.* **1965,** *69* (7), 2400-&; (b) Bruno, T. J.; Martire, D. E.; Harbison, M. W. P.; Nikolic, A.; Hammer, C. F., Gas-liquid chromatographic and nuclear magnetic resonance study of haloform + di-n-alkyl ether + n-alkane mixtures at 30.degree. *J. Phys. Chem.* **1983,** *87* (13), 2430-2436; (c) Martire, D. E.; Sheridan, J. P.; King, J. W.; Odonnell, S. E., Thermodynamics of molecular association. 9. An NMR study of hydrogen bonding of chloroform and bromoform to di-n-octyl ether, di-n-octyl thioether, and di-n-octylmethylamine. *J. Am. Chem. Soc.* **1976,** *98* (11), 3101-3106; (d) Green, R. D.; Martin, J. S., Anion-molecule complexes in solution. I. Nuclear magnetic resonance and infrared studies of halide ion-trihalomethane association. *J. Am. Chem. Soc.* **1968,** *90* (14), 3659-&; (e) Bertran, J. F.; Rodriguez, M., Detection of halogen bond formation by correlation of proton solvent shifts. 1. Haloforms inn-electron donor solvents. *Organic Magnetic Resonance* **1979,** *12* (2), 92-94; (f) Bertran, J. F.; Rodriguez, M., Detection of halogen bond formation by correlation of proton solvent shifts. II—methylene halides inn-electron

donor solvents. *Organic Magnetic Resonance* **1980,** *14* (4), 244-246; (g) Messina, M. T.; Metrangolo, P.; Panzeri, W.; Ragg, E.; Resnati, G., Perfluorocarbon-hydrocarbon self-assembly. Part 3. Liquid phase interactions between perfluoroalkylhalides and heteroatom containing hydrocarbons. *Tetrahedron Lett.* **1998,** *39* (49), 9069-9072; (h) Metrangolo, P.; Panzeri, W.; Recupero, F.; Resnati, G., Perfluorocarbon-hydrocarbon self-assembly - Part 16. F-19 NMR study of the halogen bonding between halo-perfluorocarbons and heteroatom containing hydrocarbons. *Journal of Fluorine Chemistry* **2002,** *114* (1), 27-33; (i) Messina, M. T.; Metrangolo, P.; Navarrini, W.; Radice, S.; Resnati, G.; Zerbi, G., Infrared and Raman analyses of the halogen-bonded non-covalent adducts formed by alpha,omega-diiodoperfluoroalkanes with DABCO and other electron donors. *J. Mol. Struct.* **2000,** *524*, 87-94; (j) Tiers, G. V., Detection of oriented association via NMR dilution shifts in tetramethylsilane solvent. 4. Temperature coefficients for perfluoroalkyl halide systems. *Journal of Fluorine Chemistry* **2000,** *102* (1-2), 175-184; (k) Sarwar, M. G.; Dragisic, B.; Salsberg, L. J.; Gouliaras, C.; Taylor, M. S., Thermodynamics of Halogen Bonding in Solution: Substituent, Structural, and Solvent Effects. *J. Am. Chem. Soc.* **2010,** *132* (5), 1646-1653; (l) Sarwar, M. G.; Dragisic, B.; Sagoo, S.; Taylor, M. S., A Tridentate Halogen-Bonding Receptor for Tight Binding of Halide Anions. *Angew. Chem.-Int. Edit.* **2010,** *49* (9), 1674-1677; (m) Carlsson, A.-C. C.; Grafenstein, J.; Laurila, J. L.; Bergquist, J.; Erdelyi, M., Symmetry of N-X-N (+) halogen bonds in solution. *Chem. Commun.* **2012,** *48* (10), 1458-1460; (n) Carlsson, A.-C. C.; Grafenstein, J.; Budnjo, A.; Laurila, J. L.; Bergquist, J.; Karim, A.; Kleinmaier, R.; Brath, U.; Erdelyi, M., Symmetric Halogen Bonding Is Preferred in Solution. *J. Am. Chem. Soc.* **2012,** *134* (12), 5706-5715.

10. (a) Larsen, D. W.; Allred, A. L., Halogen Complexes. II. The Types and Mean Lifetimes of Complexes Formed by Iodine and 2,4,6-Trimethylpyridine. *J. Am. Chem. Soc.* **1965,** *87* (6), 1219-&; (b) Larsen, D. W.; Allred, A. L., Halogen Complexes. I. An Investigation by Nuclear Magnetic Resonance of Complexes Formed by Iodine and Some para-Substituted Phenyl Methyl Sulfides. *J. Am. Chem. Soc.* **1965,** *87* (6), 1216-&.

11. Beweries, T.; Brammer, L.; Jasim, N. A.; McGrady, J. E.; Perutz, R. N.; Whitwood, A. C., Energetics of Halogen Bonding of Group 10 Metal Fluoride Complexes. *J. Am. Chem. Soc.* **2011,** *133* (36), 14338-14348.

12. M. J. Frisch., G. W. Trucks, H. B. Schlegel, G. E. Scuseria, M. A. Robb, J. R. Cheeseman, G. Scalmani, V. Barone, B. Mennucci, G. A. Petersson, H. Nakatsuji, M. Caricato, X. Li, H. P. Hratchian, A. F. Izmaylov, J. Bloino, G. Zheng, J. L. Sonnenberg, M. Hada, M. Ehara, K. Toyota, R. Fukuda, J. Hasegawa, M. Ishida, T. Nakajima, Y. Honda, O. Kitao, H. Nakai, T. Vreven, J. A. Montgomery, Jr., J. E. Peralta, F. Ogliaro, M. Bearpark, J. J. Heyd, E. Brothers, K. N. Kudin, V. N. Staroverov, R. Kobayashi, J. Normand, K. Raghavachari, A. Rendell, J. C. Burant, S. S. Iyengar, J. Tomasi, M. Cossi, N. Rega, J. M. Millam, M. Klene, J. E. Knox, J. B. Cross, V. Bakken, C. Adamo, J. Jaramillo, R. Gomperts, R. E. Stratmann, O. Yazyev, A. J. Austin, R. Cammi, C. Pomelli, J. W. Ochterski, R. L. Martin, K. Morokuma, V. G. Zakrzewski, G. A. Voth, P. Salvador, J. J. Dannenberg, S. Dapprich, A. D. Daniels, Ö. Farkas, J. B. Foresman, J. V. Ortiz, J. Cioslowski, and D. J. Fox, Gaussian 09, Revision D.01. Gaussian, I., Wallingford CT, Ed. 2009.

13. (a) Becke, A. D., Density-functional exchange-energy approximation with correct asymptotic behavior. *Physical Review A* **1988,** *38* (6), 3098-3100; (b) Lee, C. T.; Yang, W. T.; Parr, R. G., Development of the Colle-Salvetti correlation-energy formula into a functional of the electron density. *Physical Review B* **1988,** *37* (2), 785-789; (c) Becke, A. D., Density-functional thermochemistry. III. The role of exact exchange. *J. Chem. Phys.* **1993,** *98* (7), 5648-5652.

14. Harihara.P. C; Pople, J. A., The influence of polarization functions on molecular orbital hydrogenation energies. *Theoretica Chimica Acta* **1973,** *28* (3), 213-222.

15. Tomasi, J.; Mennucci, B.; Cammi, R., Quantum mechanical continuum solvation models. *Chem. Rev.* **2005,** *105* (8), 2999-3093.

16. Chudzinski, M. G.; McClary, C. A.; Taylor, M. S., Anion Receptors Composed of Hydrogen- and Halogen-Bond Donor Groups: Modulating Selectivity With

Combinations of Distinct Noncovalent Interacitons. *J. Am. Chem. Soc.* **2011,** *133* (27), 10559-10567.

17. Tsuzuki, S,. Uchimaru, T,. Accuracy of intermolecular interaction energies, particularly those of hetero-atom containing molecules obtained by DFT calculations with Grimme's D2, D3 and D3BJ dispersion corrections. *Phys Chem Chem Phys*. **2020**, 22 (39), 22508-22519

CHAPTER 6

Interactions of Iodopentafluorobenzene with 4-benzyl-1,3-thiazolidine-2-thione in Solution

6.1 Introduction

In the past decade a specific intermolecular interaction which involves a halogen bond as the acceptor of electron density, also defined as σ-hole donor, has been widely researched.[3a] To emphasize the similarity of this interaction with the hydrogen bond, this interaction is called halogen bonding. Despite the structural similarities, halogen bonds are unique in terms of the directionality, tunability, hydrophobicity and the donor atom dimensions.[13] Such characteristics have allowed the halogen bond to compete or surrender to the hydrogen bond in the solution.[14] We previously defined Halogen bond (X-bond) as R–X bond which provides two sites for electrophilic and nucleophilic attacks. The first one is perpendicular to R–X and it is called the halogen bond and the latter one is along the R–X bond on the side of the halogen atom which is not considered as the halogen bond according to IUPAC definition (Figure 6.1)

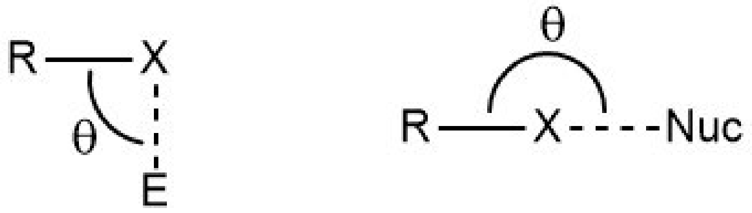

Figure 6.1. A Nucleophilic (left) and electrophilic (right) sites of R–X bond.

A schematic representation of the halogen bond is provided in figure 6.2.[1]

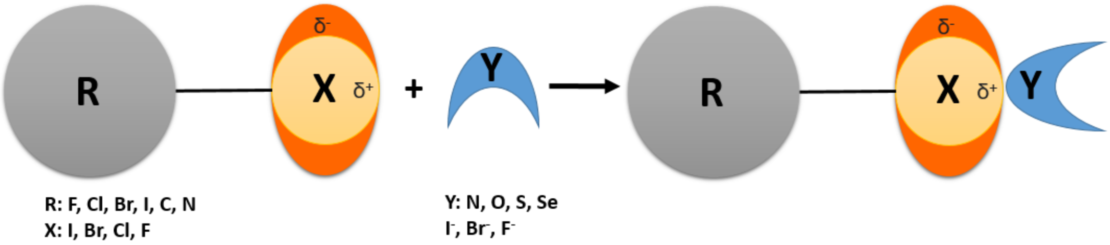

Figure 6.2. A schematic representation of the halogen bond bond.

More recently, computational methods have been applied to investigate the nature of X-bond interactions, leading to some significant progress.[15] The concept of "sigma hole" was developed to explain the X-bond donor,[2] analogous to the H-bond donor. The sigma hole represents an area with positive electrostatic potential along the covalent R-X bond where R can be F, Cl, Br, I, C, N and so on. Sigma hole is the consequence of anisotropic distribution of electron density along the same bond. This makes the radius of halogen atom smaller along the covalent C-X bond but larger on the perpendicular direction. Politzer, Murray and Clark[3] provided an atomic and molecular orbital view to demonstrate how the sigma hole is formed. Group VII atoms (halogens) have seven electrons in their p and s-orbitals of the valence shell which creates a configuration of $s^2p_x^2p_y^2p_z^1$ configuration where p_z is along the C-X bond to form a covalent bond with carbon. As a result, there is a depopulation of electron at this p_z orbital due to the formation of covalent bond with carbon, and a partial positive charge is created on the X atom. Since the electrons of the p_x and p_y are maintained around the C-X bond, an electron rich ring is created around the C-X bond.

Nuclear magnetic resonance (NMR) has aided the study of halogen bond formation. Wang et al. studied the X-bond interaction between C_6F_5Br and C_6F_5Cl with C_6D_6 and found out there is no X-bond interaction between C-Br or C-Cl and the phenyl π system and the only interaction was π…π between C_6F_5X (X: Cl, Br) and C_6D_6.[4] However, there was a X-bond interaction when C_6D_6 and C_6F_5I were in the solution. Interestingly there was no π…π interaction between C_6F_5I and C_6D_6.[4] Figure 6.3 demonstrates the competition sites in C_6F_5X (X: Cl, Br, I) in the interaction with C_6D_6.

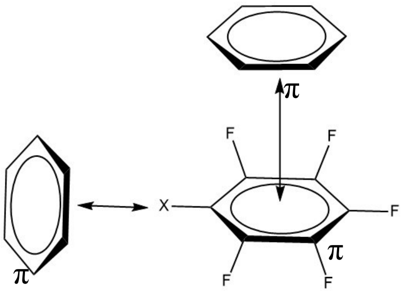

Figure 6.3. Available interaction sites for π…π interaction and X-bond interaction between C_6F_5X (X: Cl, Br, I) and C_6D_6. Blue region represents positive electrostatic potential (lower electron density) and the red surface represents negative electrostatic potential (higher electron density)[4].

Bryce et al. have performed single crystal ^{17}O-NMR and ^{31}P-NMR studies on the halogen bond interaction between triphenylphosphine oxide as X-bond acceptor and 1,4-diiodotetrafluorobenzene and1,3,5-trifluoro-2,4,6-triiodobenzene as halogen bond donors.[5] They found out that the angular deviations of the directions of the pseudo-unique components of the ^{31}P and ^{17}O chemical shift tensors, and the ^{17}O quadrupole coupling tensors is correlated to the deviations of the P=O···I halogen bond from a linear structure.[5] Among halogens, fluorine has ½ spin quantum number which makes it easier to study it by the solution NMR. Chemical shift of the binding sites or atoms close to the binding sites are correlated with the halogen bond interaction. There is always an equilibrium between the free molecules and the halogen bond complex. Now if the exchange rate between these two are smaller compared to the NMR timescale to detect the chemical shift difference; two types of NMR signal will appear related to the free and halogen bond complex.[6] However if the exchange rate is faster than the NMR time scale, one signal will be observed.[6a]

In order to evaluate the strength and the possibility of formation of halogen bond from different acceptor sites, we have chosen a system capable of providing halogen bonding, hydrogen bonding, as well as π bonding sites. As a result we will be able to compare the extent of interaction between an electron deficient site (iodine of Iodopentafluorobenzene) and an electron rich site (thiocarbonyl) and observe the effect of such interaction on the absolute configuration of the electron rich molecule. Thus, 4-benzyl-1,3-thiazolidine-2-thione, abbreviated as NSS is used to interact with Iodopentafluorobenzene abbreviated as F_5BnI (Figure 6.4).

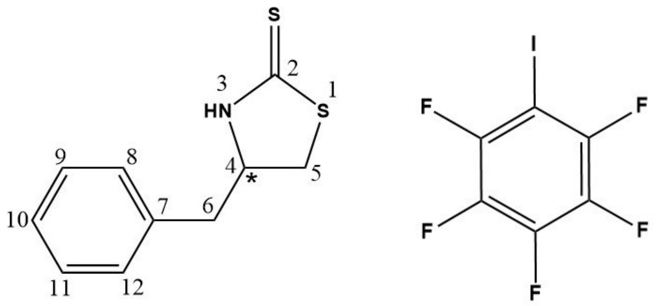

Figure 6.4. Chemical structures of 4-benzyl-1,3-thiazolidine-2-thione (NSS) (left) and Iodopentafluorobenzene (F_5BnI) (right).

4-benzyl-1,3-thiazolidine-2-thione has two delocalized π bond systems on benzene ring and N-C=S conjugated system and a thiocarbonyl functionality. Each of the three π systems can act as the acceptor site in the interaction with Iodopentafluorobenzene. 4-benzyl-1,3-thiazolidine-2-thione molecules can form hydrogen bonds in the solution so we would be able to compare the strength of the halogen with hydrogen bond in the solution. To reduce the interference with the solvent, chloroform and carbon tetrachloride have been chosen as the solvent throughout the study. This system, due to its size, would be suitable for ab-initio and DFT studies.

6.2 Experimental and Theoretical Details

4-benzyl-1,3-thiazolidine-2-thione was purchased from Astatech. F_5BnI was purchased from Sigma-Aldrich. ^{1}H-NMR and ^{19}F-NMR spectra of the compounds were recorded on a Bruker (400 MHz) spectrometer to confirm the purity of reagents. VA and VCD spectra were measured using a Bruker FTIR (Vertex 70) spectrometer equipped with a PMA 50 module for VCD measurements. The data were collected at 4 cm^{-1} resolution in the wavenumber region of 1700-1100 cm^{-1} using a liquid nitrogen cooled MCT detector for a period of 5 hours (~4300 scans per hour). A range of solutions were used for the VA and VCD measurements. The solution samples were placed between a pair of BaF_2 windows with a path-length of 0.1 mm, 0.015mm and 0.005mm. The Gaussian 09 program package[7] was used for all geometrical searches and optimizations, harmonic frequency calculations, and VA and VCD intensity predictions using density functional theory (DFT).[8] Becke three parameters, Lee-Yang-Parr, functional (B3LYP)[8] and 6-311++G(d,p)[9] was used for the calculations. Polarizable continuum model (PCM) using the universal force field radii was used to account for the bulk solvent environment[10] of $CDCl_3$. A Lorentzian line shape with a half-width at half-height of 4 cm^{-1} was used for the simulations of VA and VCD spectra VCD spectra.

6.3 Results and Discussions

6.3.1 Dispersion effect and the relative stability of conformers of NOS

Previous study of the conformers of the 4-benzyl-1,3-thiazolidine-2-thione yielded three conformers gauche-, gauche+ and syn (Figure 6.5).

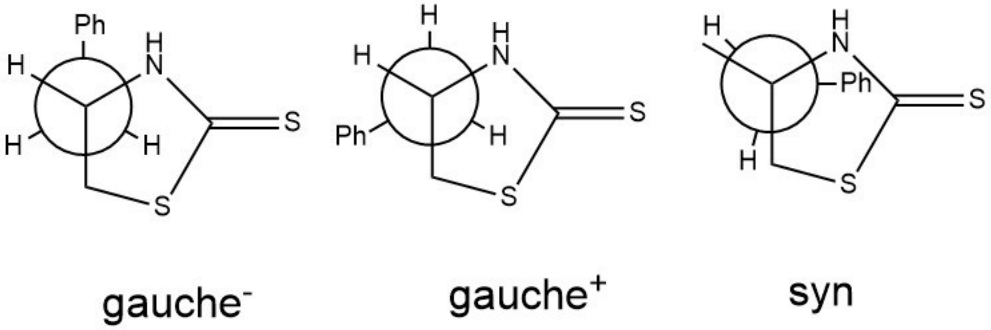

Figure 6.5. Newman projection of conformers of 4-benzyl-1,3-thiazolidine-2-thione (NSS).

Since relative stability of the conformers are determined by the volume of the groups participating in the gauche interaction with C_7, empirical dispersion correction D3BJ[16] was introduced to see the effect of the relative stability of the conformers. Figure 6.6 demonstrates the relative stability of the conformers. Exact values are brought in Table 6.1.

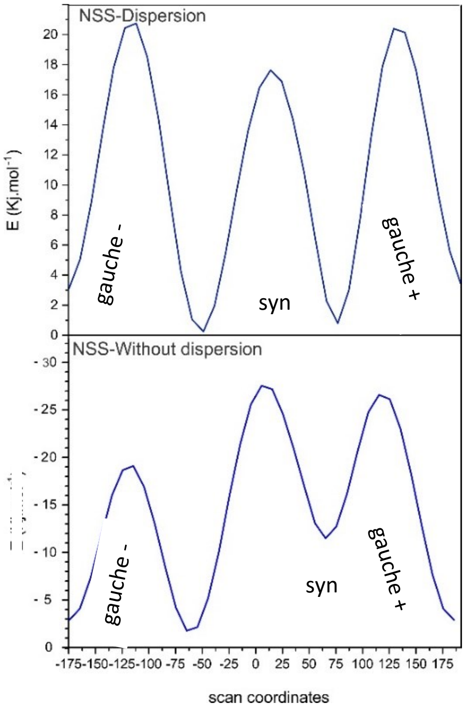

Figure 6.6. Relative stability of conformers of NSS in kJ.mol^{-1}. Scan coordinates is the dihedral angle of N-C_4-C_6-C_7 scanned over 360°. Energy of the conformer with the lowest energy is defined as zero.

The gauche- conformer is 2.7 kJ mol^{-1} and 0.8 kJ. mol^{-1} more stable than the gauche+ and syn conformers with the dispersion effect, respectively. Such an energy gap has made gauche- conformer with the highest Boltzmann population (Table 6.1). Applying the dispersion effect changed the relative stability of the conformers for this molecule.

Table 6.1 Comparison of the relative Energies and Boltzmann Distribution of Conformers of NSS

Conformer	ΔE (kJ. mol^{-1}) With||Without dispersion	%Boltzmann Distribution With||Without dispersion
gauche-	0||0	62.5||67
gauche+	2.7||1.3	20.35||32.2
syn	0.8||9.5	17.15||0.8

6.3.2 ^{1}H-NMR and ^{19}F-NMR Study of NSS

To evaluate the interaction between F_5BnI and 4-benzyl-1,3-thiazolidine-2-thione ^{1}H-NMR and ^{19}F-NMR titrations were carried out in $CDCl_3$. NSS shows a shielding pattern with occurs below 7.7 ppm for the N-H proton of this molecule. The shielding effect upon addition of F_5BnI which moves the N-H proton into the aromatic region is demonstrated in Figure 6.7.

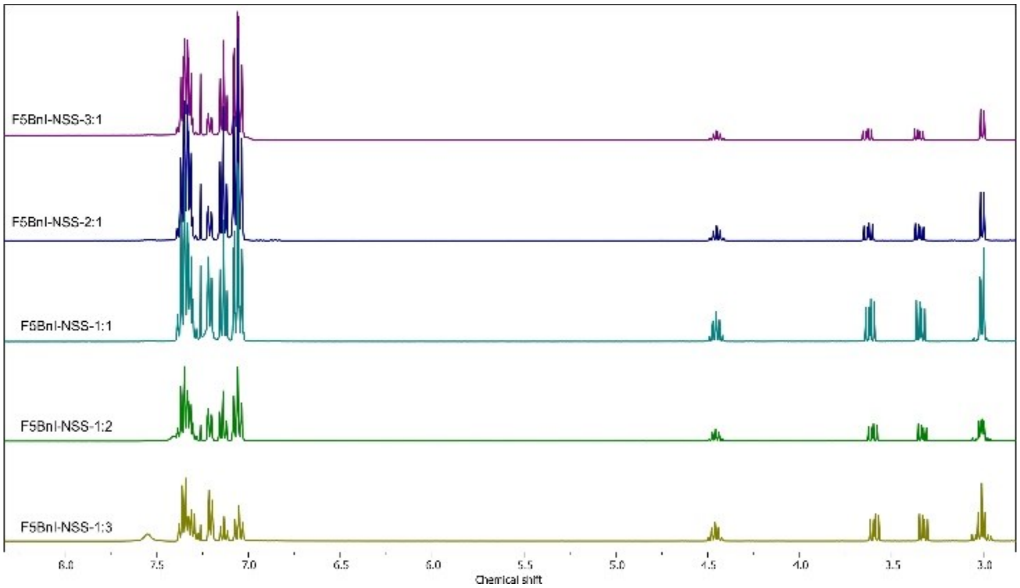

Figure 6.7. Shielding effect on N-H proton of NSS upon interacting with various concentrations of F_5BnI. Ratios from the bottom are F_5BnI/NSS:1/3; F_5BnI/NSS:1/2; F_5BnI/NSS:1; F_5BnI/NSS:2; F_5BnI/NSS:3.

^{19}F-NMR data allows to monitor the changes of the electron density around each of the fluorine atoms. Para fluorine was monitored during the titration experiments and experiments and ratios of F_5BnI/NOS varied among 1/3, 1/2, 1, 2, and 3 values and the respective para-F shifts were 152.08, -152.09, -152.06, -152.06, and -152.05 respectively as illustrated in (Fig 6.8). Initial concentration of NSS solution was 0.238 M in $CDCl_3$ and the concentration of F_5BnI was adjusted to provide the required ratio between F_5BnI and the NSS.

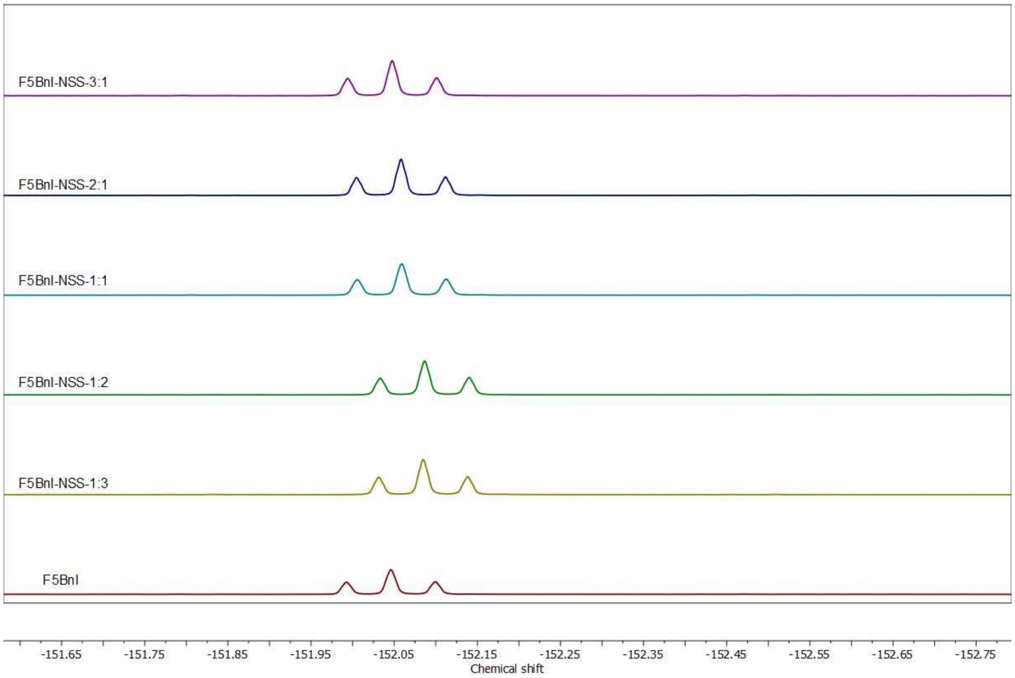

Figure 6.8. Changes in the chemical shifts of Para-F of NSS upon interacting with various concentrations of F_5BnI. Ratios from the bottom are $F_5BnI/NSS:1/3$; $F_5BnI/NSS:1/2$; $F_5BnI/NSS:1$; $F_5BnI/NSS:2$; $F_5BnI/NSS:3$.

^{19}F-NMR signals shows various behaviors depending on the environment and the type of interaction they are involved with. Halo-perfluorocarbons could show ^{19}F-NMR signals that might not be distinguishable from the ones in the presence of the trace amount of halogen bond acceptors and in dilute solutions.[11] Lunghi and his coworkers studied the formation of complex between diiodoperfuoroalkanes as the halogen bond donor and 1,4,10,13-tetraoxa-7,16-diazacyclooctadecane or with 4,7,13,16,21,24-hexaoxa- 1,10-diazabicyclo [8,8,8]hexacosane as the halogen bond acceptors (Figure 6.9).[11]

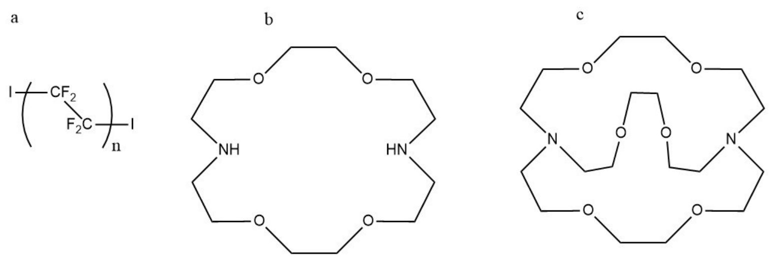

Figure 6.9. Chemical structures of a) diiodoperfuoroalkanes (n=1,2,3,4) as the halogen bond donor and b) 1,4,10,13-tetraoxa-7,16-diazacyclooctadecane and c) 4,7,13,16,21,24-hexaoxa- 1,10-diazabicyclo [8,8,8]hexacosane as the halogen bond acceptors.

The ^{19}F-NMR spectra of the complexes of a with b and c, to form [ab] or [ac] complexes, showed an upfield shift compared to the diiodoperfuoroalkanes. Dilution experiments on the above mixtures shifted back (downfield) the chemical shift of the CF_2I group to the pure diiodoperfuoroalkane signal where it could not be distinguished with the original diiodoperfuoroalkanes signal. Change in the chemical shifts were acquired by subtracting the ^{19}F-NMR signal of the complex from the ^{19}F-NMR signal of the pure diiodoperfuoroalkanes. Decreasing the concentration of the [ab] complex where n=1 from 0.13M to 0.04M, reduced the change in the chemical shift from 1.24 ppm to 0.55 ppm, and decreasing the concentration of the [ac] complex where n=1 from 0.13M to 0.03M, reduced the change in the chemical shift from 0.51 ppm to 0.11 ppm. Metrangolo and his coworkers found out that upon increasing the concentration of the halogen bond donor, an upfield in the ^{19}F-NMR signal is observed.[12] They did not observe any signal splitting or broadening feature in the ^{19}F-NMR signals which is due the rapid equilibrium between the donor and acceptor species compared to the NMR time scale. In this study 1,8-diiodo- and 1,8-dibromoperfluorooctane was the halogen bond donor and variety of binding and non-binding solvents (such as 1-Methylpiperidine; tetrahydrofuran; pyridine; etc) as the halogen bond acceptors. The halogen bonding between the electron deficient halide atoms of the dihalo-PFCs and the donor sites of the relevant solvents moved the ^{19}F-NMR signals upfield. The change in the chemical shift of the ^{19}F-NMR signals of 1,8-diiodo- and 1,8-dibromo- and 1,8-dichloro- and1 1,8-difluoroperfluorohexanes (Figure 6.10) showed the decrease on moving from diiodo- to dichloro- substituted moieties. Thus the ^{19}F-NMR signal could be used as a tool to show the extent of interaction between the donor and acceptor species in the solution.

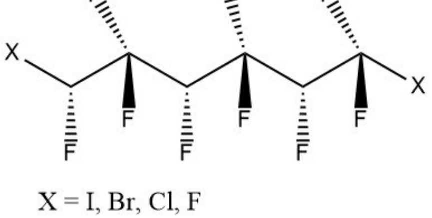

X = I, Br, Cl, F

Figure 6.10. Structures of the 1,8-diiodo- and 1,8-dibromo- and 1,8-dichloro- and1 1,8-difluoroperfluorohexanes.

In the same study Metrangolo and his coworkers found out that iodo- and bromoperfuoroarenes (Figure 6.11) behave in a similar way to the iodo- and bromoperfuoroalkanes.

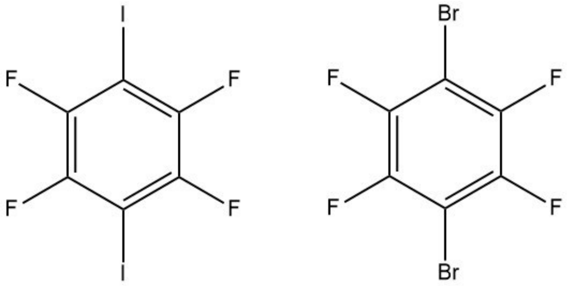

Figure 6.11. Structures of the iodo- and bromoperfuoroarenes used in the study.

It was observed that iodoarene showed a larger shift of the ^{19}F-NMR signal than the bromoarene. They also found out that nitrogen is a better donor than oxygen and sulfur. This shows that the iodine would be a better candidate than other halides to act as the halogen bond donor.

6.3.3 IR Study of NSS-F$_5$BnI Interaction

IR study of NSS with various concentration ratios of F$_5$BnI in CDCl$_3$ unlike the interaction with I$_2$ did not show an extra peak around 3310 cm^{-1}. However, the region of 3125cm^{-1}-3450cm^{-1} which includes a broader band distinctive of NSS dimer and monomer species does not show a significant change (Figure 6.12)

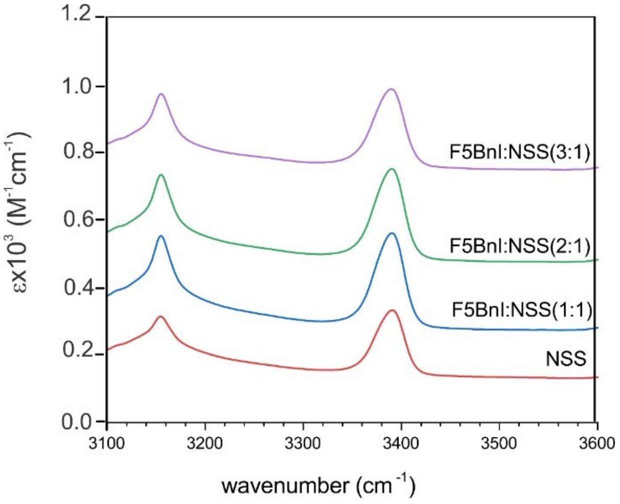

Figure 6.12. NH stretching region of NSS.

The broad peak at the N-H region confirms the formation of $(NSS)_2$ at lower and higher concentrations of F_5BnI in the solution. This region does not show formation of a new band which means there is no detectable interaction with the NH proton in this region. Infrared analysis of the optimized structures of NSS and $(NSS)_2$ was performed to find the best model to define structural behavior in this region (Figure 6.13).

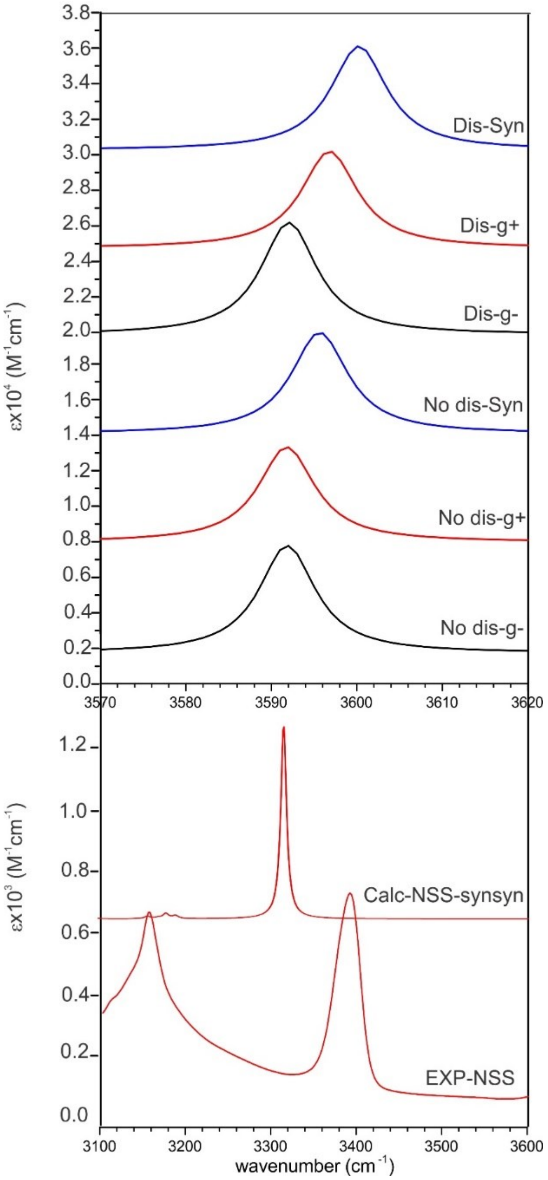

Figure 6.13. Comparison of selected calculated structures with the experimental data in the NH stretching region of NSS with and without dispersion effect.

The synsyn dimer conformation was selected due to its relative stability compared to other conformers. Table 6.2 demonstrates the relative energies and Boltzmann distribution of possible dimeric species of NSS with and without dispersion effect.

Table 6.2 Relative energies and Boltzmann distribution of NSS dimers formed from different conformers

Conformer	ΔE (kJ .mol^{-1}) With||Without dispersion	%Boltzmann Distribution With||Without dispersion
g-g-	3.64||11.05	10.36||1.06
g+g-	4.73||7.32	6.67||4.82
g+g+	1.96||0	20.43||92.66
g+syn	2.96||10.82	13.63||1.17
g-syn	6.12||15.07	3.80||0.21
synsyn	0||18.04	45.09||0.063

Thiocarbonyl stretching frequency had overlap with several other peaks and it was not possible to monitor the changes of this functional group during the spectroscopic measurements. Thus to increase our knowledge on the interaction between the NSS and the F_5BnI we further probed the bending frequency region of the NH functionality. According to our previous study monomeric form of the NSS demonstrates two bands next to one another between 1480 cm^{-1} and 1520 cm^{-1}. The NH bending bands show a blue shift to higher frequency upon introduction of F_5BnI to the solution. Figure 6.14 illustrates the difference between the location and shape of this peak among possible conformers.

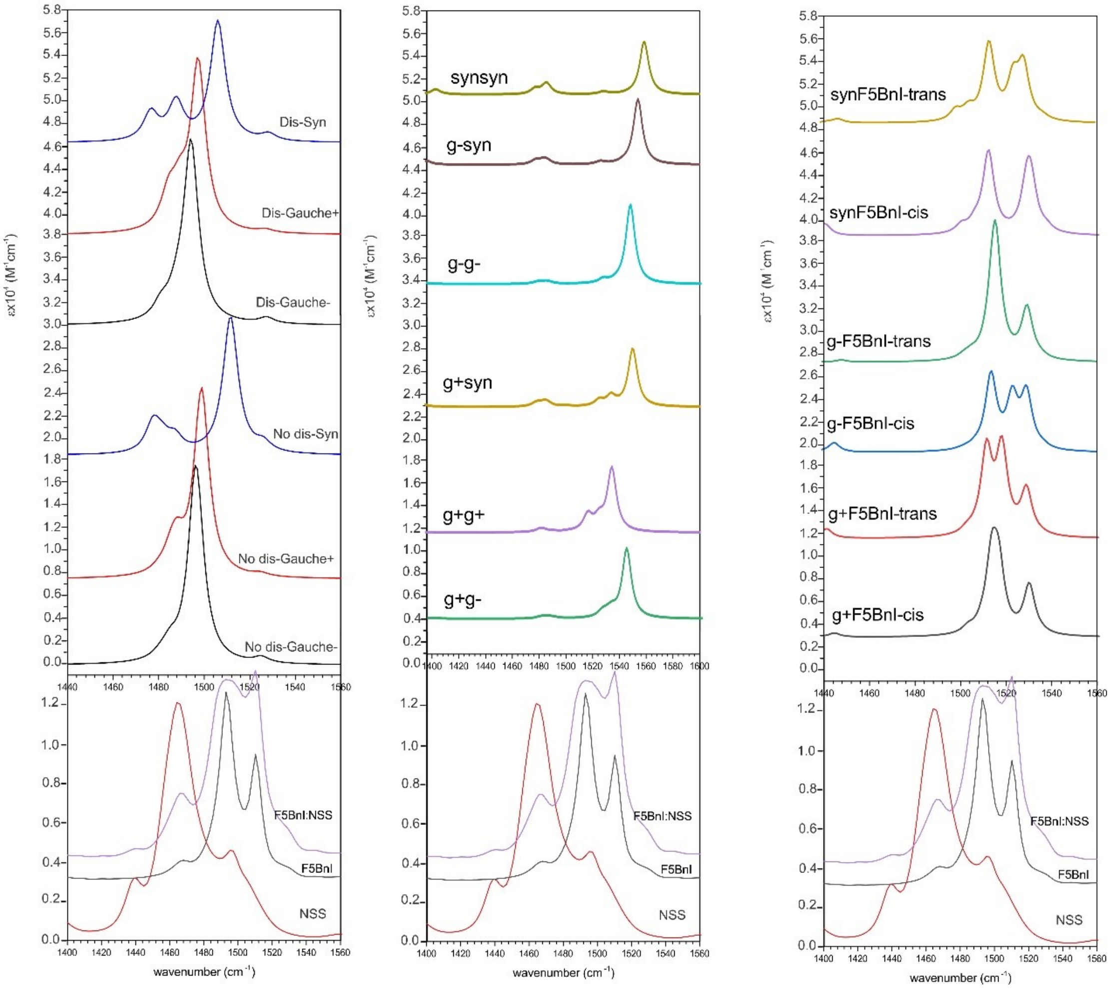

Figure 6.14. Comparison of the bending region of N-H in the experimental data (at the bottom) with the simulated spectra. The simulated spectra on the left illustrates with and without dispersion effect. The two simulated spectra on the right illustrate with the dispersion effect. The NH bending has shifted toward higher frequencies upon addition of the F_5BnI to the solution.

In the dimer these peaks appear at 1520cm^{-1} and 1580 cm^{-1} in the calculated data. Looking at the energetics of dimers we see that the g+g+ and synsyn dimers have the highest population among dimers with and without the dispersion effect. Now if we take a look at the trends of the energetics among possible conformers of the NSS-F_5BnI complex the following trend in Table 6.3 is observed.

Table 6.3 Relative energies and Boltzmann distribution of NSS-F_5BnI complexes formed from different conformers

Conformer	ΔE (kJ .mol^{-1}) With‖Without dispersion	%Boltzmann Distribution With‖Without dispersion
g-F_5BnI-cis	0‖1.08	94.78‖31.39
g- F_5BnI-trans	13.74‖5.71	0.36‖4.83
g+ F_5BnI-cis	16.80‖3.01	0.10‖14.39
g+ F_5BnI-trans	13.01‖0	0.49‖48.5
syn F_5BnI-cis	8.88‖12.01	2.62‖0.38
syn F_5BnI-trans	9.96‖11.72	1.69‖0.42

Although this table shows that g+F_5BnI-trans (without dispersion) and g-F_5BnI-cis (with dispersion) are favored energetically for the interaction between the two moieties, several possible conformers could be responsible for the change of the energy of NH bending mode upon addition of the F_5BnI to the NSS solution.

6.3.4 VCD Study

VCD study of NSS-F_5BnI was done at the same level of concentration as the NSS. Figure 6.15 shows the infrared and VCD spectrum of NSS- F_5BnI solution.

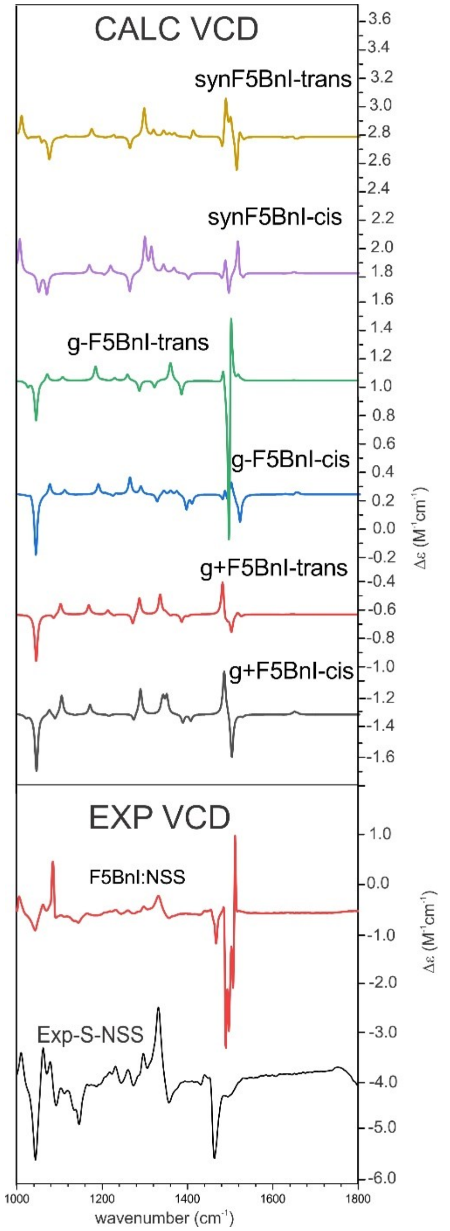

Figure 6.15. VCD of of NSS-F5BnI in 1000 cm^{-1}- 1800 cm^{-1} and the simulated possible conformer interactions.

Comparison between the acquired VCD spectra and the simulated data in Figure 6.16 shows that the signal of the bending region can be reproduced by g-F_5BnI-trans and syn-F_5BnI-cis.

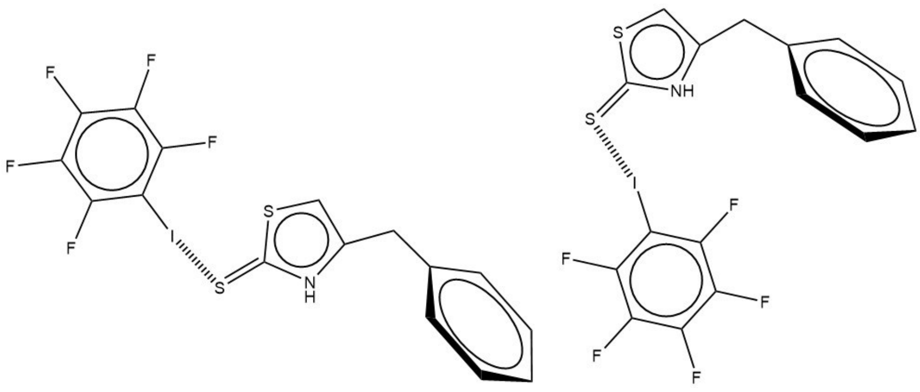

Figure 6.16. Structures of the g-F5BnI-trans and syn-F5BnI-cis.

6.4 Conclusion

^{1}H-NMR data suggest a shielding process which was previously observed in the dilution experiments. On the contrary for this type of halogen bond donor there is not a considerable dilution effect since the donor is in pure liquid form. Thus we can attribute this shift to the interaction between the donor and acceptor species. ^{19}F-NMR data also confirms the interaction between the two species although the strength of the interaction is not high enough to make a considerable shift in the NMR signals. This interaction has not largely affected the stretching frequency of the NH band, but has made a considerable blue shift in the NH bending region. VCD spectra of the bending region is reproducible via the two conformers which are g-F$_5$BnI-trans and syn-F$_5$BnI-cis. Thus, these two conformers would be the dominant species in the interaction among the two molecules.

6.5 References

1. Cavallo, G.; Metrangolo, P.; Milani, R.; Pilati, T.; Priimagi, A.; Resnati, G.; Terraneo, G., The Halogen Bond. *Chem. Rev.* **2016,** *116* (4), 2478-2601.

2. Politzer, P.; Lane, P.; Concha, M. C.; Ma, Y. G.; Murray, J. S., An overview of halogen bonding. *J. Mol. Model.* **2007,** *13* (2), 305-311.

3. (a) Clark, T.; Hennemann, M.; Murray, J. S.; Politzer, P., Halogen bonding: the sigma-hole. *J. Mol. Model.* **2007,** *13* (2), 291-296; (b) Politzer, P.; Murray, J. S.; Lane, P., sigma-hole bonding and hydrogen bonding: Competitive interactions. *Int. J. Quantum Chem.* **2007,** *107* (15), 3046-3052.

4. Zhang, Y.; Ji, B.; Tian, A.; Wang, W., Communication: Competition between pi center dot center dot center dot pi interaction and halogen bond in solution: A combined C-13 NMR and density functional theory study. *J. Chem. Phys.* **2012,** *136* (14).

5. Xu, Y.; Gabidullin, B.; Bryce, D. L., Single-Crystal NMR Characterization of Halogen Bonds. *J. Phys. Chem. A* **2019,** *123* (29), 6194-6209.

6. (a) Hirose, K., A practical guide for the determination of binding constants. *Journal of Inclusion Phenomena and Macrocyclic Chemistry* **2001,** *39* (3-4), 193-209; (b) Thordarson, P., Determining association constants from titration experiments in supramolecular chemistry. *Chem. Soc. Rev.* **2011,** *40* (3), 1305-1323.

7. M. J. Firsch., G. W. Trucks, H. B. Schlegel, G. E. Scuseria, M. A. Robb, J. R. Cheeseman, G. Scalmani, V. Barone, B. Mennucci, G. A. Petersson, H. Nakatsuji, M. Caricato, X. Li, H. P. Hratchian, A. F. Izmaylov, J. Bloino, G. Zheng, J. L. Sonnenberg, M. Hada, M. Ehara, K. Toyota, R. Fukuda, J. Hasegawa, M. Ishida, T. Nakajima, Y. Honda, O. Kitao, H. Nakai, T. Vreven, J. A. Montgomery, Jr., J. E. Peralta, F. Ogliaro, M. Bearpark, J. J. Heyd, E. Brothers, K. N. Kudin, V. N. Staroverov, R. Kobayashi, J. Normand, K. Raghavachari, A. Rendell, J. C. Burant, S. S. Iyengar, J. Tomasi, M. Cossi, N. Rega, J. M. Millam, M. Klene, J. E. Knox, J. B. Cross, V. Bakken, C. Adamo, J. Jaramillo, R. Gomperts, R. E. Stratmann, O. Yazyev, A. J. Austin, R. Cammi, C. Pomelli, J. W. Ochterski, R. L. Martin, K. Morokuma, V. G. Zakrzewski, G. A. Voth, P. Salvador, J. J. Dannenberg, S. Dapprich, A. D. Daniels, Ö. Farkas, J. B. Foresman, J. V. Ortiz, J. Cioslowski, and D. J. Fox, Gaussian 09, Revision D.01. Gaussian, I., Wallingford CT, Ed. 2009.

8. (a) Becke, A. D., Density-functional exchange-energy approximation with correct asymptotic behavior. *Physical Review A* **1988,** *38* (6), 3098-3100; (b) Lee, C. T.; Yang, W. T.; Parr, R. G., Development of the Colle-Salvetti correlation-energy formula into a functional of the electron density. *Physical Review B* **1988,** *37* (2), 785-789; (c) Becke, A. D., Density-functional thermochemistry. III. The role of exact exchange. *J. Chem. Phys.* **1993,** *98* (7), 5648-5652.

9. Harihara.Pc; Pople, J. A., The influence of polarization functions on molecular orbital hydrogenation energies. *Theoretica Chimica Acta* **1973,** *28* (3), 213-222.

10. Tomasi, J.; Mennucci, B.; Cammi, R., Quantum mechanical continuum solvation models. *Chem. Rev.* **2005,** *105* (8), 2999-3093.

11. Lunghi, A.; Cardillo, P.; Messina, T.; Metrangolo, P.; Panzeri, W.; Resnati, G., Perfluorocarbon-hydrocarbon self assembling. Thermal and vibrational analyses of one-dimensional networks formed by alpha,omega-diiodoperfluoroalkanes with K.2.2. and K.2.2.2. *Journal of Fluorine Chemistry* **1998,** *91* (2), 191-194.

12. Metrangolo, P.; Panzeri, W.; Recupero, F.; Resnati, G., Perfluorocarbon-hydrocarbon self-assembly - Part 16. F-19 NMR study of the halogen bonding between halo-perfluorocarbons and heteroatom containing hydrocarbons. *Journal of Fluorine Chemistry* **2002,** *114* (1), 27-33.

13. (a) Saccone, M.; Cavallo, G.; Metrangolo, P.; Pace, A.; Pibiri, I.;Pilati, T.; Resnati, G.; Terraneo, G. Halogen Bond Directionality Translates Tecton Geometry into Self-Assembled Architecture Geometry. *CrystEngComm* **2013**, 15, 3102−3105 (b) Messina, M. T.; Metrangolo, P.; Panzeri, W.; Ragg, E.; Resnati, G. Perfluorocarbon-Hydrocarbon Self-Assembly. Part 3. Liquid Phase Interactions between Perfluoroalkylhalides and Heteroatom Containing Hydrocarbons. *Tetrahedron Lett.* **1998**, 39, 9069−9072 (c) Vargas Jentzsch, A.; Emery, D.; Mareda, J.; Metrangolo, P.; Resnati, G.; Matile, S. Ditopic Ion Transport Systems: Anion-π Interactions and Halogen Bonds at Work. *Angew. Chem., Int. Ed.* **2011**, 50, 11675−11678 (d) Huber, S. M.; Jimenez-Izal, E.; Ugalde, J. M.; Infante, I. Unexpected Trends in Halogen-Bond Based Noncovalent Adducts. *Chem. Commun.* **2012**, 48, 7708−7710.

14. Carlsson, A. C. C.; Uhrbom, M.; Karim, A.; Brath, U.; Grafenstein, J.; Erdelyi, M., Solvent effects on halogen bond symmetry. *Crystengcomm* **2013,** *15* (16), 3087-3092

15. Tsuzuki, S.; Wakisaka, A.; Ono, T.; Sonoda, T., Magnitude and Origin of the Attraction and Directionality of the Halogen Bonds of the Complexes of C_6F_5X and C_6H_5X (X=I, Br, Cl and F) with Pyridine. *Chem.-Eur. J.* **2012,** *18* (3), 951-960.

16. Tsuzuki, S,. Uchimaru, T,. Accuracy of intermolecular interaction energies, particularly those of hetero-atom containing molecules obtained by DFT calculations with Grimme's D2, D3 and D3BJ dispersion corrections. *Phys Chem Chem Phys*. **2020**, 22 (39), 22508-22519.

CHAPTER 7

Conclusions and Future Work

7.1 Conclusions

Understanding of the nature of the halogen bond in the solution has largely advanced in the recent years due to availability of different experimental and theoretical techniques. Such techniques would allow us to take a small step closer to the actual composition of the interacting species and try to reduce our uncertainties of the interacting structures in the dynamic of solution to some extent. Our current understanding of the dynamics of the solution could change in the future. In our study we have utilized experimental observation and theoretical modelling to develop our understanding of the nature of the halogen bond interaction and possible competition between the halogen bond and the hydrogen bond.

NOS has showed a higher tendency to participate in the inter-molecular hydrogen bonding through formation of a dimer. As a result iodine was not able to form a halogen bond with the NOS. When F_5BnI is used instead of iodine as the halogen bond donor we don't have the effect of dilution. Here we observed that the NH and carbonyl stretching frequencies did not show any shift during the interaction of the two species. However, we were able to observe a slight shift in the ^{19}F-NMR signal upon addition of the F_5BnI to the solution. ^{19}F-NMR is very sensitive to the environment and this could suggest a slight interaction between the two species. Although the reported ^{19}F-NMR signals in the literature among other halocarbons and haloarenes show a larger shift,[1] our interacting species may not be able to form a strong halogen bond between them. VCD is a sensitive technique which could provide deeper insight into the structure of interacting species when combined with the theoretical calculations. In order to produce the VCD signals of the interacting species gauche- conformer was suggested to interact with the F_5BnI from the trans position that is on the opposite side of the NH functionality.

NSS dimer on the other hand is not as strong as the NOS dimer and thus a better halogen bond acceptor for the iodine. Such interaction increases the energy gap between the HOMO and LUMO of the iodine molecule and as a result we observed a blue shift in the UV-vis spectroscopy. Both NH stretching and bending vibrations of NSS molecule showed a change in the shape of the spectrum indicative of the interaction between the donor and acceptor species.

NSS showed a different behavior while interacting with the F_5BnI. NH stretching band of the NSS did not show a change upon introduction of the F5BnI to the solution. Thiocarbonyl stretching frequency has overlap with other peaks and thus we were not able to monitor the change of this peak during the experiments. NH bending vibration however showed a blue shift upon addition of the F_5BnI to the solution. This peaked was probed with the simulated data and several possible conformers were suggested to be responsible for such a shift. By studying the energetics of the possible conformers we understood that not always the most stable structures are responsible for the observation of detected signals. VCD signals of the bending region of the NSS-F_5BnI can be produced through interaction of the F_5BnI with g- conformer from the trans position and the syn conformer from the cis position. These two conformers are not the most abundant ones among the possible conformers. ^{19}F-NMR signals also showed a similar trend to NOS here and we observed a slight upfield upon addition of F_5BnI to the solution. F_5BnI is not a chiral molecule and shows a doublet in the IR spectrum around 1510 cm^{-1}. We also observed that this doublet also appears in VCD spectrum of the NOS-F_5BnI (Figure 7.1), which could be a sign of chirality transfer from the NOS over to the halogen bond donor.

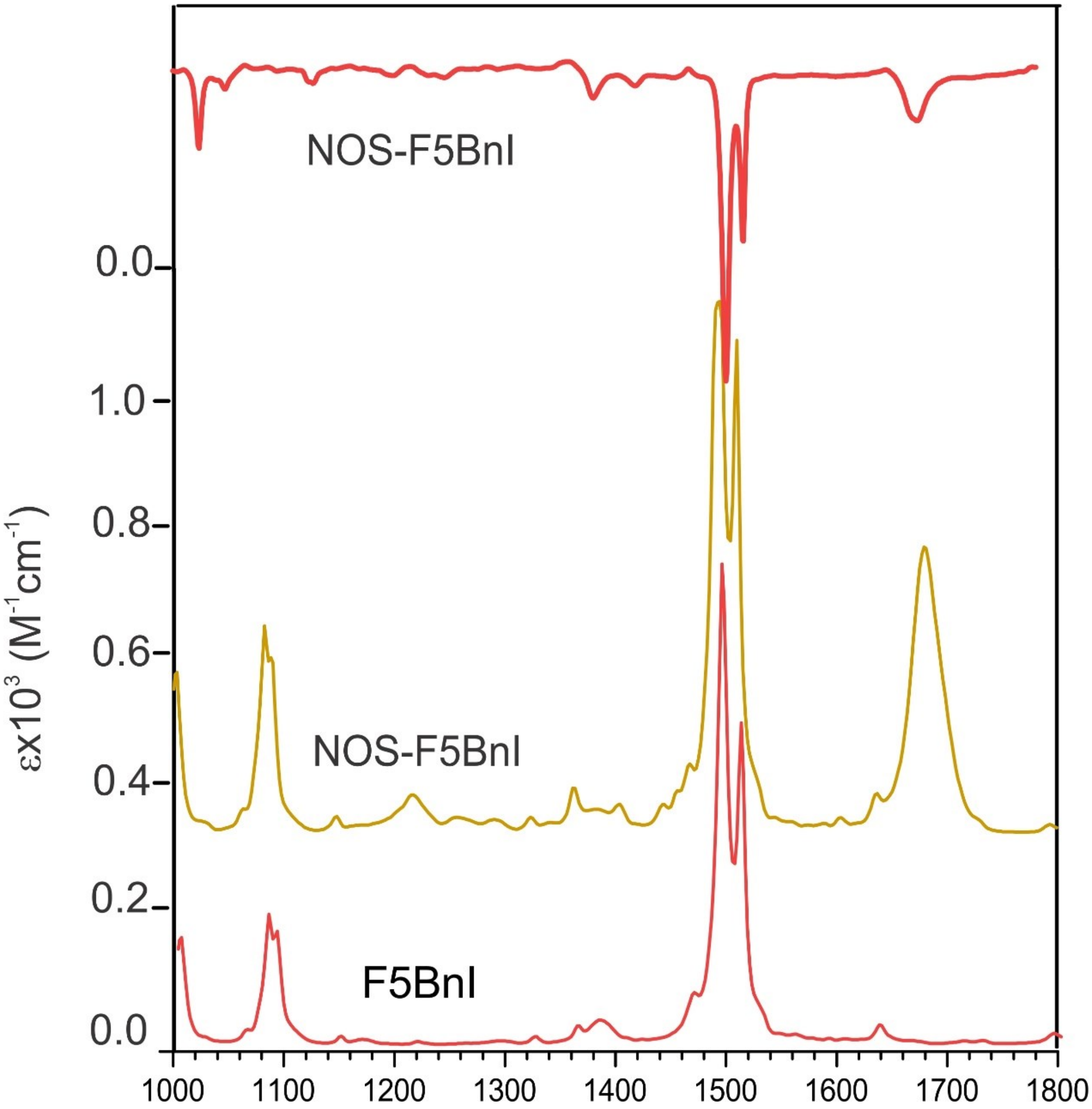

Figure 7.1. IR and VCD spectra of F_5BnI and NOS-F_5BnI.

7.2 Future work

Future work can be expanded through experimenting on various halogen bond donor and acceptor species and study their behavior through different spectroscopy and theoretical technics. One such halogen bond donor candidate is 1-(2-iodoethynyl)-4-methylbenzene) which could be used to study of the interaction of this molecule with the NOS and NSS (Figure 7.2).

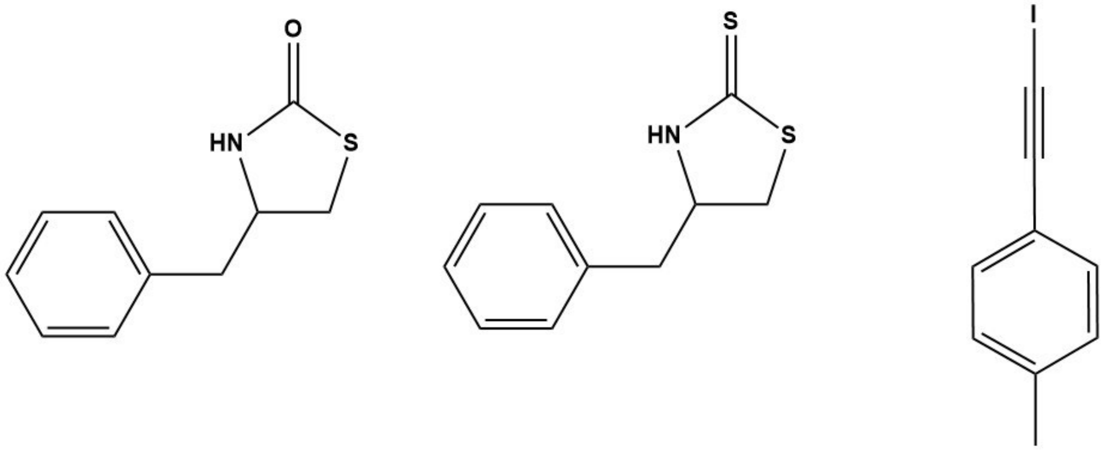

Figure 7.2. Chemical structures of NOS and NSS (left) and 1-(2-iodoethynyl)-4-methylbenzene (abbreviated as MeBnEtnl) (right).

Initial theoretical study on the trans MeBnEtnl complexes with NSS and NOS is done and is summarized in Table 7.1. This initial comparison showed that for the g- conformer of the NOS is more stable in trans complexation with the MeBnEtnl compared to g+ and syn conformers. However for the NSS, syn conformer was more stable in trans position complexation compared to g- and g+ conformers.

Table 6.1 Comparison of the relative energies and Boltzmann distribution of trans MeBnEtnl complexes with NOS B3LYP-6-311++G(d,p) with the dispersion effect.

Conformer	ΔE (kJ .mol^{-1}) Of the trans NOS interaction	ΔE (kJ .mol^{-1}) Of the trans NSS interaction
gauche-	0	2.68
gauche+	4.83	6.33
syn	9.94	0

Infrared and VCD spectra of the above complexes of NSS and NOS have been simulated. Figure 7.2 illustrates the relevant spectra of the NSS molecule.

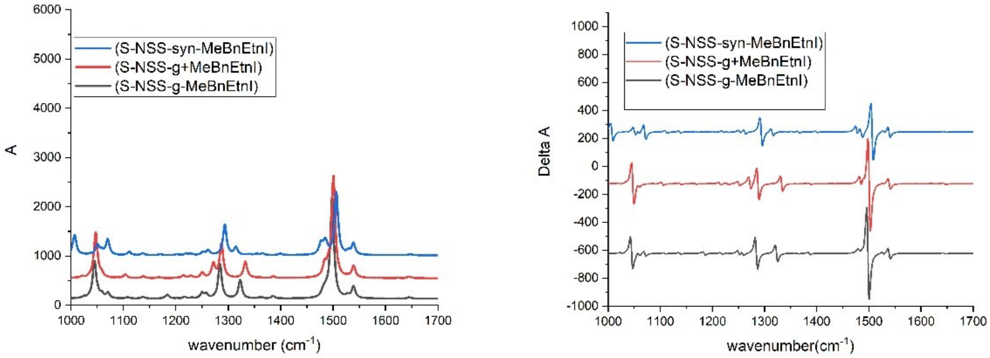

Figure 7.2. Simulated IR and VCD of spectra of trans interaction of the MeBnEtnl with NSS conformers.

In order to further justify the effect of the nature of the halogen bond acceptor on the formation of halogen bond it is also beneficial to probe this bond with different halogen bond acceptors. One such promising candidate is 1-phenylethylamine (Figure 7.3).

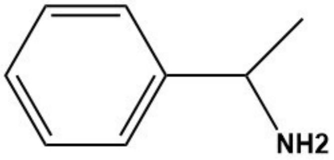

Figure 7.3. Chemical structures of 1-phenylethylamine.

1-phenylethylamine is able to compete with the halogen bond through formation of the inter-molecular hydrogen bond. Initial IR and VCD on this molecule have been performed (Figure 7.4).

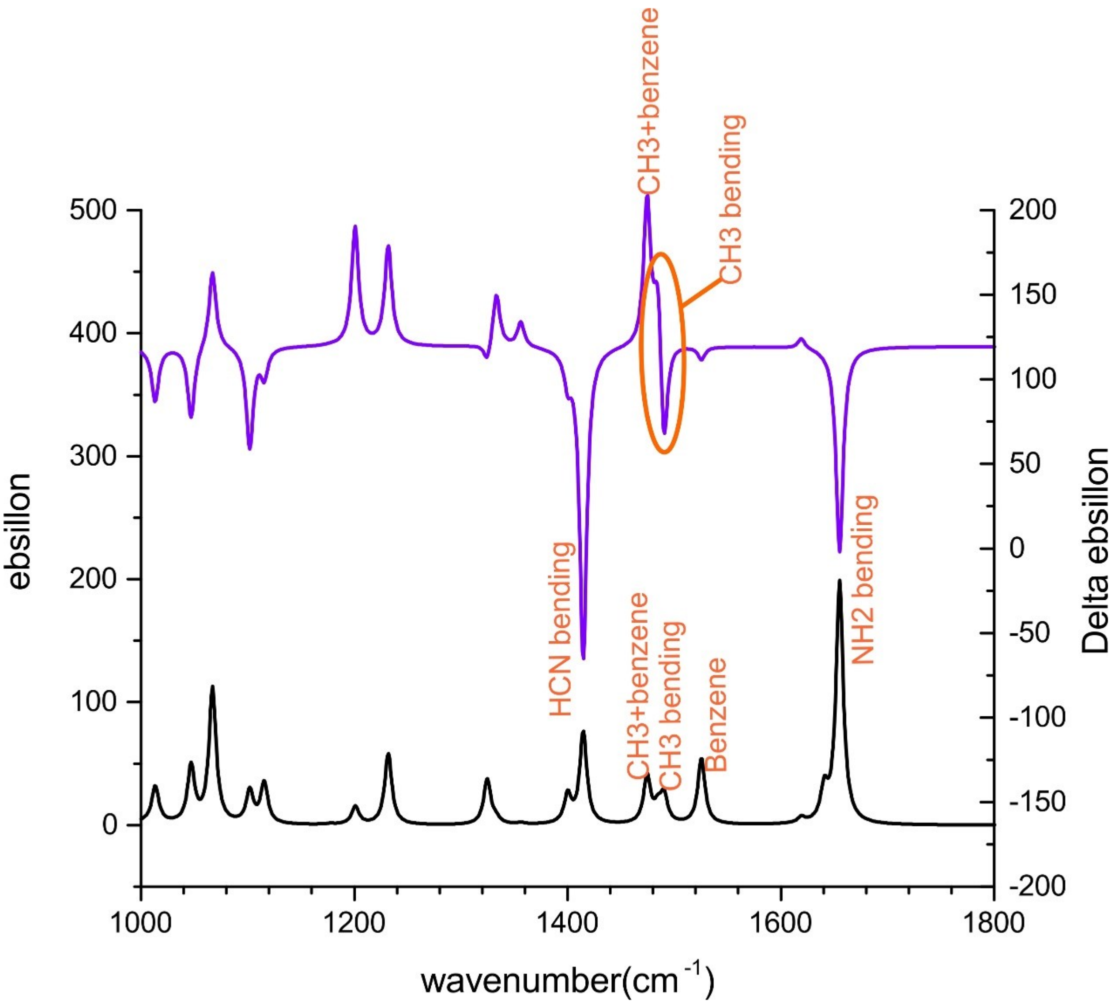

Figure 7.4. Illustration of the selected peaks in the IR and VCD of the 1-phenylethylamine in the range of 1000cm^{-1} to 1800 cm^{-1}.

Studying the halogen bond formation of the above halogen bond acceptor with halogen bond donors such as iodine, F5BnI, or MeBnEtnl could further expand the path of this study.

7.3 References

1. Metrangolo, P.; Panzeri, W.; Recupero, F.; Resnati, G., Perfluorocarbon-hydrocarbon self-assembly - Part 16. F-19 NMR study of the halogen bonding between halo-perfluorocarbons and heteroatom containing hydrocarbons. *Journal of Fluorine Chemistry* **2002,** *114* (1), 27-33

Bibliography

1. Guthrie, F., XXVIII.—On the iodide of iodammonium. *Journal of the Chemical Society* **1863,** *16* (0), 239-244.

2. Mulliken, R. S., Structures of Complexes Formed by Halogen Molecules with Aromatic and with Oxygenated Solvents. *J. Am. Chem. Soc.* **1950,** *72* (1), 600-608.

3. (a) Mulliken, R. S., Molecular Compounds and their Spectra. III. The Interaction of Electron Donors and Acceptors. *J. Phys. Chem.* **1952,** *56* (7), 801-822; (b) Mulliken, R. S., Molecular Compounds and their Spectra. II *J. Am. Chem. Soc.* **1952,** *74* (3), 811-824.

4. Hassel, O.; Hvoslef, J., The Structure of Bromine 1,4-Dioxanate. *Acta Chem. Scand.* **1954,** *8* (5), 873-873.

5. Eia, G.; Hassel, O., Structure of an Addition Compound Containing two Bromine Molecules and one Molecule of Hexamethylene Tetramine. *Acta Chem. Scand.* **1956,** *10* (1), 139-141.

6. (a) Hassel, O.; Stromme, K. O., Halogen-Molecule Bridges in Solid Addition Compounds. *Nature* **1958,** *182* (4643), 1155-1156; (b) Hassel, O.; Stromme, K. O., Crystal Structure of the 1:1 Addition Compound Formed by Acetone and Bromine. *Acta Chem. Scand.* **1959,** *13* (2), 275-280.

7. (a) Hassel, O.; Stromme, K. O., Crystal Structure of the Addition Compound 1,4-Dioxan-Chlorine. *Acta Chem. Scand.* **1959,** *13* (9), 1775-1780; (b) Hassel, O.; Hvoslef, J., Structure of an Addition Compound Containing two Molecules of Iodine Monochloride and One Molecule of 1,4-Dioxan. *Acta Chem. Scand.* **1956,** *10* (1), 138-139; (c) Hassel, O., The structure of addition compounds, especially those in which halogens act as electron-acceptors. *Proceedings of the Chemical Society of London*

1957, (9), 250-255; (d) Hassel, O.; Romming, C., Crystal Structure of the 1:1 Molecular Compound 1,4-Dioxan, Sulphuric Acid. *Acta Chem. Scand.* **1960,** *14* (2), 398-406; (e) Romming, C., The Crystal Structure of the 1:1 Addition Compound Formed by Benzyl Sulphide and Iodine. *Acta Chem. Scand.* **1960,** *14* (10), 2145-2151; (f) Chao, G. Y.; McCullough, J. D., 1960-The refinement of the structure of the complex of iodine with 1,4 dithiane. C4H8S2.2I2. *Acta Crystallographica* **1960,** *13* (9), 727-732; (g) Chao, G. Y.; McCullough, J. D., 1961-The refinement of the structure of the complex of iodine with 1,4-diselenane. C4H8SE2.2I2. *Acta Crystallographica* **1961,** *14* (9), 940-&; (h) McCullough, J. D., The structure of the compounds of iodine with 1,4 diselenane and 1,4 dithiane. *Acta Crystallographica* **1959,** *12* (10), 815-816.

8. Hassel, O., Structural Aspects of Interatomic Charge-Transfer Bonding. *Science* **1970,** *170* (3957), 497-&.

9. Lommerse, J. P. M.; Stone, A. J.; Taylor, R.; Allen, F. H., The nature and geometry of intermolecular interactions between halogens and oxygen or nitrogen. *J. Am. Chem. Soc.* **1996,** *118* (13), 3108-3116.

10. (a) Metrangolo, P.; Neukirch, H.; Pilati, T.; Resnati, G., Halogen bonding based recognition processes: A world parallel to hydrogen bonding. *Accounts Chem. Res.* **2005,** *38* (5), 386-395; (b) Rissanen, K., Halogen bonded supramolecular complexes and networks. *Crystengcomm* **2008,** *10* (9), 1107-1113.

11. Pearson, R. G., Hard and Soft Acids and Bases. *J. Am. Chem. Soc.* **1963,** *85* (22), 3533-&.

12. (a) Cametti, M.; Crousse, B.; Metrangolo, P.; Milani, R.; Resnati, G., The fluorous effect in biomolecular applications. *Chem. Soc. Rev.* **2012,** *41* (1), 31-42; (b) Cardillo, P.; Corradi, E.; Lunghi, A.; Meille, S. V.; Messina, M. T.; Metrangolo, P.; Resnati, G., The N center dot center dot center dot I intermolecular interaction as a general protocol for the formation of perfluorocarbon-hydrocarbon supramolecular architectures. *Tetrahedron* **2000,** *56* (30), 5535-5550; (c) Gilday, L. C.; Robinson, S. W.; Barendt, T. A.; Langton, M. J.; Mullaney, B. R.; Beer, P. D., Halogen Bonding in Supramolecular Chemistry. *Chem. Rev.* **2015,** *115* (15), 7118-7195; (d) Metrangolo, P.; Murray, J. S.; Pilati, T.; Politzer, P.; Resnati, G.; Terraneo, G., Fluorine-Centered

Halogen Bonding: A Factor in Recognition Phenomena and Reactivity. *Cryst. Growth Des.* **2011,** *11* (9), 4238-4246; (e) Parisini, E.; Metrangolo, P.; Pilati, T.; Resnati, G.; Terraneo, G., Halogen bonding in halocarbon-protein complexes: a structural survey. *Chem. Soc. Rev.* **2011,** *40* (5), 2267-2278; (f) Politzer, P.; Murray, J. S.; Clark, T., Halogen bonding: an electrostatically-driven highly directional noncovalent interaction. *Phys. Chem. Chem. Phys.* **2010,** *12* (28), 7748-7757.

13. Politzer, P.; Lane, P.; Concha, M. C.; Ma, Y. G.; Murray, J. S., An overview of halogen bonding. *J. Mol. Model.* **2007,** *13* (2), 305-311.

14. (a) Clark, T.; Hennemann, M.; Murray, J. S.; Politzer, P., Halogen bonding: the sigma-hole. *J. Mol. Model.* **2007,** *13* (2), 291-296; (b) Politzer, P.; Murray, J. S.; Lane, P., sigma-hole bonding and hydrogen bonding: Competitive interactions. *Int. J. Quantum Chem.* **2007,** *107* (15), 3046-3052.

15. (a) Riley, K. E.; Hobza, P., Investigations into the nature of halogen bonding including symmetry adapted perturbation theory analyses. *J. Chem. Theory Comput.* **2008,** *4* (2), 232-242; (b) Wu, J. Y.; Zhang, J. C.; Wang, Z. X.; Cao, W. L., Theoretical study on intermolecular interactions in BrF/HnX adducts. *Chem. Phys.* **2007,** *338* (1), 69-74; (c) Riley, K. E.; Hobza, P., Strength and Character of Halogen Bonds in Protein-Ligand Complexes. *Cryst. Growth Des.* **2011,** *11* (10), 4272-4278; (d) Lu, Y. X.; Zou, J. W.; Wang, Y. H.; Jiang, Y. J.; Yu, Q. S., Ab initio investigation of the complexes between bromobenzene and several electron donors: Some insights into the magnitude and nature of halogen bonding interactions. *J. Phys. Chem. A* **2007,** *111* (42), 10781-10788; (e) Murray, J. S.; Riley, K. E.; Politzer, P.; Clark, T., Directional Weak Intermolecular Interactions: sigma-Hole Bonding. *Aust. J. Chem.* **2010,** *63* (12), 1598-1607.

16. (a) Metrangolo, P.; Meyer, F.; Pilati, T.; Resnati, G.; Terraneo, G., Halogen bonding in supramolecular chemistry. *Angew. Chem.-Int. Edit.* **2008,** *47* (33), 6114-6127; (b) Fox, D.; Metrangolo, P.; Pasini, D.; Pilati, T.; Resnati, G.; Terraneo, G., Site-selective supramolecular synthesis of halogen-bonded cocrystals incorporating the photoactive azo group. *Crystengcomm* **2008,** *10* (9), 1132-1136.

17. Szell, P. M. J.; Zablotny, S.; Bryce, D. L., Halogen bonding as a supramolecular dynamics catalyst. *Nat. Commun.* **2019,** *10*, 8.

18. Gentry, C. L.; Egleton, R. D.; Gillespie, T.; Abbruscato, T. J.; Bechowski, H. B.; Hruby, V. J.; Davis, T. P., The effect of halogenation on blood-brain barrier permeability of a novel peptide drug. *Peptides* **1999,** *20* (10), 1229-1238.

19. Prelog, V., Problems in Chemical Topology. *Chem. Br.* **1968,** *4* (9), 382-&.

20. Sokolov, V. I., Stereochemistry of optically active compounds. Problems and prospects. *Russ. Chem. Bull.* **2001,** *50* (8), 1339-1355.

21. Cahn, R. S.; Ingold, C.; Prelog, V., Specification of Molecular Chirality. *Angew. Chem.-Int. Edit.* **1966,** *5* (4), 385-&.

22. Moss, G. P., Basic terminology of stereochemistry. *Pure Appl. Chem.* **1996,** *68* (12), 2193-2222.

23. Adams, S. S.; Bresloff, P.; Mason, C. G., Pharmacological differences between the optical isomers of ibuprofen: evidence for metabolic inversion of the (-)-isomer. *J. Pharm. Pharmacol.* **1976,** *28* (3), 256-257.

24. Flack, H. D.; Bernardinelli, G., Absolute structure and absolute configuration. *Acta Crystallogr. Sect. A* **1999,** *55*, 908-915.

25. Hoye, T. R.; Hamad, A. S. S.; Koltun, D. O.; Tennakoon, M. A., An NMR method for determination of configuration of beta-substituted carboxylic acids. *Tetrahedron Lett.* **2000,** *41* (14), 2289-2293.

26. Uray, G.; Verdino, P.; Belaj, F.; Kappe, C. O.; Fabian, W. M. F., Absolute configuration in 4-alkyl- and 4-aryl-3,4-dihydro-2(1H)-pyrimidones: A combined theoretical and experimental investigation. *J. Org. Chem.* **2001,** *66* (20), 6685-6694.

27. (a) Bouman, T. D.; Moscowitz, A., Optical Activity of Saturated Ketones. *J. Chem. Phys.* **1968,** *48* (7), 3115-+; (b) Schellman, J. A., Vibrational Optical Activity. *J. Chem. Phys.* **1973,** *58* (7), 2882-2886; (c) Stigter, D.; Schellman, J. A., Approximations in the One-Electron Theory of Optical Rotation. *J. Chem. Phys.* **1969,** *51* (8), 3397-+; (d) Holzwart.G; Chabay, I., Optical Activity of Vibrational Transitions: A Coupled Oscillator Model. *J. Chem. Phys.* **1972,** *57* (4), 1632-&; (e) Faulkner, T. R.; Moscowit.A; Holzwart.G; Hsu, E. C.; Mosher, H. S., Infrared circular dichroism of

carbon-hydrogen and carbon-deuterium stretching modes. Calculations. *J. Am. Chem. Soc.* **1974,** *96* (1), 252-253.

28. Holzwart.G; Hsu, E. C.; Mosher, H. S.; Faulkner, T. R.; Moscowit.A, Infrared circular dichroism of carbon-hydrogen and carbon-deuterium stretching modes. Calculations. *J. Am. Chem. Soc.* **1974,** *96* (1), 251-252.

29. (a) Lipp, E. D.; Nafie, L. A., Fourier Transform Infrared Vibrational Circular Dichroism: Improvements in Methodology and Mid-Infrared Spectral Results. *Appl. Spectrosc.* **1984,** *38* (1), 20-26; (b) Lipp, E. D.; Zimba, C. G.; Nafie, L. A., Vibrational circular dichroism in the mid-infrared using fourier transform spectroscopy. *Chem. Phys. Lett.* **1982,** *90* (1), 1-5; (c) Nafie, L. A.; Diem, M., Theory of High Frequency Differential Interferometry: Application to the Measurement of Infrared Circular and Linear Dichroism via Fourier Transform Spectroscopy. *Appl. Spectrosc.* **1979,** *33* (2), 130-135; (d) Nafie, L. A.; Diem, M.; Vidrine, D. W., Fourier transform infrared vibrational circular dichroism. *J. Am. Chem. Soc.* **1979,** *101* (2), 496-498.

30. Nafie, L. A., Infrared and Raman vibrational optical activity: Theoretical and experimental aspects. *Annu. Rev. Phys. Chem.* **1997,** *48*, 357-386.

31. (a) Freedman, T. B.; Cao, X. L.; Dukor, R. K.; Nafie, L. A., Absolute configuration determination of chiral molecules in the solution state using vibrational circular dichroism. *Chirality* **2003,** *15* (9), 743-758; (b) Polavarapu, P. L.; He, J. T., Chiral analysis using Mid-IR vibrational CD spectroscopy. *Analytical Chemistry* **2004,** *76* (3), 61A-67A.

32. Polavarapu, P. L., The absolute configuration of bromochlorofluoromethane. *Angew. Chem.-Int. Edit.* **2002,** *41* (23), 4544-+.

33. (a) Stephens, P. J.; Lowe, M. A., Vibrational circular dichroism. *Annu. Rev. Phys. Chem.* **1985,** *36*, 213-241; (b) Stephens, P. J., Theory of vibrational circular dichroism. *J. Phys. Chem.* **1985,** *89* (5), 748-752; (c) Nafie, L. A.; Freedman, T. B., Vibronic coupling theory of infrared vibrational transitions. *J. Chem. Phys.* **1983,** *78* (12), 7108-7116; (d) Craig, D. P.; Thirunamachandran, T., A theory of vibrational circular dichroism in terms of vibronic interactions. *Mol. Phys.* **1978,** *35* (3), 825-840.

34. Schellman, J. A., Circular dichroism and optical rotation. *Chem. Rev.* **1975,** *75* (3), 323-331.

35. Faulkner, T. R.; Marcott, C.; Moscowitz, A.; Overend, J., Anharmonic effects in vibrational circular dichroism. *J. Am. Chem. Soc.* **1977,** *99* (25), 8160-8168.

36. Schellman, J. A., Vibrational optical-activity. *J. Chem. Phys.* **1973,** *58* (7), 2882-2886.

37. Holzwart.G; Chabay, I., Optical activity of vibrational transitions: A coupled oscillator model. *J. Chem. Phys.* **1972,** *57* (4), 1632-&.

38. Barnett, C. J.; Drake, A. F.; Kuroda, R.; Mason, S. F., A dynamic polarization model for vibrational optical activity and the infrared circular dichroism of a dihydro[5]helicene. *Mol. Phys.* **1980,** *41* (2), 455-468.

39. (a) Nafie, L. A.; Walnut, T. H., Vibrational circular-dichroism theory - localized molecular-orbital model. *Chem. Phys. Lett.* **1977,** *49* (3), 441-446; (b) Walnut, T. H.; Nafie, L. A., IR absorption and Born-Oppenheimer approximation .2. vibrational circular-dichroism. *J. Chem. Phys.* **1977,** *67* (4), 1501-1510.

40. Hunt, K. L. C.; Harris, R. A., Vibrational circular dichroism and electric-field shielding tensors: A new physical interpretation based on nonlocal susceptibility densities. *J. Chem. Phys.* **1991,** *94* (11), 6995-7002.

41. (a) Stephens, P. J., Gauge dependence of vibrational magnetic dipole transition moments and rotational strengths. *J. Phys. Chem.* **1987,** *91* (7), 1712-1715; (b) Buckingham, A. D.; Fowler, P. W.; Galwas, P. A., Velocity-dependent property surfaces and the theory of vibrational circular dichroism. *Chem. Phys.* **1987,** *112* (1), 1-14.

42. Nafie, L. A.; Diem, M.; Vidrine, D. W., Fourier transform infrared vibrational circular dichroism. *J. Am. Chem. Soc.* **1979,** *101* (2), 496-498.

43. Keiderling, T. A.; Stephens, P. J., Vibrational circular dichroism of overtone and combination bands. *Chem. Phys. Lett.* **1976,** *41* (1), 46-48.

44. Nafie, L. A., Dual polarization modulation: A real-time, spectral-multiplex separation of circular dichroism from linear birefringence spectral intensities. *Appl. Spectrosc.* **2000,** *54* (11), 1634-1645.

45. Busch, K. W. B. M. A., Chiral Analysis: Instrumental aspects of chiroptical detection. **2006**.

46. Gunther, H., *NMR spectroscopy: basic principles, concepts, and applications in*

chemistry. 2013; Vol. 3rd.

47. Gunther, H., *NMR spectroscopy: basic principles, concepts, and applications in chemistry*. **2013**; Vol. 3rd.

48. Zerbe, O. J., S., *Applied NMR spectroscopy for chemists and life scientists*. Wiley-VCH: Weinheim: 2014.

49. Skoog, D. A. H., F. James; Crouch, Stanley R., *Principles of Instrumental Analysis*. Belmont, CA: Thomson Brooks/Cole: 2007.

50. Keeler, J,. Understanding NMR Spectroscopy. **2010.**

51. Alkorta, I.; Rozas, I.; Elguero, J., Charge-transfer complexes between dihalogen compounds and electron donors. *J. Phys. Chem. A* **1998,** *102* (46), 9278-9285.

52. Kerenskaya, G.; Goldschleger, I. U.; Apkarian, V. A.; Janda, K. C., Spectroscopic signatures of halogens in clathrate hydrate cages. 1. Bromine. *J. Phys. Chem. A* **2006,** *110* (51), 13792-13798.

53. (a) Bruinsma, R. F., Physics of protein-DNA interaction. *Physica A* **2002,** *313* (1-2), 211-237; (b) Degennes, P. G., Interactions between polymers and surfactants. *J. Phys. Chem.* **1990,** *94* (22), 8407-8413; (c) Cabane, B.; Duplessix, R., Decoration of semidilute polymer solutions with surfactant micelles. *Journal De Physique* **1987,** *48* (4), 651-662; (d) Cabane, B.; Duplessix, R., Organization of surfactant micelles adsorbed on a polymer molecule in water : a neutron scattering study. *Journal De Physique* **1982,** *43* (10), 1529-1542; (e) Kekicheff, P.; Cabane, B.; Rawiso, M., Macromolecules dissolved in a lamellar lyotropic mesophase. *Journal of Colloid and Interface Science* **1984,** *102* (1), 51-70.

54. (a) Hunter, C. A., Quantifying intermolecular interactions: Guidelines for the molecular recognition toolbox. *Angew. Chem.-Int. Edit.* **2004,** *43* (40), 5310-5324; (b) Singh, R. N.; Baboo, V.; Rawat, P.; Gupta, V. P., Studies on molecular weaker

interactions, spectroscopic analysis and chemical reactivity of synthesized ethyl 3,5-dimethyl-4- 3-(2-nitro-phenyl)-acryloyl -1H-pyrrole-2-carboxylate through experimental and quantum chemical approaches. *J. Mol. Struct.* **2013,** *1037*, 338-351.

55. (a) Parks, J. S.; Cistola, D. P.; Small, D. M.; Hamilton, J. A., Interactions of the carboxyl group of oleic-acid with bovine serum-albumin - a c-13 nmr-study. *J. Biol. Chem.* **1983,** *258* (15), 9262-9269; (b) Sahu, P. K.; Nanda, R.; Seth, S.; Ghosh, A.; Sarkar, M., Nuclear magnetic resonance, fluorescence correlation spectroscopy and time-resolved fluorescence anisotropy studies of intermolecular interactions in bis(1-methyl-1H-imidazol-3-ium-3-yl)dihydroborate bis (trifluoromethylsulfonyl)amide and its mixtures with various cosolvents. *Chem. Phys. Lett.* **2016,** *661*, 100-106; (c) Sethio, D.; Raggi, G.; Lindh, R.; Erdelyi, M., Halogen Bond of Halonium Ions: Benchmarking DFT Methods for the Description of NMR Chemical Shifts. *J. Chem. Theory Comput.* **2020,** *16* (12), 7690-7701; (d) von der Heiden, D.; Vanderkooy, A.; Erdelyi, M., Halogen bonding in solution: NMR spectroscopic approaches. *Coordination Chemistry Reviews* **2020,** *407*; (e) Bryce, D. L., Preparation Strategies and Solid-State NMR Characterization of Supramolecular Architectures based on Halogen Bonds, Chalcogen Bonds, and Pnictogen Bonds. *Acta Crystallographica a-Foundation and Advances* **2021,** *77*, C252-C252.

56. Gavezzotti, A., Comparing the strength of covalent bonds, intermolecular hydrogen bonds and other intermolecular interactions for organic molecules: X-ray diffraction data and quantum chemical calculations. *New J. Chem.* **2016,** *40* (8), 6848-6853.

57. Tsai, C. E.; Hwang, B. J., Intermolecular interactions between methanol/water molecules and Nafion (TM) membrane: An infrared spectroscopy study. *Fuel Cells* **2007,** *7* (5), 408-416.

58. Mazzeo, G.; Abbate, S.; Longhi, G.; Castiglioni, E.; Villani, C., Vibrational Circular Dichroism (VCD) Reveals Subtle Conformational Aspects and Intermolecular Interactions in the Carnitine Family. *Chirality* **2015,** *27* (12), 907-913.

59. Lewis, G. N., The atom and the molecule. *J. Am. Chem. Soc.* **1916,** *38*, 762-785.

60. Pauling, L., *The Nature of the Chemical Bond and the Structure of Molecules and Crystals: An Introduction to Modern Struc-tural Chemistry*. Cornell University Press: 1960.

61. (a) Hobza, P.; Zahradnik, R., Intermolecular interactions between medium-sized systems. Nonempirical and empirical calculations of interaction energies. Successes and failures. *Chem. Rev.* **1988,** *88* (6), 871-897; (b) Jeffrey, G. A.; Saenger, W., *Hydrogen bonding in biological structures*. 1991; p XIV+569P-XIV+569P.

62. Wang, S.; Taniguchi, T.; Monde, K.; Kawahata, M.; Yamaguchi, K.; Otani, Y.; Ohwada, T., Hydrogen bonding to carbonyl oxygen of nitrogen-pyramidalized amide - detection of pyramidalization direction preference by vibrational circular dichroism spectroscopy. *Chem. Commun.* **2016,** *52* (21), 4018-4021.

63. (a) Magyarfalvi, G.; Tarczay, G.; Vass, E., Vibrational circular dichroism. *Wiley Interdiscip. Rev.-Comput. Mol. Sci.* **2011,** *1* (3), 403-425; (b) Gobi, S.; Vass, E.; Magyarfalvi, G.; Tarczay, G., Effects of strong and weak hydrogen bond formation on VCD spectra: a case study of 2-chloropropionic acid. *Phys. Chem. Chem. Phys.* **2011,** *13* (31), 13972-13984.

64. Xia, Y. Y.; Koenis, M. A. J.; Collados, J. F.; Ortiz, P.; Harutyunyan, S. R.; Visscher, L.; Buma, W. J.; Nicu, V. P., Regional Susceptibility in VCD Spectra to Dynamic Molecular Motions: The Case of a Benzyl -Hydroxysilane. *ChemPhysChem* **2018,** *19* (5), 561-565.

65. Kwac, K.; Lee, K. K.; Han, J. B.; Oh, K. I.; Cho, M., Classical and quantum mechanical/molecular mechanical molecular dynamics simulations of alanine dipeptide in water: Comparisons with IR and vibrational circular dichroism spectra. *J. Chem. Phys.* **2008,** *128* (10), 13.

66. Yang, G. C.; Xua, Y. J., Probing chiral solute-water hydrogen bonding networks by chirality transfer effects: A vibrational circular dichroism study of glycidol in water. *J. Chem. Phys.* **2009,** *130* (16), 9.

67. Yamamoto, K.; Nakao, Y.; Kyogoku, Y.; Sugeta, H., Vibrational circular dichroism in hydrogen bond systems: Part III. Vibrational circular dichroism of the OH

stretching vibrations of 1,2-diols and β-methoxyalcohols. *J. Mol. Struct.* **1991,** *242*, 75-86.

68. Nakao, Y.; Kyogoku, Y.; Sugeta, H., Vibrational circular-dichroism in hydrogen-bond systems .2. vibrational circular-dichroism of the oh stretching vibration in 2,2-dimethyl-1,3-dioxolane-4-methanol. *J. Mol. Struct.* **1986,** *146*, 85-90.

69. (a) Arunan, E.; Desiraju, G. R.; Klein, R. A.; Sadlej, J.; Scheiner, S.; Alkorta, I.; Clary, D. C.; Crabtree, R. H.; Dannenberg, J. J.; Hobza, P.; Kjaergaard, H. G.; Legon, A. C.; Mennucci, B.; Nesbitt, D. J., Definition of the hydrogen bond (IUPAC Recommendations 2011). *Pure Appl. Chem.* **2011,** *83* (8), 1637-1641; (b) Arunan, E.; Desiraju, G. R.; Klein, R. A.; Sadlej, J.; Scheiner, S.; Alkorta, I.; Clary, D. C.; Crabtree, R. H.; Dannenberg, J. J.; Hobza, P.; Kjaergaard, H. G.; Legon, A. C.; Mennucci, B.; Nesbitt, D. J., Defining the hydrogen bond: An account (IUPAC Technical Report). *Pure Appl. Chem.* **2011,** *83* (8), 1619-1636.

70. (a) Clark, T.; Hennemann, M.; Murray, J. S.; Politzer, P., Halogen bonding: the sigma-hole. *J. Mol. Model.* **2007,** *13* (2), 291-296; (b) Murray, J. S.; Lane, P.; Politzer, P., Expansion of the sigma-hole concept. *J. Mol. Model.* **2009,** *15* (6), 723-729; (c) Politzer, P.; Murray, J. S.; Clark, T., Halogen bonding and other sigma-hole interactions: a perspective. *Phys. Chem. Chem. Phys.* **2013,** *15* (27), 11178-11189.

71. Cavallo, G.; Metrangolo, P.; Milani, R.; Pilati, T.; Priimagi, A.; Resnati, G.; Terraneo, G., The Halogen Bond. *Chem. Rev.* **2016,** *116* (4), 2478-2601.

72. Nyburg, S. C.; Faerman, C. H., A revision of van der Waals atomic radii for molecular crystals: N, O, F, S, Cl, Se, Br and I bonded to carbon. *Acta Crystallographica Section B-Structural Science* **1985,** *41* (AUG), 274-279.

73. Losada, M.; Xu, Y., Chirality transfer through hydrogen-bonding: Experimental and ab initio analyses of vibrational circular dichroism spectra of methyl lactate in water. *Phys. Chem. Chem. Phys.* **2007,** *9* (24), 3127-3135.

74. M. J. Firsch., G. W. Trucks, H. B. Schlegel, G. E. Scuseria, M. A. Robb, J. R. Cheeseman, G. Scalmani, V. Barone, B. Mennucci, G. A. Petersson, H. Nakatsuji, M. Caricato, X. Li, H. P. Hratchian, A. F. Izmaylov, J. Bloino, G. Zheng, J. L. Sonnenberg, M. Hada, M. Ehara, K. Toyota, R. Fukuda, J. Hasegawa, M. Ishida, T. Nakajima, Y.

Honda, O. Kitao, H. Nakai, T. Vreven, J. A. Montgomery, Jr., J. E. Peralta, F. Ogliaro, M. Bearpark, J. J. Heyd, E. Brothers, K. N. Kudin, V. N. Staroverov, R. Kobayashi, J. Normand, K. Raghavachari, A. Rendell, J. C. Burant, S. S. Iyengar, J. Tomasi, M. Cossi, N. Rega, J. M. Millam, M. Klene, J. E. Knox, J. B. Cross, V. Bakken, C. Adamo, J. Jaramillo, R. Gomperts, R. E. Stratmann, O. Yazyev, A. J. Austin, R. Cammi, C. Pomelli, J. W. Ochterski, R. L. Martin, K. Morokuma, V. G. Zakrzewski, G. A. Voth, P. Salvador, J. J. Dannenberg, S. Dapprich, A. D. Daniels, Ö. Farkas, J. B. Foresman, J. V. Ortiz, J. Cioslowski, and D. J. Fox, Gaussian 09, Revision D.01. Gaussian, I., Wallingford CT, Ed. 2009.

75. (a) Becke, A. D., Density-functional thermochemistry. III. The role of exact exchange. *J. Chem. Phys.* **1993,** *98* (7), 5648-5652; (b) Becke, A. D., Density-functional exchange-energy approximation with correct asymptotic behavior. *Physical Review A* **1988,** *38* (6), 3098-3100; (c) Lee, C. T.; Yang, W. T.; Parr, R. G., Development of the Colle-Salvetti correlation-energy formula into a functional of the electron density. *Physical Review B* **1988,** *37* (2), 785-789.

76. Harihara.P. C; Pople, J. A., The influence of polarization functions on molecular orbital hydrogenation energies. *Theoretica Chimica Acta* **1973,** *28* (3), 213-222.

77. Tomasi, J.; Mennucci, B.; Cammi, R., Quantum mechanical continuum solvation models. *Chem. Rev.* **2005,** *105* (8), 2999-3093.

78. A., S., *Solubilities of inorganic and metal organic compounds*. 3 ed.; New York: D. Van Nostrand Company: 1940; Vol. 1.

79. Greenwood, N,. Earnshaw, A,. *Chemistry of the Elements*. Butterworth-Heinemann: 1997.

80. Cavallo, G.; Metrangolo, P.; Milani, R.; Pilati, T.; Priimagi, A.; Resnati, G.; Terraneo, G., The Halogen Bond. *Chem. Rev.* **2016,** *116* (4), 2478-2601.

81. Politzer, P.; Lane, P.; Concha, M. C.; Ma, Y. G.; Murray, J. S., An overview of halogen bonding. *J. Mol. Model.* **2007,** *13* (2), 305-311.

82. (a) Clark, T.; Hennemann, M.; Murray, J. S.; Politzer, P., Halogen bonding: the sigma-hole. *J. Mol. Model.* **2007,** *13* (2), 291-296; (b) Politzer, P.; Murray, J. S.; Lane,

P., sigma-hole bonding and hydrogen bonding: Competitive interactions. *Int. J. Quantum Chem.* **2007,** *107* (15), 3046-3052.

83. Zhang, Y.; Ji, B.; Tian, A.; Wang, W., Communication: Competition between pi center dot center dot center dot pi interaction and halogen bond in solution: A combined C-13 NMR and density functional theory study. *J. Chem. Phys.* **2012,** *136* (14).

84. Xu, Y.; Gabidullin, B.; Bryce, D. L., Single-Crystal NMR Characterization of Halogen Bonds. *J. Phys. Chem. A* **2019,** *123* (29), 6194-6209.

85. (a) Hirose, K., A practical guide for the determination of binding constants. *Journal of Inclusion Phenomena and Macrocyclic Chemistry* **2001,** *39* (3-4), 193-209; (b) Thordarson, P., Determining association constants from titration experiments in supramolecular chemistry. *Chem. Soc. Rev.* **2011,** *40* (3), 1305-1323.

86. (a) Becke, A. D., Density-functional exchange-energy approximation with correct asymptotic behavior. *Physical Review A* **1988,** *38* (6), 3098-3100; (b) Lee, C. T.; Yang, W. T.; Parr, R. G., Development of the Colle-Salvetti correlation-energy formula into a functional of the electron density. *Physical Review B* **1988,** *37* (2), 785-789; (c) Becke, A. D., Density-functional thermochemistry. III. The role of exact exchange. *J. Chem. Phys.* **1993,** *98* (7), 5648-5652.

87. Harihara.Pc; Pople, J. A., The influence of polarization functions on molecular orbital hydrogenation energies. *Theoretica Chimica Acta* **1973,** *28* (3), 213-222.

88. Tomasi, J.; Mennucci, B.; Cammi, R., Quantum mechanical continuum solvation models. *Chem. Rev.* **2005,** *105* (8), 2999-3093.

89. Lunghi, A.; Cardillo, P.; Messina, T.; Metrangolo, P.; Panzeri, W.; Resnati, G., Perfluorocarbon-hydrocarbon self assembling. Thermal and vibrational analyses of one-dimensional networks formed by alpha,omega-diiodoperfluoroalkanes with K.2.2. and K.2.2.2. *Journal of Fluorine Chemistry* **1998,** *91* (2), 191-194.

90. Metrangolo, P.; Panzeri, W.; Recupero, F.; Resnati, G., Perfluorocarbon-hydrocarbon self-assembly - Part 16. F-19 NMR study of the halogen bonding between halo-perfluorocarbons and heteroatom containing hydrocarbons. *Journal of Fluorine Chemistry* **2002,** *114* (1), 27-33.

91. Rezac, R., Description of Halogen Bonding in SemiempiricalQuantum-Mechanical and Self-Consistent ChargeDensity-Functional Tight-Binding Methods. J. Comput. Chem. 2019, 40, 1633–1642.

92. Jason T. A. Gall, Javix, T., Fan, X, Zhibo, W., Jäger, W, Xu, Y,. Rotational spectroscopy of the methyl glycidate–water complex: conformation and water and methyl rotor tunneling motions, Phys. Chem. Chem. Phys., 2017, 19, 29508–29515

93. Hansen, P, E,. Vakili, M,. Kamounah, F, S,. Spanget-Larsen, J,. NH Stretching Frequencies of Intramolecularly Hydrogen-Bonded Systems: An Experimental and Theoretical Study. *Molecules*. **2021**. 26 (24), 7651-7669.

94. Devillanova, F. A.; Verani, G., Charge transfer complexes between I_2 and 1,3-imidazolidine-2-thione and its n-mono- and n,n'-di-substituted derivatives. *Tetrahedron* **1979,** *35* (4), 511-514.

95. Tsuzuki, S,. Uchimaru, T,. Accuracy of intermolecular interaction energies, particularly those of hetero-atom containing molecules obtained by DFT calculations with Grimme's D2, D3 and D3BJ dispersion corrections. *Phys Chem Chem Phys*. **2020**, 22 (39), 22508-22519.

96. Harihara.P. C; Pople, J. A., The influence of polarization functions on molecular orbital hydrogenation energies. *Theoretica Chimica Acta* **1973,** *28* (3), 213-222.

97. Saccone, M.; Cavallo, G.; Metrangolo, P.; Pace, A.; Pibiri, I.;Pilati, T.; Resnati, G.; Terraneo, G. Halogen Bond Directionality Translates Tecton Geometry into Self-Assembled Architecture Geometry. *CrystEngComm* **2013**, 15, 3102−3105.

98. Messina, M. T.; Metrangolo, P.; Panzeri, W.; Ragg, E.; Resnati, G. Perfluorocarbon-Hydrocarbon Self-Assembly. Part 3. Liquid Phase Interactions between Perfluoroalkylhalides and Heteroatom Containing Hydrocarbons. *Tetrahedron Lett.* **1998**, 39, 9069−9072.

99. Vargas Jentzsch, A.; Emery, D.; Mareda, J.; Metrangolo, P.; Resnati, G.; Matile, S. Ditopic Ion Transport Systems: Anion-π Interactions and Halogen Bonds at Work. *Angew. Chem., Int. Ed*. **2011**, 50, 11675−11678.

100. Huber, S. M.; Jimenez-Izal, E.; Ugalde, J. M.; Infante, I. Unexpected Trends in Halogen-Bond Based Noncovalent Adducts. *Chem. Commun*. **2012**, 48, 7708−7710.

101. Carlsson, A. C. C.; Uhrbom, M.; Karim, A.; Brath, U.; Grafenstein, J.; Erdelyi, M., Solvent effects on halogen bond symmetry. *Crystengcomm* **2013,** *15* (16), 3087-3092

102. Tsuzuki, S.; Wakisaka, A.; Ono, T.; Sonoda, T., Magnitude and Origin of the Attraction and Directionality of the Halogen Bonds of the Complexes of C_6F_5X and C_6H_5X (X=I, Br, Cl and F) with Pyridine. *Chem.-Eur. J.* **2012,** *18* (3), 951-960.